

## Supporting Information

### $\pi$ -Spacer Effects in 2,6-Disubstituted BODIPY Fluorophores for Mitochondrial Imaging

Charutha Kalarikkal<sup>a</sup>, Poonam Rani<sup>b</sup>, and Chinna Ayya Swamy P<sup>a\*</sup>

<sup>a</sup>Main group Organometallics Optoelectronic Materials and Catalysis lab, Department of Chemistry, National Institute of Technology, Calicut, India-673601.

<sup>b</sup>Department of Inorganic and Physical Chemistry, Indian Institute of Science, Bangalore 560012, India

Corresponding author : [swamy@nitc.ac.in](mailto:swamy@nitc.ac.in)

#### Table of Contents

<b>1. General Information</b> .....	<b>S2</b>
<b>2. Synthetic Procedures</b> .....	<b>S4</b>
<b>3. NMR and HRMS Spectra of the Compounds</b> .....	<b>S9</b>
<b>4. Photophysical Studies of the Compounds</b> .....	<b>S24</b>
<b>5. DFT Calculations</b> .....	<b>S33</b>
<b>6. Cytotoxicity Assay</b> .....	<b>S34</b>
<b>7. Co-localization Imaging</b> .....	<b>S35</b>
<b>8. Comparative Table</b> .....	<b>S37</b>
<b>9. DFT Coordinates</b> .....	<b>S40</b>
<b>10. References</b> .....	<b>S58</b>

## 1. General Information

### 1.1 Materials and Measurements

All the commercially available chemicals and solvents were purchased and used as received. Toluene was dried over sodium, freshly distilled, and then used. The chlorinated solvents were dried over CaH<sub>2</sub> and subsequently stored over 4 Å molecular sieves. All the heating reactions were performed in a reaction block on a magnetic stirrer using a temperature-controlled probe. Moisture sensitive reactions were performed under a nitrogen atmosphere. The 500 MHz <sup>1</sup>H NMR, 126 MHz <sup>13</sup>C NMR, 471 MHz <sup>19</sup>F NMR and 160.4 MHz <sup>11</sup>B NMR spectra were recorded on a JEOL JNM-ECZ-500R/M1, 500 MHz NMR spectrometer. All solution <sup>1</sup>H and <sup>13</sup>C spectra were referenced internally to the solvent signal [TMS (δ = 0)]. <sup>11</sup>B and <sup>11</sup>F spectra were referenced externally to BF<sub>3</sub>·Et<sub>2</sub>O (δ = 0) in C<sub>6</sub>D<sub>6</sub>. All the chemical shifts were reported in δ ppm, and the coupling constants (J) were given in Hertz (Hz). The HRMS was performed on a Waters Synapt XS spectrometer in the positive ion mode using acetonitrile as the solvent. The UV–Vis absorption spectra were measured using a UV-Vis spectrophotometer SHIMADZU-2600 with a slit width of 2. Fluorescence measurements were carried out on a PerkinElmer 6500 fluorescence spectrometer.

### 1.2 Fluorescence Quantum Yield

The fluorescence quantum yields of compounds in solution were evaluated by using Rhodamine B in ethanol as a standard (Φ<sub>F</sub> = 0.49 in ethanol). The quantum yield Φ is calculated using the formula:

$$\Phi = \Phi_F \times (I/I_R) \times (A_R/A) \times (\eta/\eta_R)^2$$

where Φ = quantum yield of the compound, I = integral area of the emission peak, A = absorbance at λ<sub>ex</sub>, η = refractive index of the solvent.

**1.3 Cell culture:** HeLa cells were maintained in DMEM (Dulbecco's Modified Eagle's media) supplemented with 10% (v/v) fetal bovine serum (FBS) and antibiotic-antimycotic solution (100 units/mL penicillin/ streptomycin), at 37°C with 5% CO<sub>2</sub>.

**1.4 Cell freezing and thawing:** Cells released from the culture dish were centrifuged at 1200 rpm for 4 minutes. The supernatant was then aspirated, and the cells were resuspended in freezing media (growth medium + 10% sterile DMSO). Subsequently, 1 mL aliquots were

dispensed into cryopreservative screw-cap vials. The vials were frozen at -80 °C overnight and subsequently transferred to a liquid nitrogen tank.

For cell culturing, the frozen vials were first thawed in a 37°C water bath. The contents of each vial (1 mL) were then added to 3 mL of growth medium and centrifuged at 1200 rpm for 4 minutes to eliminate DMSO from the medium. After removing the supernatant, the cells were resuspended in 4 mL of growth medium in a T-25 flask and placed in a 5% CO<sub>2</sub>/37°C incubator. The cells were cultured until confluence was achieved before proceeding with experiments.

### **1.5 MTT assay:**

5x10<sup>3</sup> cells/well were seeded in 96 well plate, after 24 h HeLa cells were treated with probes in different concentrations, and incubated for 24 h at 37 °C, CO<sub>2</sub>-5% and humidity-controlled conditions. Following incubation, the cells were washed with 1X PBS, thrice. Then cells were treated with 0.5 mg/mL of MTT for 2 h and absorbance was measured at 590 nm.

### **1.6 Confocal microscopy imaging studies:**

HeLa cells were seeded at a density of 1×10<sup>5</sup> on the coverslip in 12-well plate, 10% FBS (DMEM media). Then the cells were treated with 700 nM concentration of compounds solution prepared in 0.2 % FBS. After incubation for 30 mins, cells were washed with DPBS and then incubated with 100 nM of LysoTracker blue, 500 nM of Mitotracker green separately, and fixed the cells with ice-cold methanol at -20 °C for 15 mins, removed the methanol from each well, and washed with DPBS. Cells were then treated with Hoechst (5 µg/ml) for 15 mins to stain the nuclei, and then the cover slips were mounted on glass slides with antifade and sealed with colorless nail polish. These coverslips were subjected to Confocal Zeiss LSM880 (Airyscan) microscopy. The images were analyzed on Leica LasX software. Imaging was performed using 405, 488, 540 nm laser excitation and emission Zeiss sets 38 (green), 49 (blue) and 63 (red) filter sets for fluorescence screening and 40 x objective. Images were analyzed in Zen 3.3 and Image j software. Pearson correlation coefficient was computed using JACoP with Fiji/ImageJ.

Ex/Em (LysoTracker blue) = 405/425 nm

Ex/Em (Mitotracker green) = 488/516 nm

Ex/Em Hoechst = 405/ 454 nm

Ex/Em (probes) = 540/550-700 nm

## 2. Synthetic procedure for the precursors and target molecules

### Synthesis of *(4-(dimethylamino)phenyl)methanol* (1)

Sodium borohydride NaBH<sub>4</sub> (609 mg, 16.09 mmol) was slowly added to 4-(dimethyl)amino benzaldehyde (2 g, 13.41 mmol) in a mixture of 30 mL DCM and 10 mL ethanol and stirred the reaction mixture at room temperature (RT) for 12 h. Using thin layer chromatography (TLC), the reaction was monitored, and the complete consumption of reactant was observed. Later, the reaction mixture was quenched with water and the volatiles were evaporated under reduced pressure. The crude product was extracted multiple times using DCM and brine solution, dried over anhydrous sodium sulfate (Na<sub>2</sub>SO<sub>4</sub>) and evaporated under reduced pressure, to obtain a pure colourless oily product (1.96 g, 97 %). The characterisation data of synthesised compound matched the literature reports.<sup>1</sup> <sup>1</sup>H NMR (500 MHz, CDCl<sub>3</sub>) δ: 7.24 (d, *J* = 8.8 Hz, 2H), 6.74 (d, *J* = 8.8 Hz, 2H), 4.54 (s, 2H), 2.95 (s, 6H).

### Synthesis of *(4-(dimethylamino)benzyl)triphenylphosphonium bromide* (2)

Compound 1 (1.50 g, 9.92 mmol) and PPh<sub>3</sub>.HBr (3.61 g, 10.52 mmol) were dissolved in 25 mL of dry CHCl<sub>3</sub> under N<sub>2</sub> atmosphere. The reaction mixture was refluxed at 70 °C for 4 h. Using TLC, the reaction was monitored, and the complete consumption of reactant was observed. After completion, the volatiles were removed under reduced pressure and the precipitate was washed multiple times with diethyl ether and dried under vacuum to obtain a pure white solid (4.67 g, 99 %). The characterisation data of synthesised compound matched the literature reports.<sup>2</sup> <sup>1</sup>H NMR (500 MHz, CDCl<sub>3</sub>) δ: 7.79 – 7.74 (m, 3H), 7.69 – 7.60 (m, 12H), 6.87 (dd, *J* = 8.9, 2.5 Hz, 2H), 6.54 (d, *J* = 8.6 Hz, 2H), 5.04 (d, *J* = 13.3 Hz, 2H), 2.88 (s, 6H).

### Synthesis of *(E)-4-bromo-N-(4-(4-(dimethylamino)styryl)phenyl)-N-phenylaniline* (3)

4-bromo benzaldehyde (2 g, 10.81 mmol), K<sub>2</sub>CO<sub>3</sub> (2.99 g, 21.62 mmol), and 18 crown-6 (143 mg, 0.54 mmol), were dissolved in 20 mL of dry DMF. Compound 2 (6.18 g, 12.97 mmol) which was dissolved in 20 mL of dry DMF was slowly added to the reaction mixture with vigorous stirring for 24 h under N<sub>2</sub> atmosphere. Using TLC, the reaction was monitored, and the complete consumption of reactant was observed. After completion, the reaction mixture was added to ice cold water to obtain pale white precipitate containing both E and Z isomers which was filtered, dried and kept under vacuum. In order to convert Z isomer into E isomer, precipitate was further dissolved in 30 mL of dry THF and was added with catalytic amount of resublimed I<sub>2</sub> and refluxed at 70 °C for 12 h. Excess I<sub>2</sub> was removed by adding NaOH

solution to the reaction mixture. After cooling into RT, the volatiles were evaporated under reduced pressure and the crude product was extracted using DCM and brine solution, dried over anhydrous Na<sub>2</sub>SO<sub>4</sub> and evaporated under reduced pressure to obtain the crude product. The crude product was further purified by using silica gel column chromatography with hexane/ethyl acetate (9:1) as the eluent as well as precipitation method (since the product (compound 3) was not completely miscible with most of the organic solvents). The pure product was obtained as a white solid (2.4 g, 73 %). The characterisation data of synthesised compound matched the literature reports.<sup>3</sup> <sup>1</sup>H NMR (500 MHz, CDCl<sub>3</sub>) δ: 7.44 (d, *J* = 8.5 Hz, 2H), 7.40 (d, *J* = 8.9 Hz, 2H), 7.33 (d, *J* = 8.6 Hz, 2H), 7.03 (d, *J* = 16.3 Hz, 1H), 6.84 (d, *J* = 16.3 Hz, 1H), 6.72 (d, *J* = 9.0 Hz, 2H), 2.99 (s, 6H).

The synthesis of compound 6 was similar procedure of compound 3 and data as follows:

Compound 5 (1 g, 2.84 mmol), K<sub>2</sub>CO<sub>3</sub> (785 mg, 5.68 mmol), 18 crown-6 (37.50 mg, 0.14 mmol), and compound 2 (2.70 g, 5.67 mmol). The pure product was obtained as a yellow solid (840 mg, 63 %). <sup>1</sup>H NMR (500 MHz, CDCl<sub>3</sub>) δ: 7.44 (d, *J* = 8.9 Hz, 2H), 7.40 (d, *J* = 8.7 Hz, 2H), 7.38 – 7.34 (m, 2H), 7.32 – 7.27 (m, 2H), 7.13 (d, *J* = 8.6 Hz, 2H), 7.07 (d, *J* = 8.8 Hz, 3H), 7.03 – 6.97 (m, 3H), 6.91 (d, *J* = 16.3 Hz, 1H), 6.75 (d, *J* = 8.9 Hz, 2H), 3.01 (s, 6H). <sup>13</sup>C{<sup>1</sup>H} NMR (126 MHz, CDCl<sub>3</sub>) δ: 150.4, 147.7, 147.4, 146.4, 133.8, 132.8, 132.6, 129.9, 128.2, 127.9, 127.4, 125.9, 125.6, 124.9, 123.7, 115.3, 113.1, 41.0. HRMS (ESI) *m/z*: [M + H]<sup>+</sup> calcd for C<sub>28</sub>H<sub>25</sub>BrN<sub>2</sub>, 471.1259; found, 471.1265.

#### **Synthesis of (*E*)-*N,N*-dimethyl-4-(4-(4,4,5,5-tetramethyl-1,3,2-dioxaborolan-2-yl)styryl)aniline (4)**

A 100 mL oven-dried Schlenk flask was charged with compound 3 (1.5 g, 4.96 mmol), bis(pinacolato)diboron (1.57 g, 6.20 mmol), potassium acetate (1.46 g, 14.89 mmol), and triphenylphosphine (52 mg, 0.20 mmol), followed by purging with N<sub>2</sub> multiple times. The reactants were dissolved in 50 mL of dry toluene, and the reaction mixture was thoroughly degassed with N<sub>2</sub> for 30 minutes. Dichlorobis(triphenylphosphine)palladium(II) (70 mg, 0.10 mmol) was then added as a catalyst, and the reaction was refluxed at 110 °C for 24 h. After completion, volatiles were removed under reduced pressure, and the crude product was extracted multiple times with ethyl acetate (3–4 times) and brine solution. The organic layer was dried over anhydrous Na<sub>2</sub>SO<sub>4</sub> and was evaporated under reduced pressure, yielding a brown solid as the crude product, which was further purified by silica gel column chromatography using hexane/ethyl acetate (95:5) as the eluent. The pure product was obtained as a white solid (1.40 g, 81 %). The characterisation data of synthesised compound matched

the literature reports.<sup>4</sup> <sup>1</sup>H NMR (500 MHz, CDCl<sub>3</sub>) δ: 7.77 (d, *J* = 8.3 Hz, 2H), 7.48 (d, *J* = 8.1 Hz, 2H), 7.42 (d, *J* = 9.0 Hz, 2H), 7.12 (d, *J* = 16.3 Hz, 1H), 6.92 (d, *J* = 16.3 Hz, 1H), 6.72 (d, *J* = 9.0 Hz, 2H), 2.99 (s, 6H), 1.35 (s, 12H).

The synthesis of compound **7** was similar procedure of compound **4**. For compound **7**, we have used Bis(diphenylphosphino)ferrocene dichloropalladium(II) as the catalyst and the data as follows:

Compound **6** (1 g, 2.13 mmol), bis(pinacolato)diboron (676 mg, 2.66 mmol), potassium acetate (627 mg, 6.39 mmol), and Pd(dppf)Cl<sub>2</sub> catalyst (47 mg, 0.06 mmol). The pure product was obtained as a yellow solid (374 mg, 34 %). <sup>1</sup>H NMR (500 MHz, CDCl<sub>3</sub>) δ: 7.71 (d, *J* = 8.7 Hz, 2H), 7.43 – 7.39 (m, 4H), 7.30 – 7.27 (m, 2H), 7.15 (d, *J* = 8.6 Hz, 2H), 7.09 (d, *J* = 8.7 Hz, 5H), 7.03 – 6.87 (m, 2H), 6.74 (d, *J* = 9.0 Hz, 2H), 3.00 (s, 6H), 1.36 (s, 12H). <sup>13</sup>C{<sup>1</sup>H} NMR (126 MHz, CDCl<sub>3</sub>) δ: 150.9, 150.4, 147.7, 146.4, 136.3, 133.8, 129.8, 128.2, 127.9, 127.3, 125.5, 125.4, 124.3, 123.9, 122.3, 113.0, 84.0, 41.0, 25.3. HRMS (ESI) *m/z*: [M + H]<sup>+</sup> calcd for C<sub>34</sub>H<sub>37</sub>BN<sub>2</sub>O<sub>2</sub>, 517.3026; found, 517.3021.

### Synthesis of Compound **8**

*p*-Anisaldehyde (893 μL, 7.34 mmol) and 2, 4 dimethyl pyrrole (1.8 mL, 17.63 mmol) were added to freshly distilled DCM (350 mL), stirred at room temperature under a N<sub>2</sub> atmosphere. The reaction mixture was thoroughly degassed using N<sub>2</sub> for at least 30 minutes, followed by the addition of a catalytic amount of trifluoroacetic acid (56.2 μL, 0.73 mmol). After 1 h, DDQ (1.9 g, 8.37 mmol) was added to the reaction mixture and was stirred for 5 h at room temperature. Triethylamine (10 mL, 73.45 mmol), and BF<sub>3</sub>·Et<sub>2</sub>O (10 mL, 81.02 mmol) were then added to the resultant product and stirred at room temperature for overnight. The crude was purified by silica gel column chromatography (hexane/ethylacetate = 95:5) and yielded as an orange crystalline solid BODIPY (0.79 g, 30 %). The NMR data matches well with the literature reported values.<sup>5</sup> <sup>1</sup>H NMR (500 MHz, CDCl<sub>3</sub>) δ: 7.17 (d, *J* = 8.7, 2H), 7.01 (d, *J* = 8.7, 2H), 5.97 (s, 2H), 3.87 (s, 3H), 2.55 (s, 6H), 1.43 (s 6H).

BODIPY (200 mg, 0.56 mmol) was dissolved in 40 mL of dry DCM and degassed the reaction mixture with N<sub>2</sub>. N-iodo succinimide (318 mg, 1.41 mmol) was added and stirred the reaction mixture at RT for 3 h. The progress of the reaction was monitored using TLC and the complete consumption of reactant was observed. The volatiles were removed under reduced pressure, followed by extraction with DCM (40 mL for 3 to 4 times) and washed with brine solution. The organic fraction was dried over anhydrous Na<sub>2</sub>SO<sub>4</sub> and was evaporated under reduced

pressure and kept under vacuum. The pure product was obtained as a red solid (335 mg, 98 %). The NMR data matches well with the literature reported values.<sup>6</sup> <sup>1</sup>H NMR (500 MHz, CDCl<sub>3</sub>) δ: 7.14 (d, *J*=8.7, 2H), 7.03 (d, *J*=8.7, 2H), 3.89 (s, 3H), 2.64 (s, 6H), 1.44 (s, 6H).

### Synthesis of Ph-BDP-NMe<sub>2</sub>

Compound **4** (553 mg, 1.59 mmol), compound **8** (400 mg, 0.66 mmol), and K<sub>2</sub>CO<sub>3</sub> (912 mg, 6.60 mmol) were added to a 100 mL Schlenk flask. The reactants were dissolved in 30 mL of THF and 10 mL of water, and thoroughly degassed the reaction mixture using N<sub>2</sub> gas for 30 minutes. After degassing, tetrakis(triphenylphosphine) palladium (0) Pd(PPh<sub>3</sub>)<sub>4</sub> (61 mg, 0.05 mmol) catalyst was added to the reaction mixture and refluxed for 48 h under N<sub>2</sub> atmosphere. The volatiles were evaporated under reduced pressure and the crude product was extracted using DCM and brine solution. The organic layer was dried over anhydrous Na<sub>2</sub>SO<sub>4</sub> and was evaporated under reduced pressure. The crude was further purified by silica gel column chromatography (hexane/DCM = 1:1). The pure product was obtained as a red solid powder in moderate yield (352 mg, 67 %). <sup>1</sup>H NMR (500 MHz, CDCl<sub>3</sub>) δ: 7.50 (d, *J* = 8.3 Hz, 4H), 7.43 (d, *J* = 8.9 Hz, 4H), 7.24 (d, *J* = 8.8 Hz, 2H), 7.14 (d, *J* = 8.3 Hz, 4H), 7.08 (d, *J* = 16.3 Hz, 2H), 7.03 (d, *J* = 8.8 Hz, 2H), 6.94 (d, *J* = 16.3 Hz, 2H), 6.78 (d, *J* = 8.9 Hz, 4H), 3.87 (s, 3H), 3.00 (s, 12H), 2.58 (s, 6H), 1.39 (s, 6H). <sup>13</sup>C {<sup>1</sup>H} NMR (126 MHz, CDCl<sub>3</sub>) δ: 160.6, 154.6, 150.1, 142.5, 139.6, 137.3, 133.9, 132.6, 132.3, 130.9, 129.8, 129.3, 128.1, 127.2, 126.4, 124.9, 115.1, 113.6, 55.8, 41.4, 13.9, 13.5. <sup>11</sup>B {<sup>1</sup>H} NMR (160.4 MHz, CDCl<sub>3</sub>) δ: 0.05 (t, *J* = 33.1 Hz). <sup>19</sup>F {<sup>1</sup>H} NMR (471 MHz, CDCl<sub>3</sub>) δ: -145.79 (q, *J* = 24.4 Hz). HRMS (ESI) *m/z*: [M + H]<sup>+</sup> calcd for C<sub>52</sub>H<sub>51</sub>BF<sub>2</sub>N<sub>4</sub>O, 797.4202; found, 797.4219.

The synthesis of TPA-BDP-NMe<sub>2</sub> was similar procedure of Ph-BDP-NMe<sub>2</sub> and the data as follows:

Compound **7** (818 mg, 1.59 mmol), compound **8** (400 mg, 0.66 mmol), K<sub>2</sub>CO<sub>3</sub> (912 mg, 6.60 mmol), and Pd(PPh<sub>3</sub>)<sub>4</sub> catalyst (76 mg, 0.07 mmol). The pure product was obtained as a red solid powder in moderate yield (410 mg, 54 %). <sup>1</sup>H NMR (500 MHz, CDCl<sub>3</sub>) δ: 7.43 – 7.36 (m, 8H), 7.30 – 7.23 (m, 4H), 7.14 (d, *J* = 7.6 Hz, 5H), 7.12 – 7.07 (m, 8H), 7.06 – 7.00 (m, 9H), 7.01 – 6.84 (m, 5H), 6.73 (d, *J* = 8.6 Hz, 3H), 3.88 (s, 3H), 2.98 (s, 12H), 2.59 (s, 6H), 1.41 (s, 6H). <sup>13</sup>C {<sup>1</sup>H} NMR (126 MHz, CDCl<sub>3</sub>) δ: 160.6, 154.6, 148.0, 147.0, 146.7, 142.3, 139.5, 133.7, 133.5, 132.2, 131.3, 129.8, 128.0, 128.0, 127.9, 127.4, 125.0, 124.9, 124.4, 123.5, 115.1, 113.1, 55.8, 41.1, 14.0, 13.6. <sup>11</sup>B {<sup>1</sup>H} NMR (160.4 MHz, CDCl<sub>3</sub>) δ: 0.05 (t, *J* = 34.7

Hz).  $^{19}\text{F}\{^1\text{H}\}$  NMR (471 MHz,  $\text{CDCl}_3$ )  $\delta$ : -144.75 (q,  $J = 28.9$  Hz). HRMS (ESI)  $m/z$ :  $[\text{M}/2 + \text{H}]^+$  calcd for  $\text{C}_{76}\text{H}_{69}\text{BF}_2\text{N}_6\text{O}$ , 566.2875; found, 566.2900.

### Synthesis of Ph-BDP-NMe<sub>3</sub>

**Ph-BDP-NMe<sub>2</sub>** (75 mg, 0.09 mmol) and methyl iodide (2.34 mL, 0.04 mmol) were dissolved in 10 mL of dry acetonitrile and stirred the reaction mixture at RT overnight under  $\text{N}_2$  atmosphere. The progress of the reaction was monitored using TLC, and complete consumption of reactant was observed. The volatiles were removed under reduced pressure and washed the crude product multiple times using diethyl ether and the pure product was obtained as red solid powder (90 mg, 88 %).  $^1\text{H}$  NMR (500 MHz,  $\text{DMSO-d}_6$ )  $\delta$ : 7.97 (d,  $J = 9.2$  Hz, 4H), 7.85 (d,  $J = 9.3$  Hz, 4H), 7.70 (d,  $J = 8.5$  Hz, 4H), 7.51 – 7.39 (m, 4H), 7.38 (d,  $J = 8.7$  Hz, 2H), 7.31 (d,  $J = 8.3$  Hz, 4H), 7.15 (d,  $J = 8.9$  Hz, 2H), 3.83 (s, 3H), 3.62 (s, 18H), 1.39 (s, 6H).  $^{13}\text{C}\{^1\text{H}\}$  NMR (126 MHz,  $\text{DMSO-d}_6$ )  $\delta$ : 160.0, 153.4, 146.0, 138.8, 135.5, 132.1, 131.5, 131.5, 130.6, 130.4, 128.8, 128.7, 127.6, 126.9, 126.5, 120.9, 114.8, 56.4, 55.3, 13.3, 12.8.  $^{11}\text{B}\{^1\text{H}\}$  NMR (160.4 MHz,  $\text{DMSO-d}_6$ )  $\delta$ : -0.17 (t,  $J = 35.2$  Hz).  $^{19}\text{F}\{^1\text{H}\}$  NMR (471 MHz,  $\text{DMSO-d}_6$ )  $\delta$ : -143.03 (q,  $J = 28.3$  Hz). HRMS (ESI)  $m/z$ :  $[\text{M}/2]^+$  calcd for  $\text{C}_{54}\text{H}_{57}\text{BF}_2\text{N}_4\text{O}^{2+}$ , 413.2292; found, 413.2313.

The synthesis of **TPA-BDP-NMe<sub>3</sub>** was similar procedure of **Ph-BDP-NMe<sub>3</sub>** and the data as follows:

**TPA-BDP-NMe<sub>2</sub>** (75 mg, 0.07 mmol) and methyl iodide (1.65 mL, 0.03 mmol). The pure product was obtained as red solid powder (71 mg, 76 %).  $^1\text{H}$  NMR (500 MHz,  $\text{DMSO-d}_6$ )  $\delta$ : 7.94 (d,  $J = 6.9$  Hz, 4H), 7.80 (d,  $J = 9.3$  Hz, 4H), 7.57 (d,  $J = 9.0$  Hz, 4H), 7.36 (d,  $J = 7.3$  Hz, 6H), 7.24 – 7.08 (m, 16H), 7.04 (d,  $J = 7.2$  Hz, 8H), 3.83 (s, 3H), 3.61 (s, 18H), 2.48 (s, 6H), 1.38 (s, 6H).  $^{13}\text{C}\{^1\text{H}\}$  NMR (126 MHz,  $\text{DMSO-d}_6$ )  $\delta$ : 160.0, 147.0, 146.6, 145.8, 142.6, 134.3, 131.0, 130.6, 129.8, 128.1, 127.3, 126.9, 125.0, 124.7, 123.4, 122.8, 120.8, 114.8, 107.3, 101.6, 56.4, 55.3, 13.3, 12.8.  $^{11}\text{B}\{^1\text{H}\}$  NMR (160.4 MHz,  $\text{DMSO-d}_6$ )  $\delta$ : -0.19 (t,  $J = 33.7$  Hz).  $^{19}\text{F}\{^1\text{H}\}$  NMR (471 MHz,  $\text{DMSO-d}_6$ )  $\delta$ : -143.16 (q,  $J = 33.0$  Hz). HRMS (ESI)  $m/z$ :  $[\text{M}/2]^+$  calcd for  $\text{C}_{78}\text{H}_{75}\text{BF}_2\text{N}_6\text{O}^{2+}$ , 580.3026; found, 580.3057.

### 3. NMR and HRMS spectra of precursors and target molecules

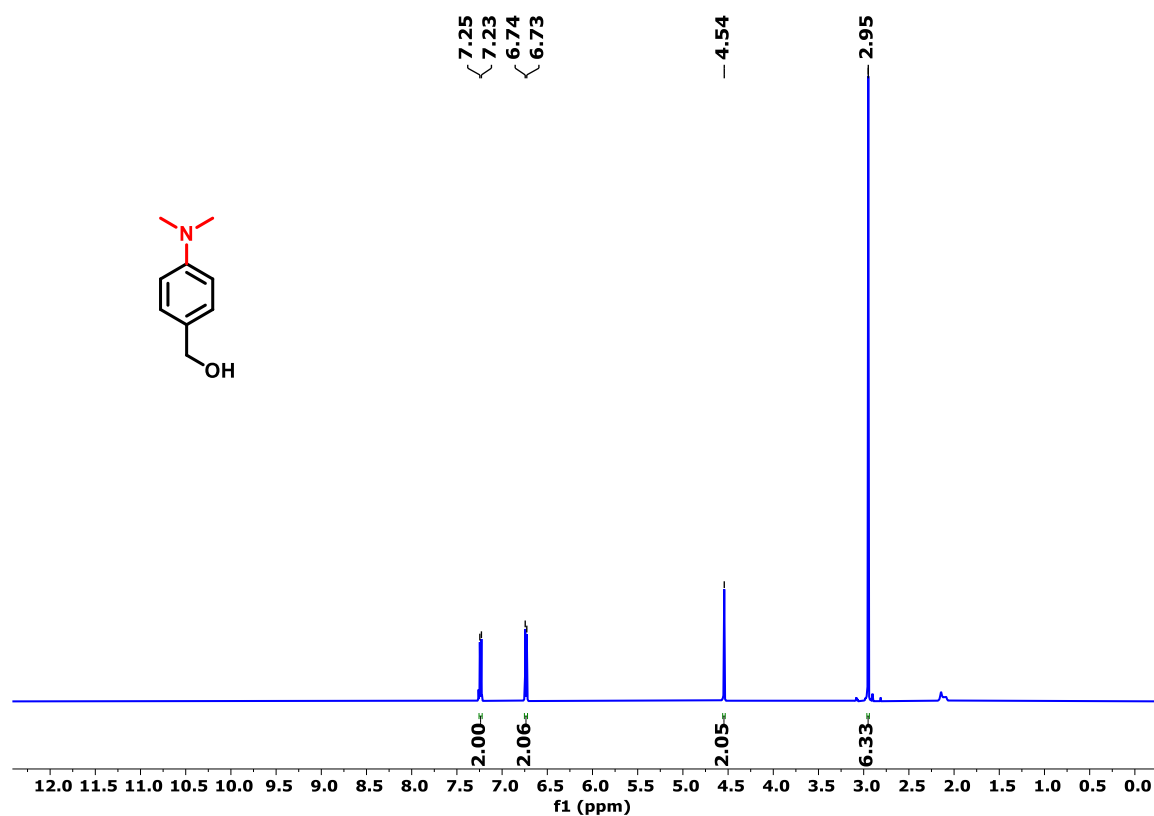


Figure S1. <sup>1</sup>H NMR spectrum (500 MHz, RT) of compound **1** in CDCl<sub>3</sub>.

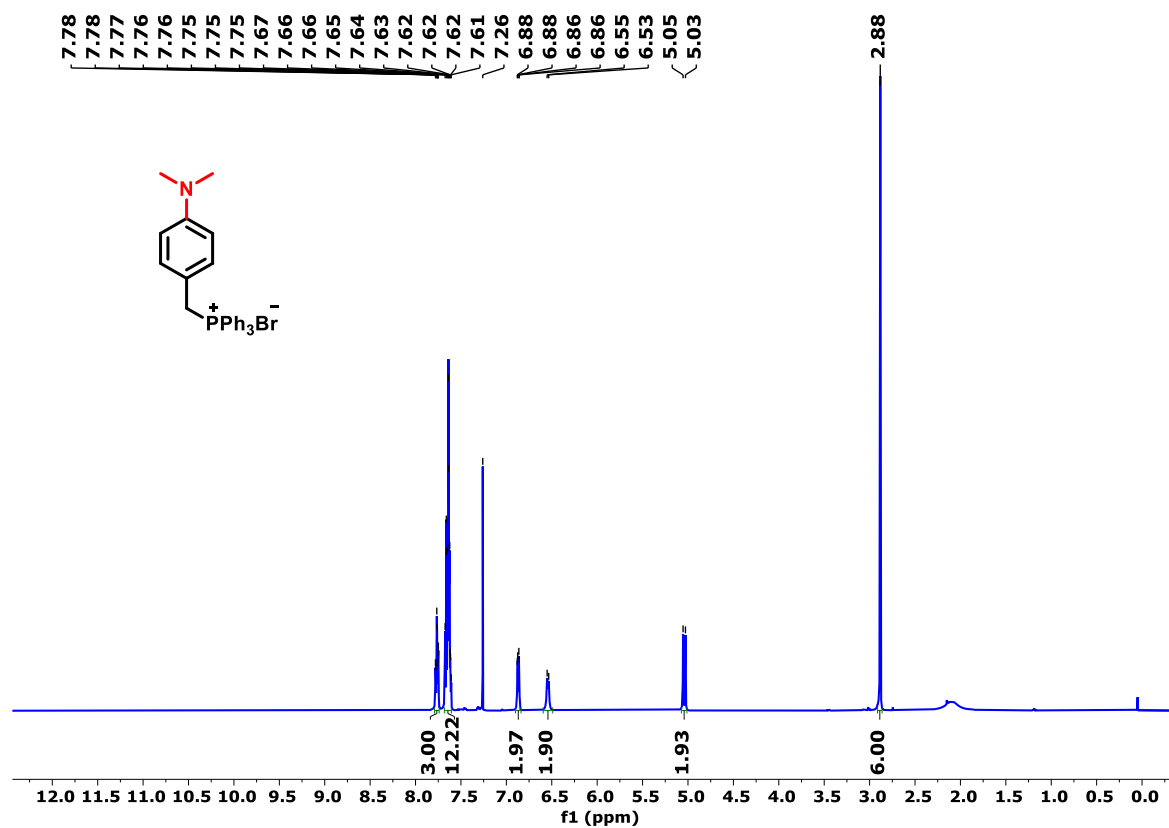


Figure S2. <sup>1</sup>H NMR spectrum (500 MHz, RT) of compound **2** in CDCl<sub>3</sub>.

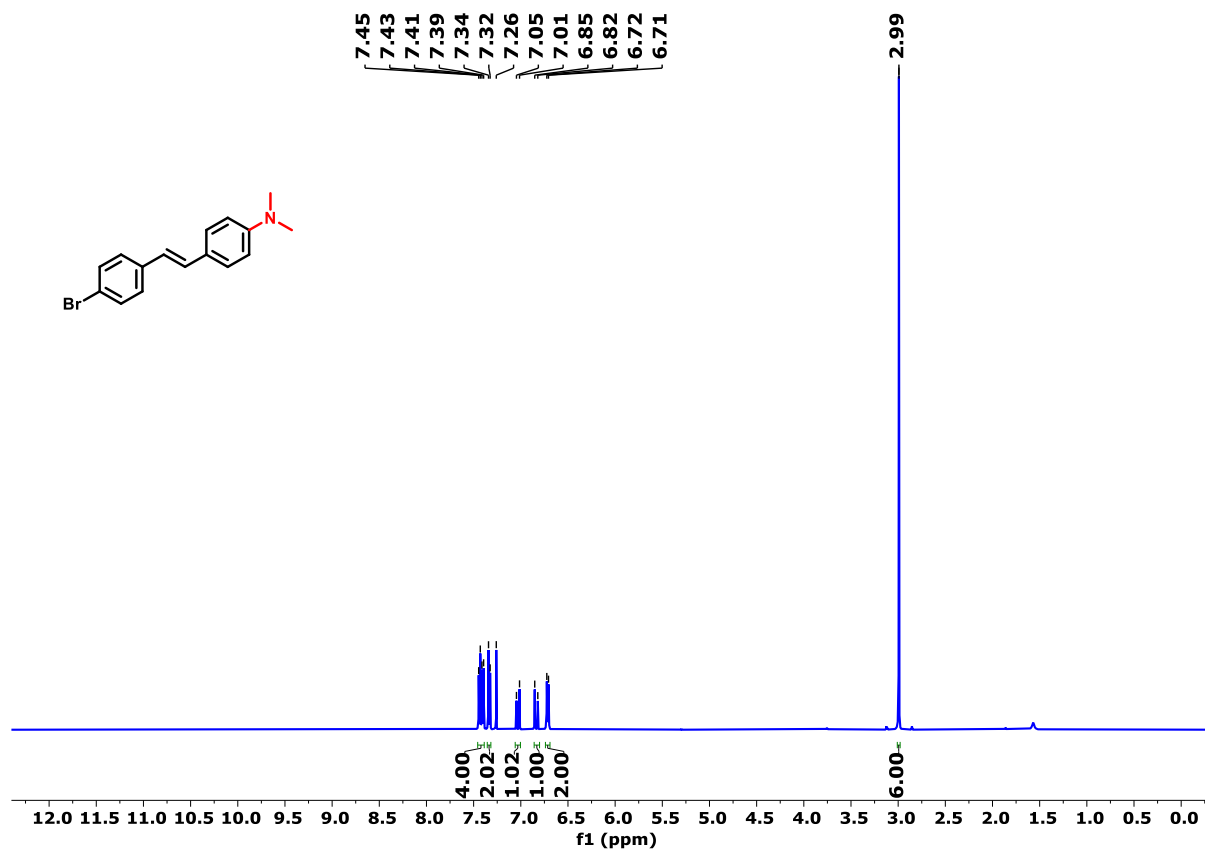


Figure S3. <sup>1</sup>H NMR spectrum (500 MHz, RT) of compound 3 in CDCl<sub>3</sub>.

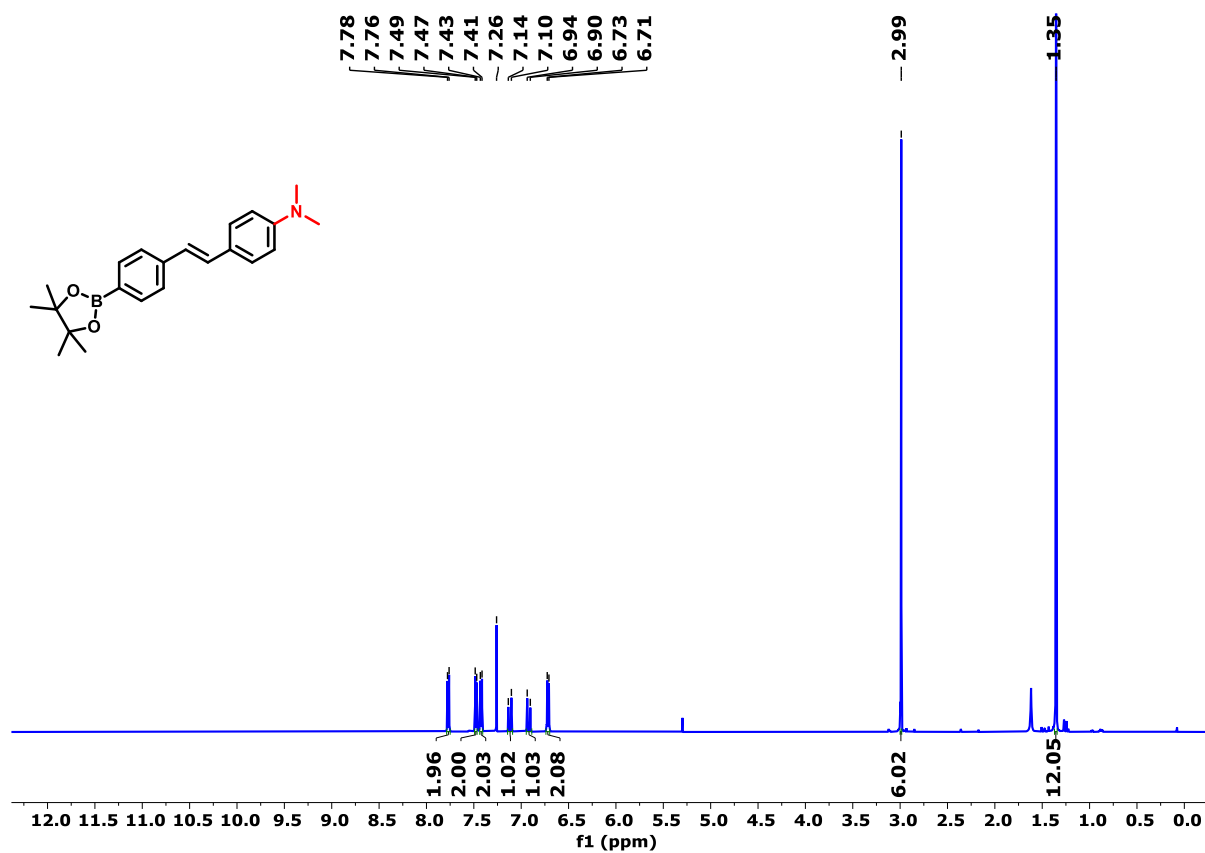


Figure S4. <sup>1</sup>H NMR spectrum (500 MHz, RT) of compound 4 in CDCl<sub>3</sub>.

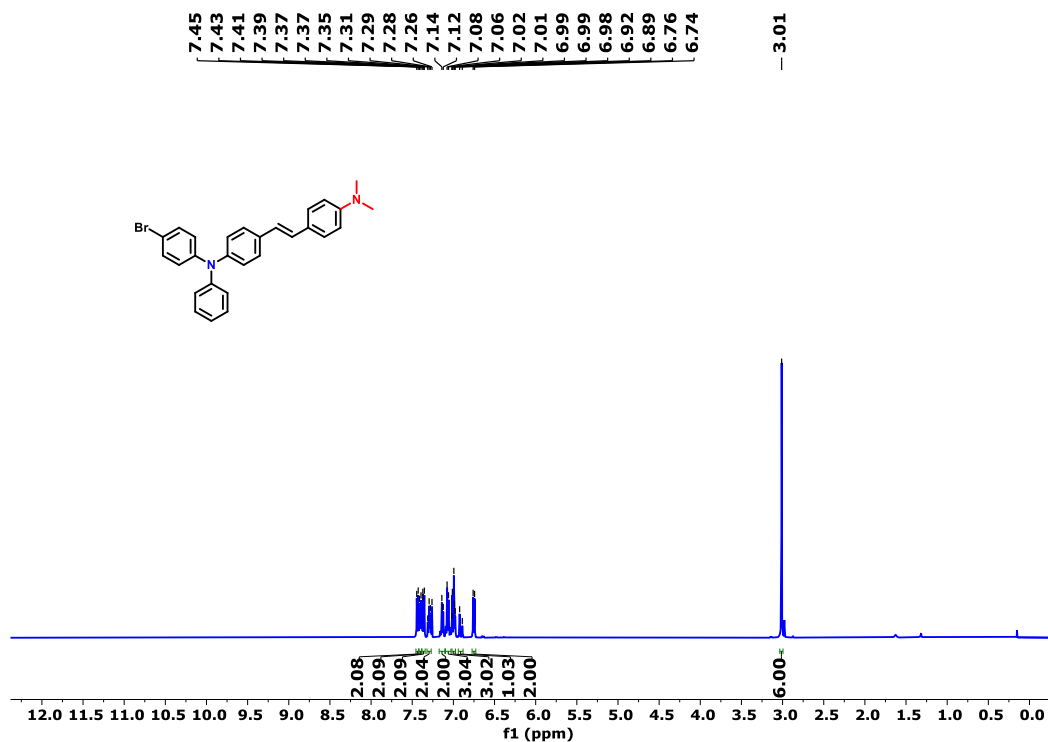


Figure S5.  $^1\text{H}$  NMR spectrum (500 MHz, RT) of compound **6** in  $\text{CDCl}_3$ .

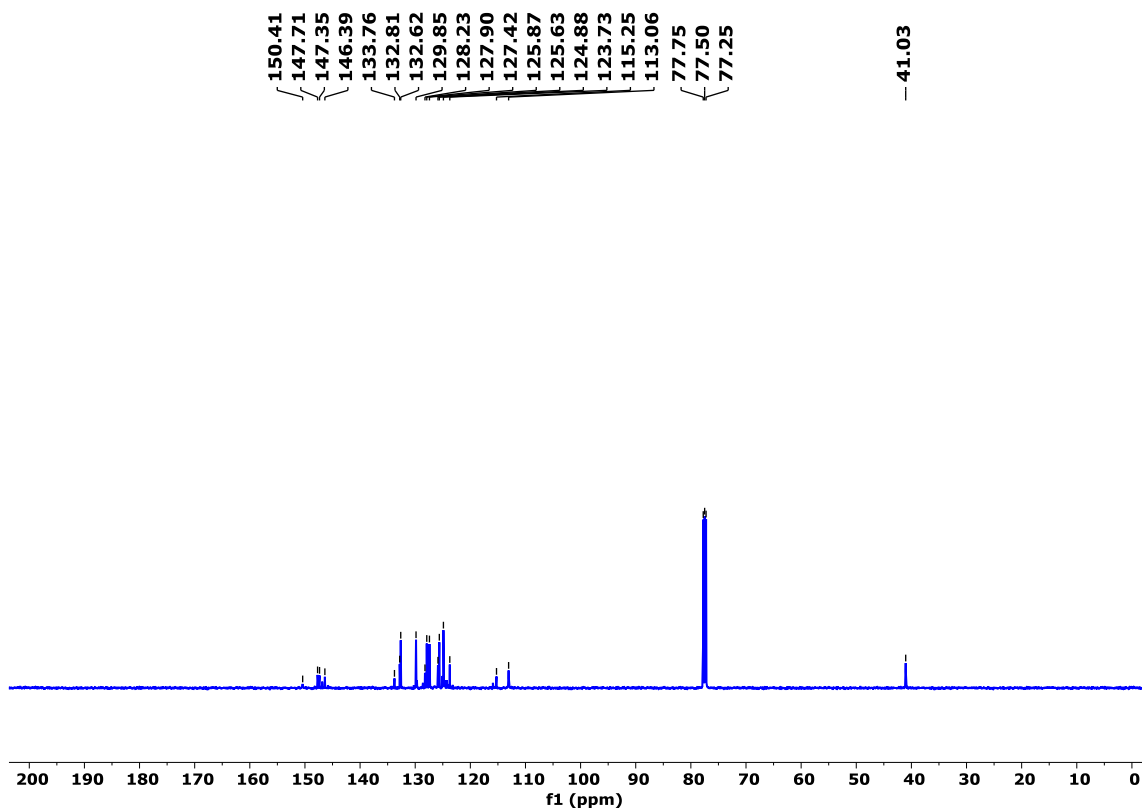


Figure S6.  $^{13}\text{C}\{^1\text{H}\}$  NMR spectrum (126 MHz, RT) of compound **6** in  $\text{CDCl}_3$ .

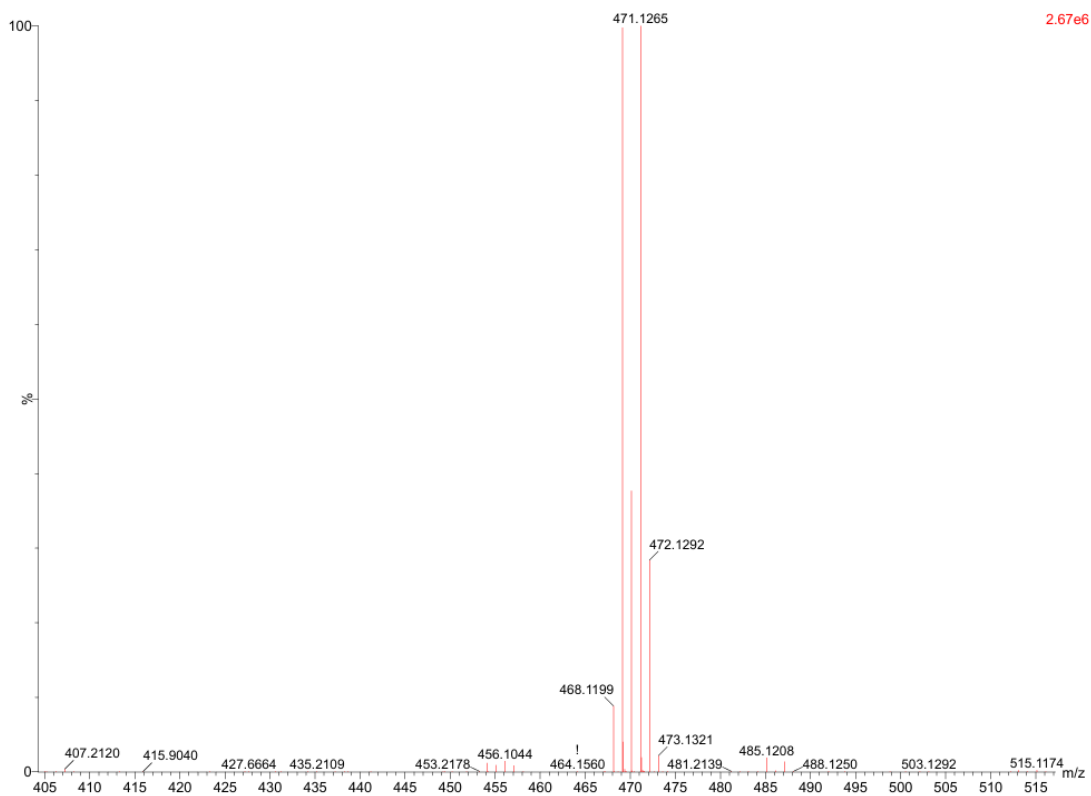


Figure S7. HRMS spectrum of compound 6.

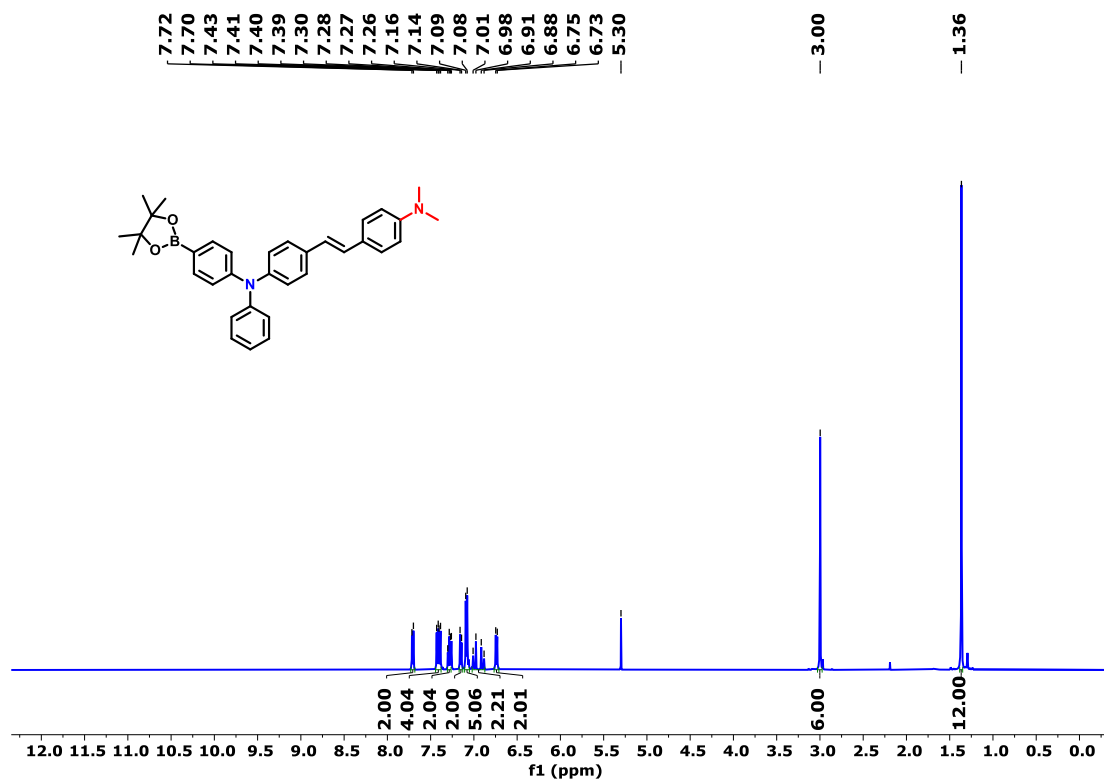


Figure S8. <sup>1</sup>H NMR spectrum (500 MHz, RT) of compound 7 in CDCl<sub>3</sub>.

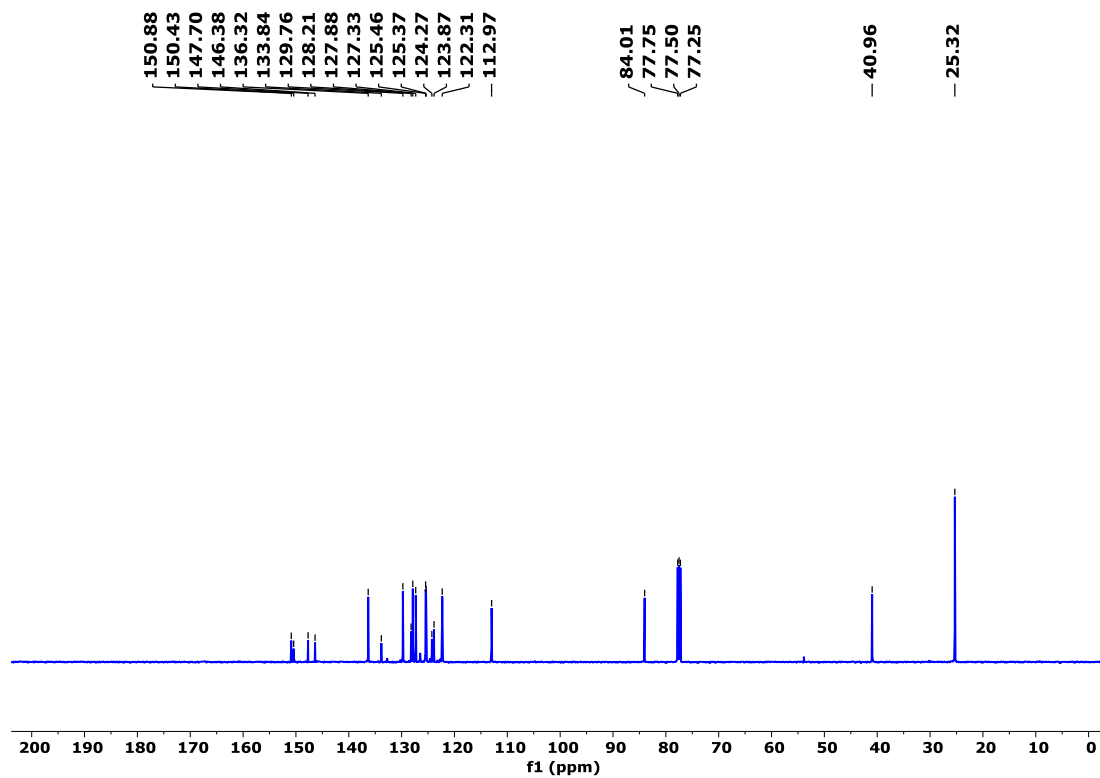


Figure S9.  $^{13}\text{C}\{^1\text{H}\}$  NMR spectrum (126 MHz, RT) of compound **7** in  $\text{CDCl}_3$ .

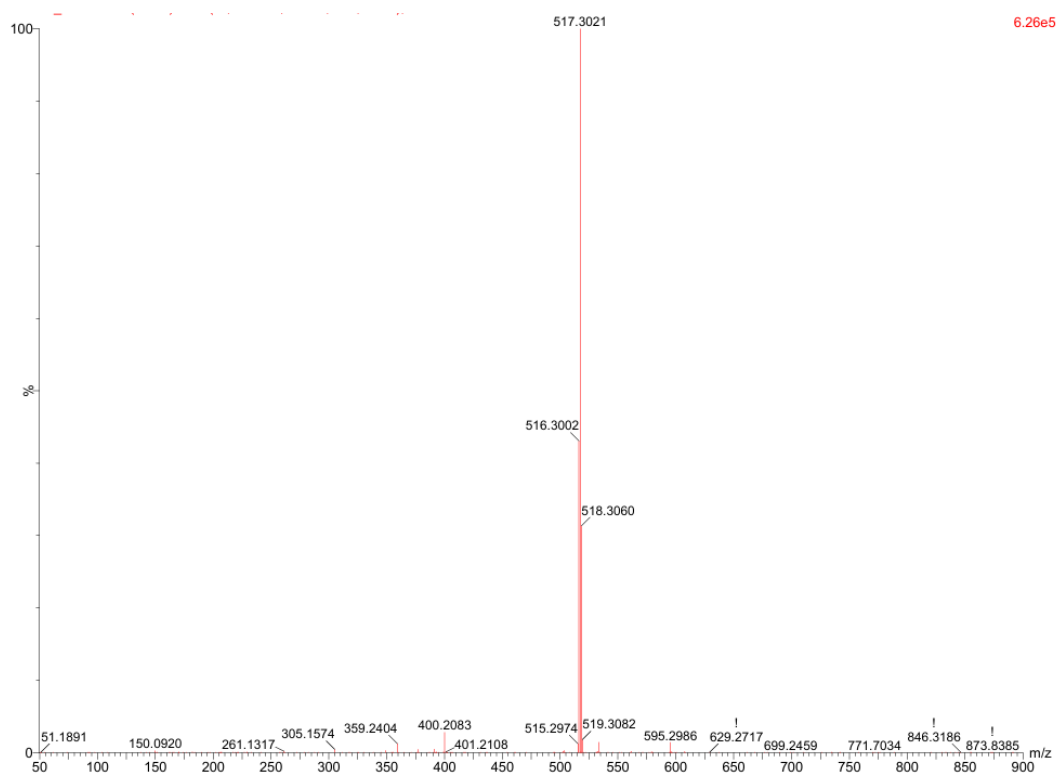


Figure S10. HRMS spectrum of compound **7**.

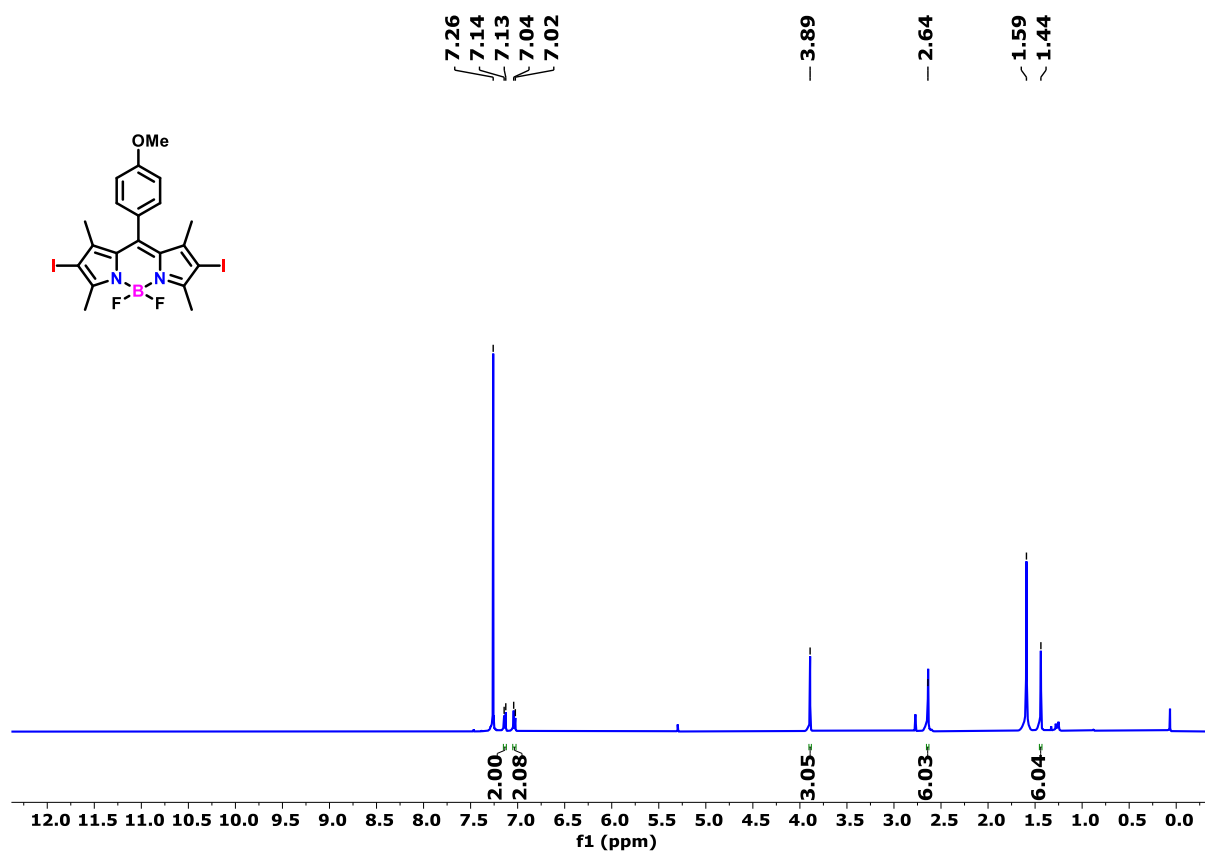


Figure S11. <sup>1</sup>H NMR spectrum (500 MHz, RT) of compound **8** in CDCl<sub>3</sub>.

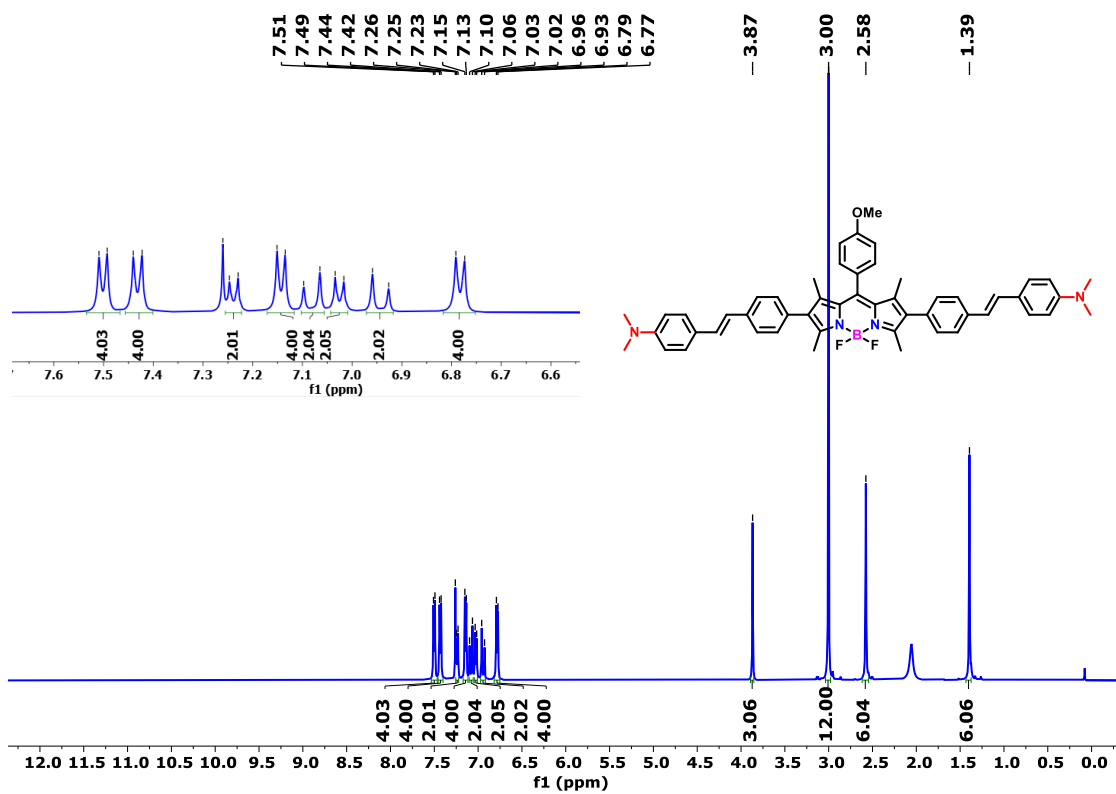


Figure S12. <sup>1</sup>H NMR spectrum (500 MHz, RT) of Ph-BDP-NMe<sub>2</sub> in CDCl<sub>3</sub>.

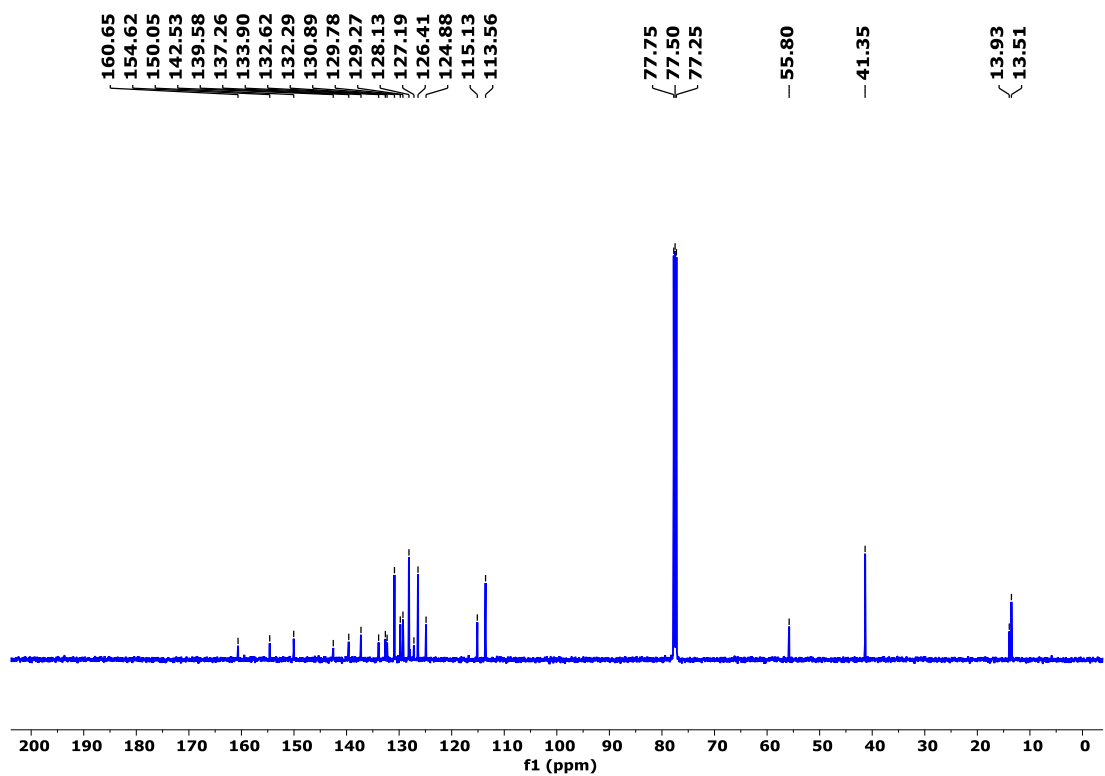


Figure S13.  $^{13}\text{C}\{^1\text{H}\}$  NMR spectrum (126 MHz, RT) of **Ph-BDP-NMe<sub>2</sub>** in  $\text{CDCl}_3$ .

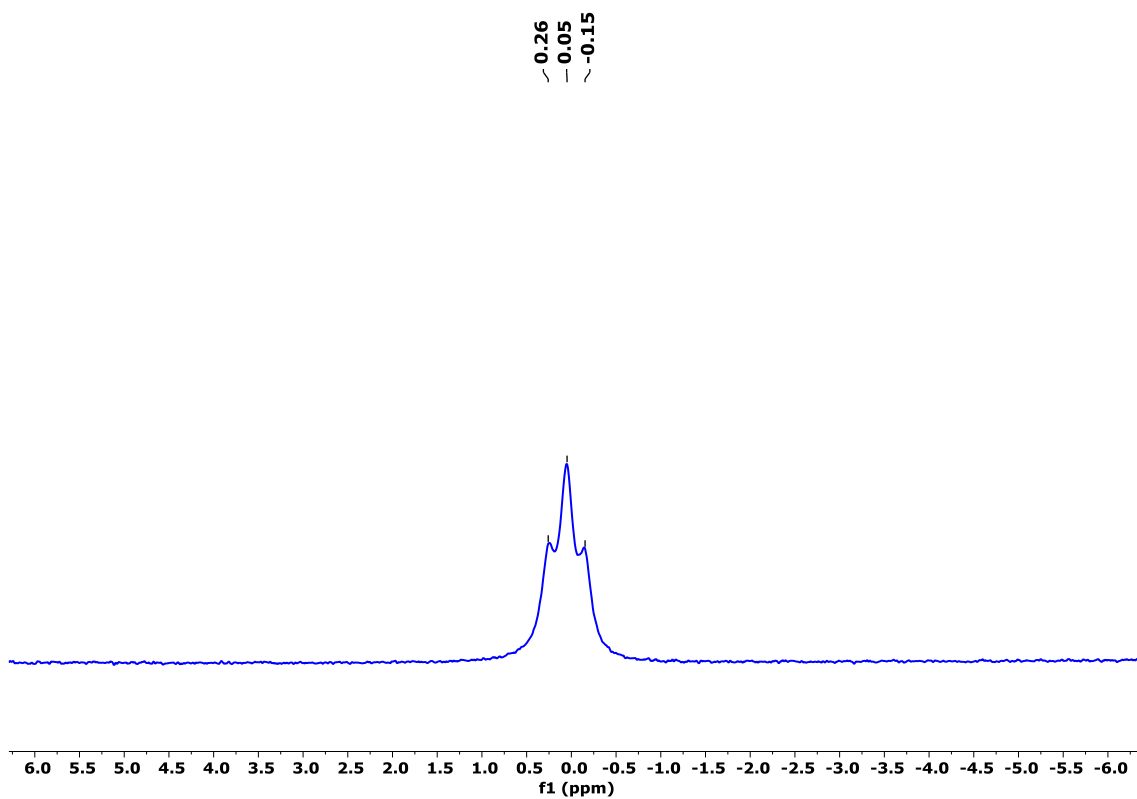
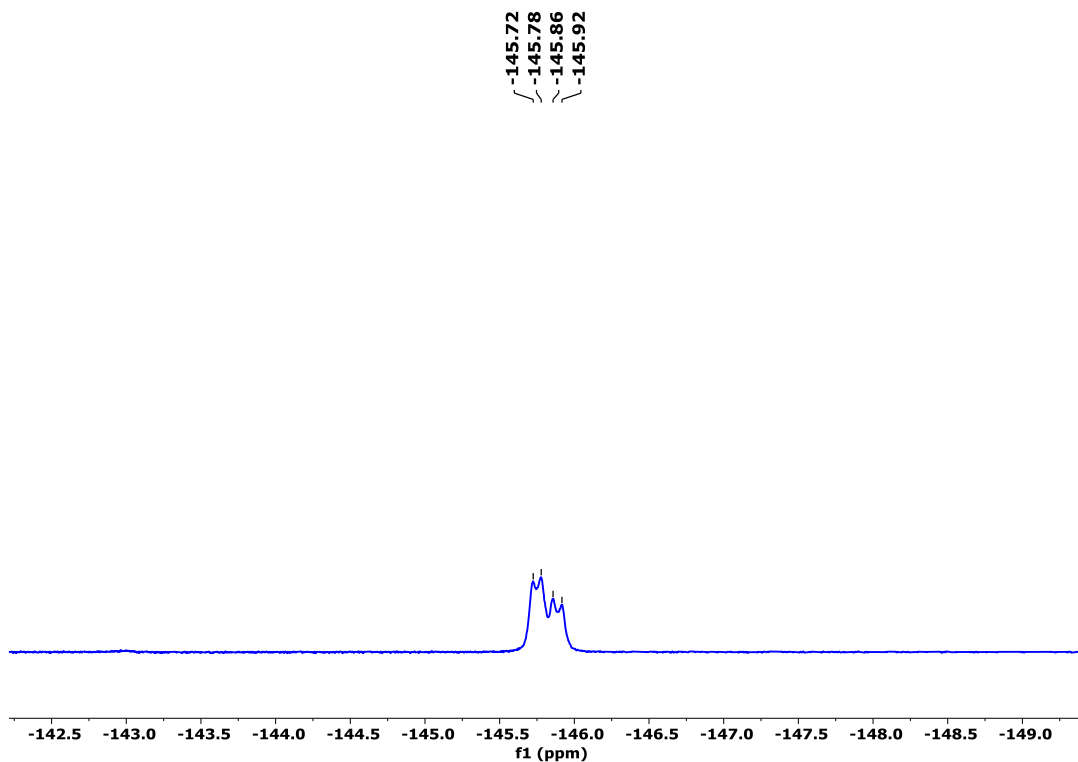
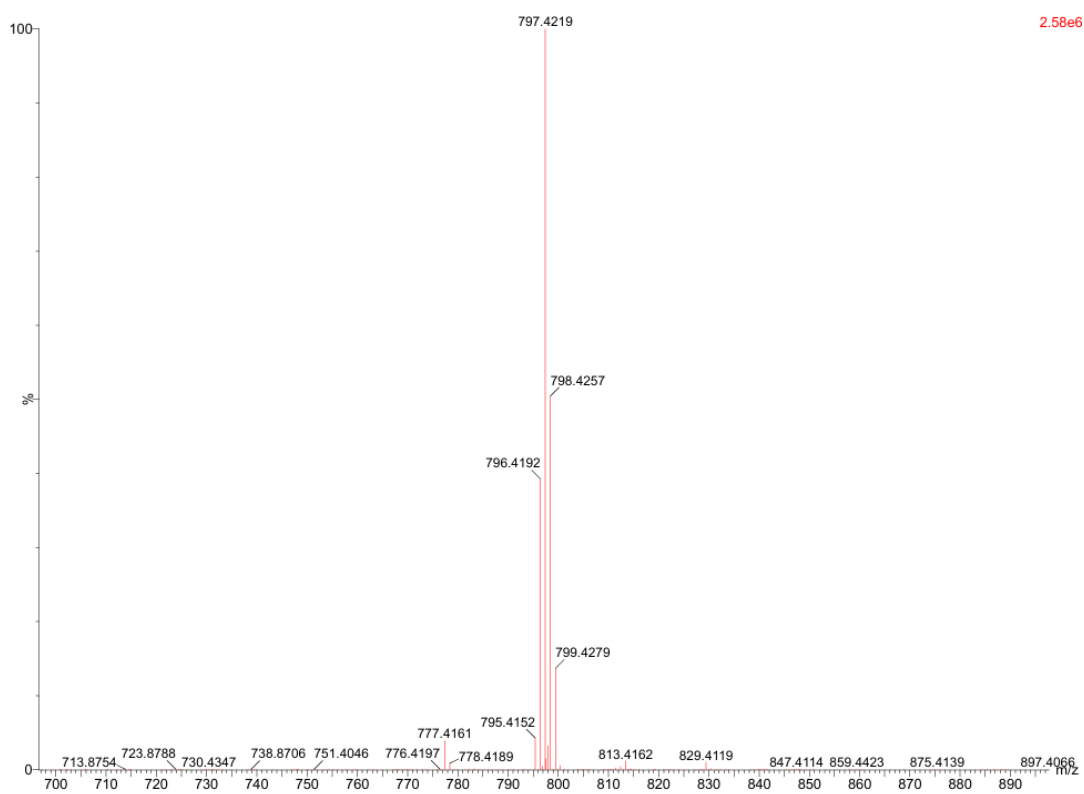


Figure S14.  $^{11}\text{B}\{^1\text{H}\}$  NMR spectrum (160.4 MHz, RT) of **Ph-BDP-NMe<sub>2</sub>** in  $\text{CDCl}_3$ .



**Figure S15.**  $^{19}\text{F}\{^1\text{H}\}$  NMR spectrum (471 MHz, RT) of **Ph-BDP-NMe<sub>2</sub>** in  $\text{CDCl}_3$ .



**Figure S16.** HRMS spectrum of compound **Ph-BDP-NMe<sub>2</sub>**.

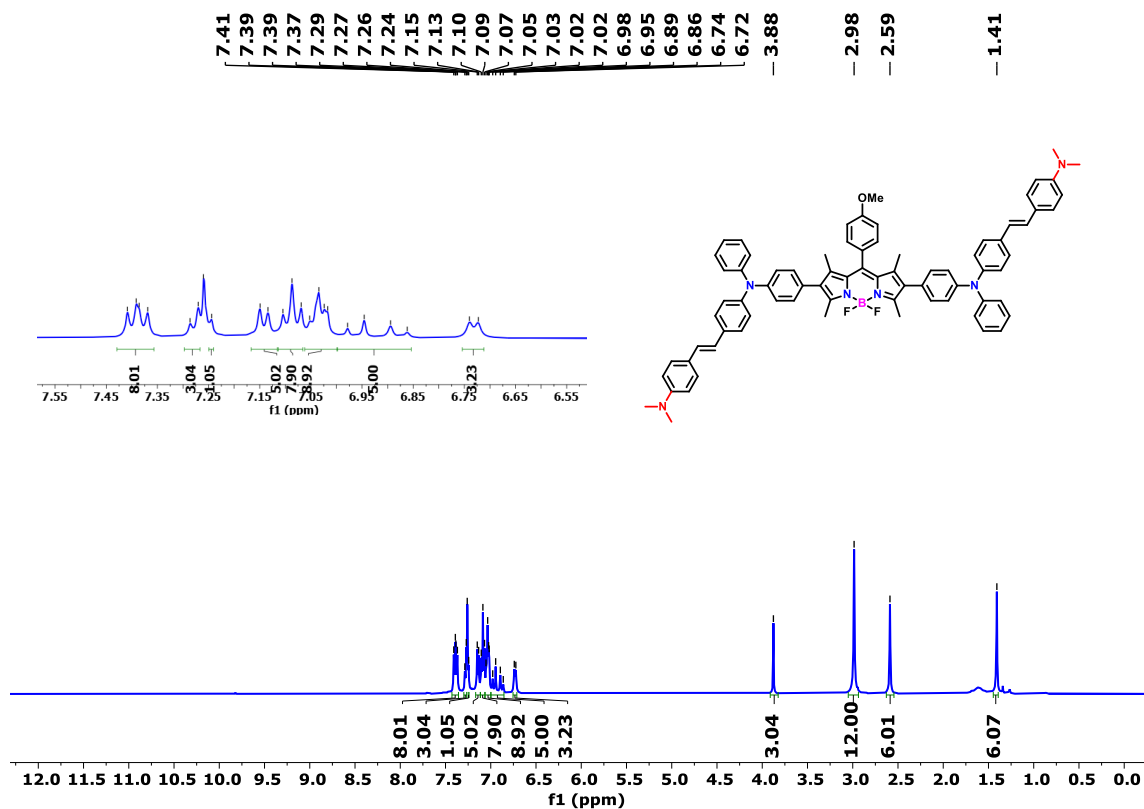


Figure S17. <sup>1</sup>H NMR spectrum (500 MHz, RT) of TPA-BDP-NMe<sub>2</sub> in CDCl<sub>3</sub>.

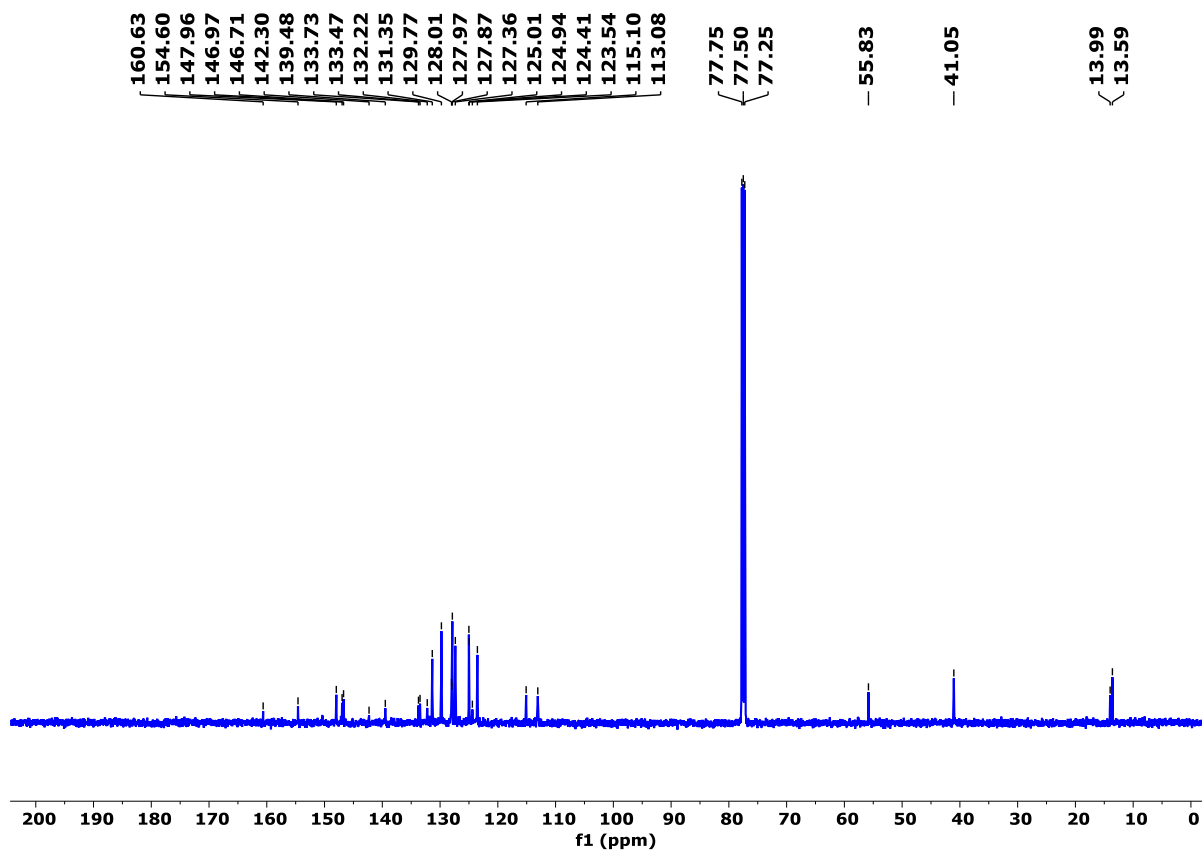


Figure S18. <sup>13</sup>C{<sup>1</sup>H} NMR spectrum (126 MHz, RT) of TPA-BDP-NMe<sub>2</sub> in CDCl<sub>3</sub>.

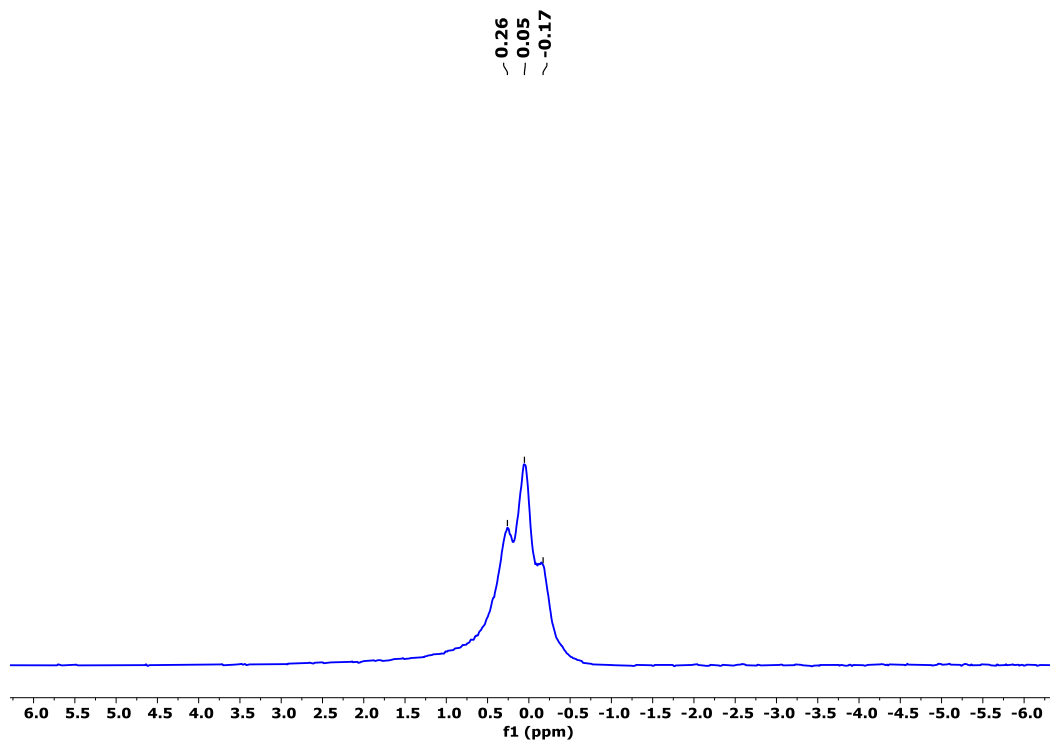


Figure S19.  $^{11}\text{B}\{^1\text{H}\}$  NMR spectrum (160.4 MHz, RT) of TPA-BDP-NMe<sub>2</sub> in CDCl<sub>3</sub>.

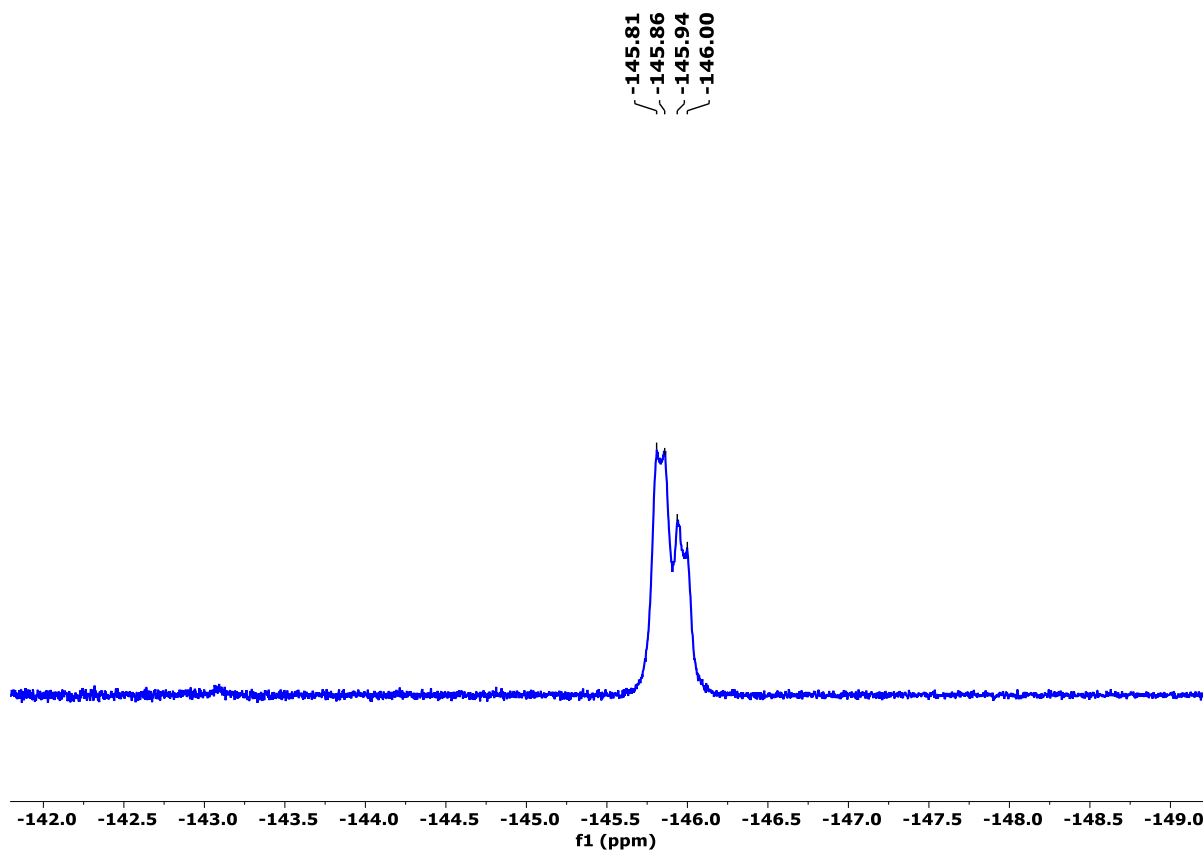


Figure S20.  $^{19}\text{F}\{^1\text{H}\}$  NMR spectrum (471 MHz, RT) of TPA-BDP-NMe<sub>2</sub> in CDCl<sub>3</sub>.

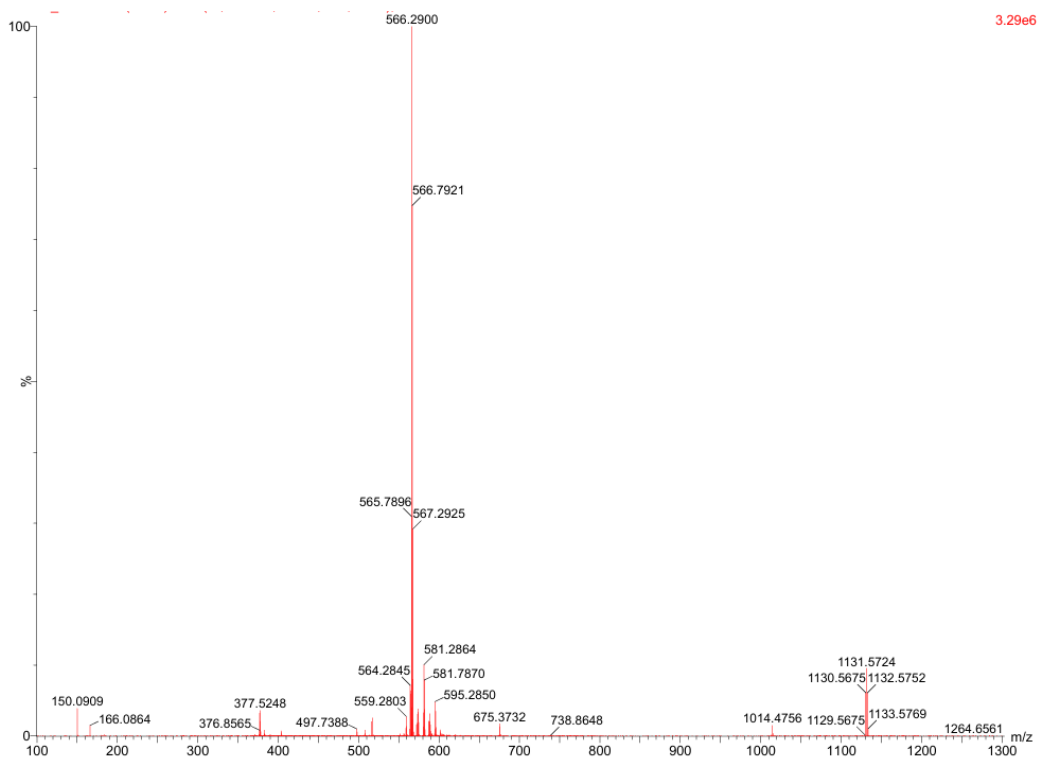


Figure S21. HRMS spectrum of TPA-BDP-NMe<sub>2</sub>.

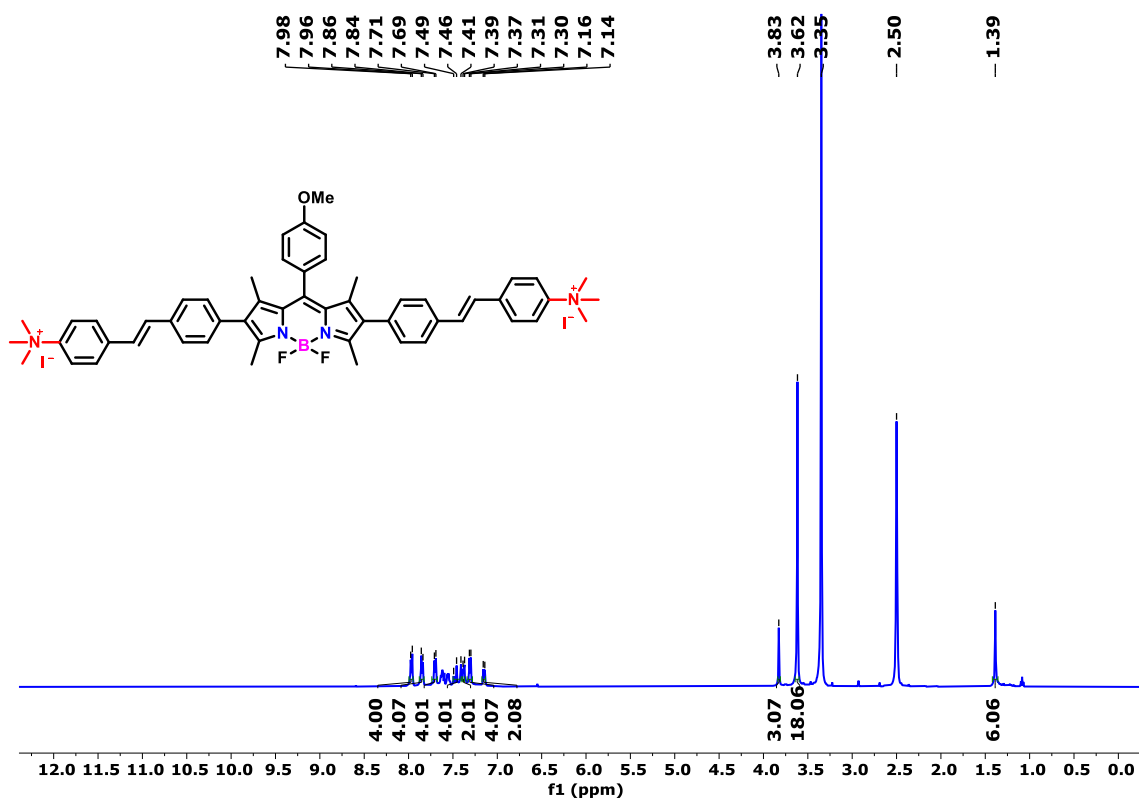


Figure S22. <sup>1</sup>H NMR spectrum (500 MHz, RT) of Ph-BDP-NMe<sub>3</sub> in DMSO-d<sub>6</sub>.

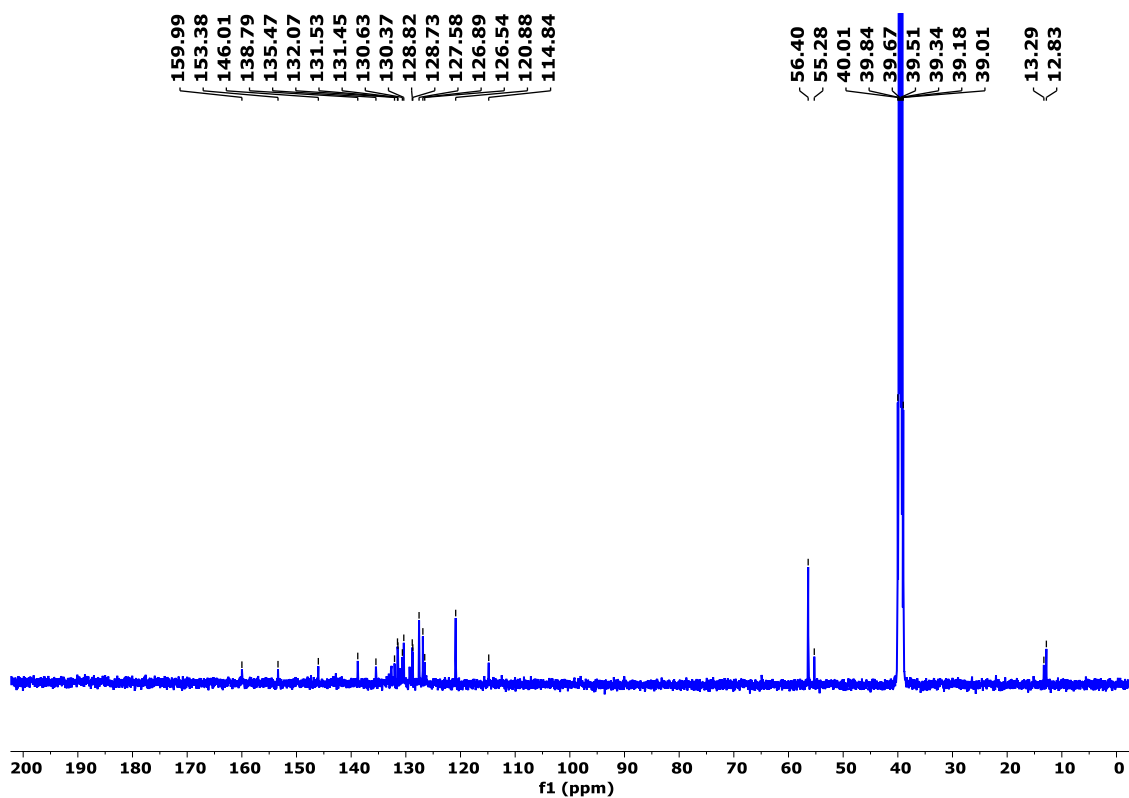


Figure S23.  $^{13}\text{C}\{^1\text{H}\}$  NMR spectrum (126 MHz, RT) of **Ph-BDP-NMe<sub>3</sub>** in DMSO- $\text{d}_6$ .

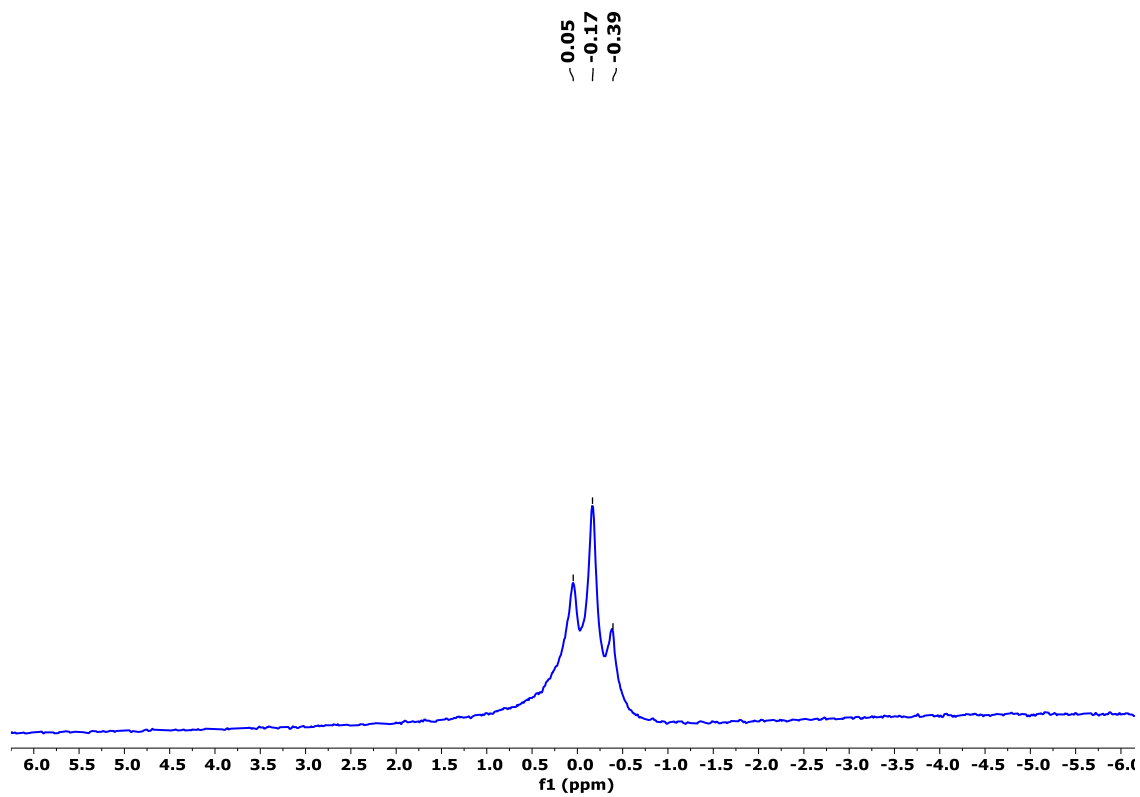
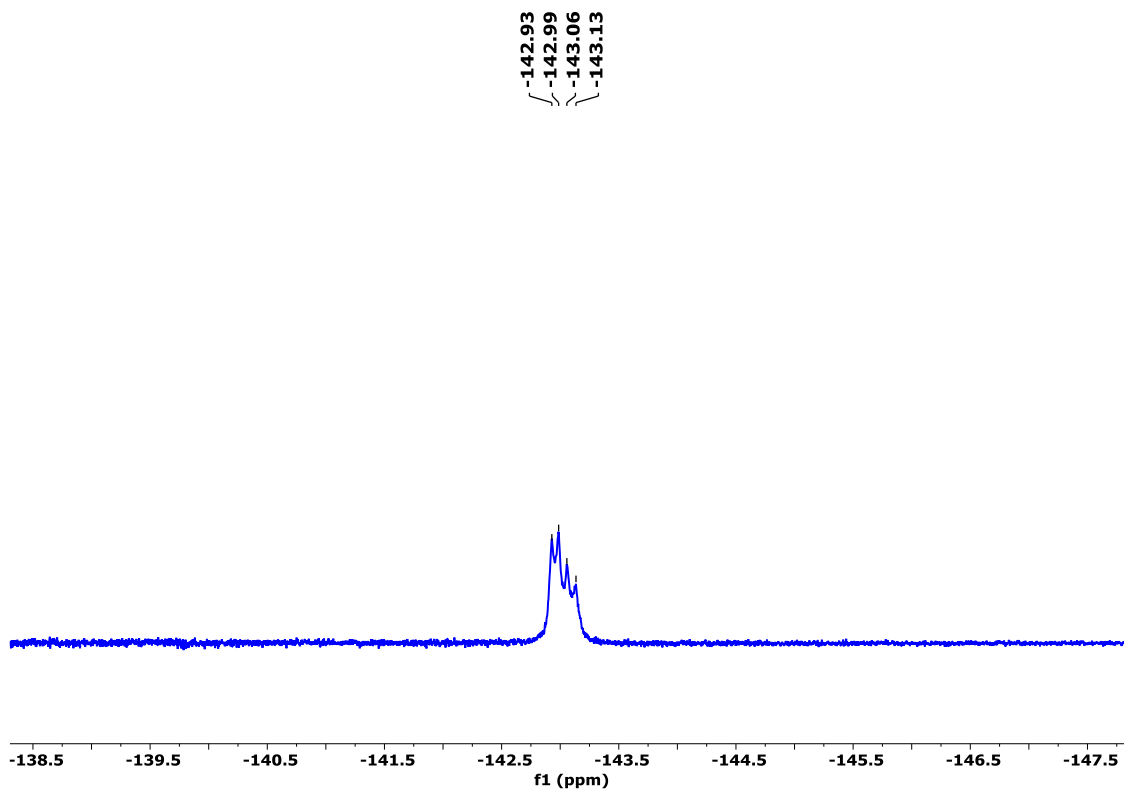
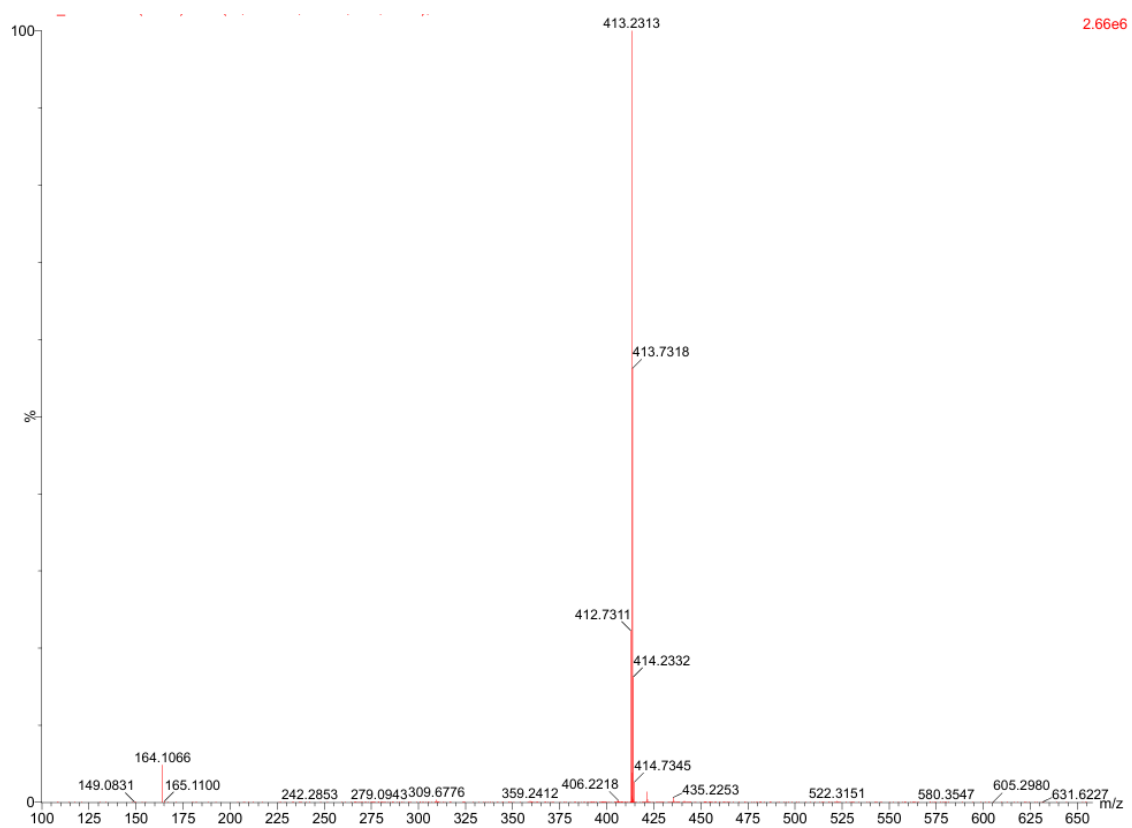


Figure S24.  $^{11}\text{B}\{^1\text{H}\}$  NMR spectrum (160.4 MHz, RT) of **Ph-BDP-NMe<sub>3</sub>** in DMSO- $\text{d}_6$ .



**Figure S25.**  $^{19}\text{F}\{^1\text{H}\}$  NMR spectrum (471 MHz, RT) of **Ph-BDP-NMe<sub>3</sub>** in DMSO- $\text{d}_6$ .



**Figure S26.** HRMS spectrum of **Ph-BDP-NMe<sub>3</sub>**.

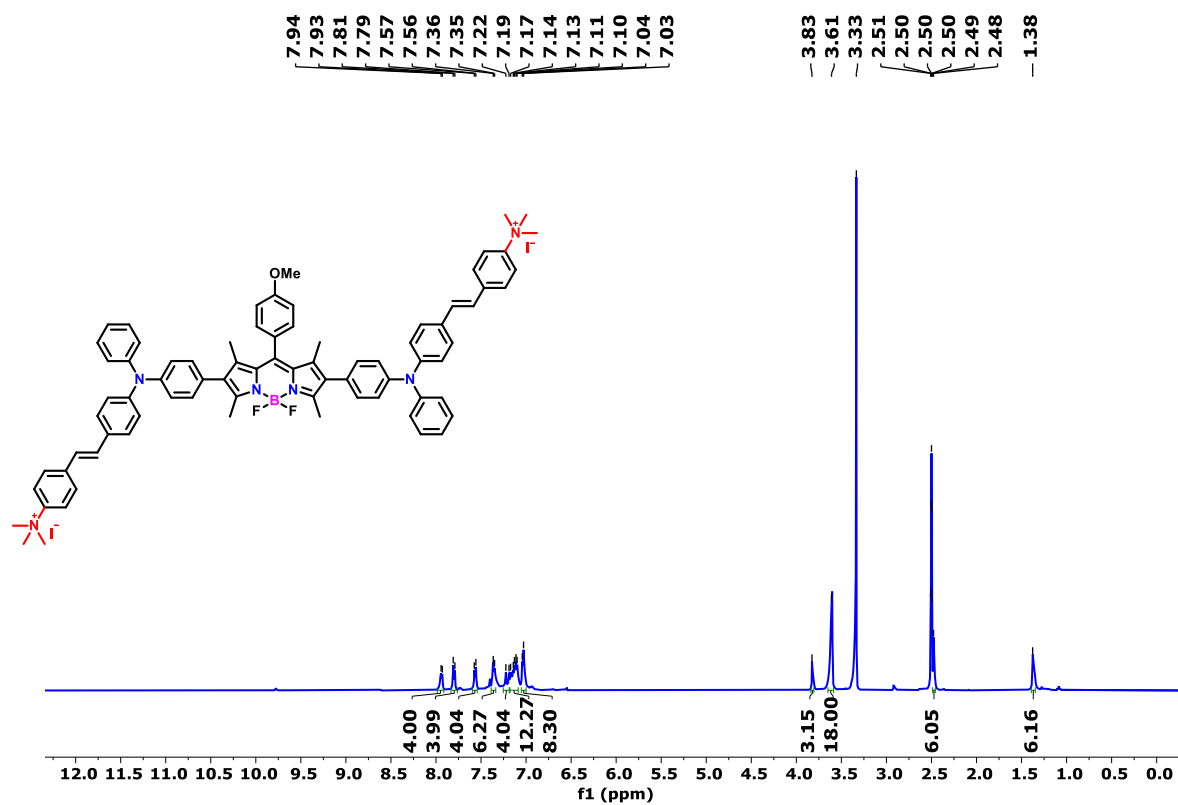


Figure S27. <sup>1</sup>H NMR spectrum (500 MHz, RT) of TPA-BDP-NMe<sub>3</sub> in DMSO-d<sub>6</sub>.

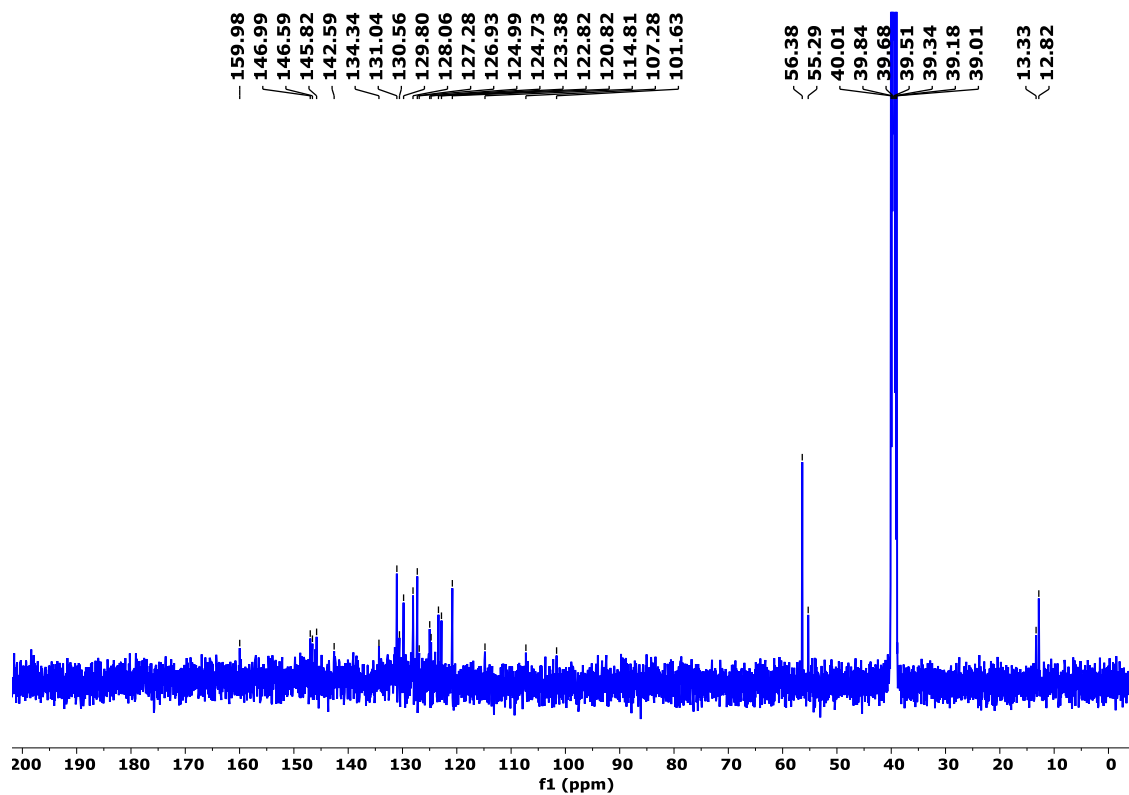
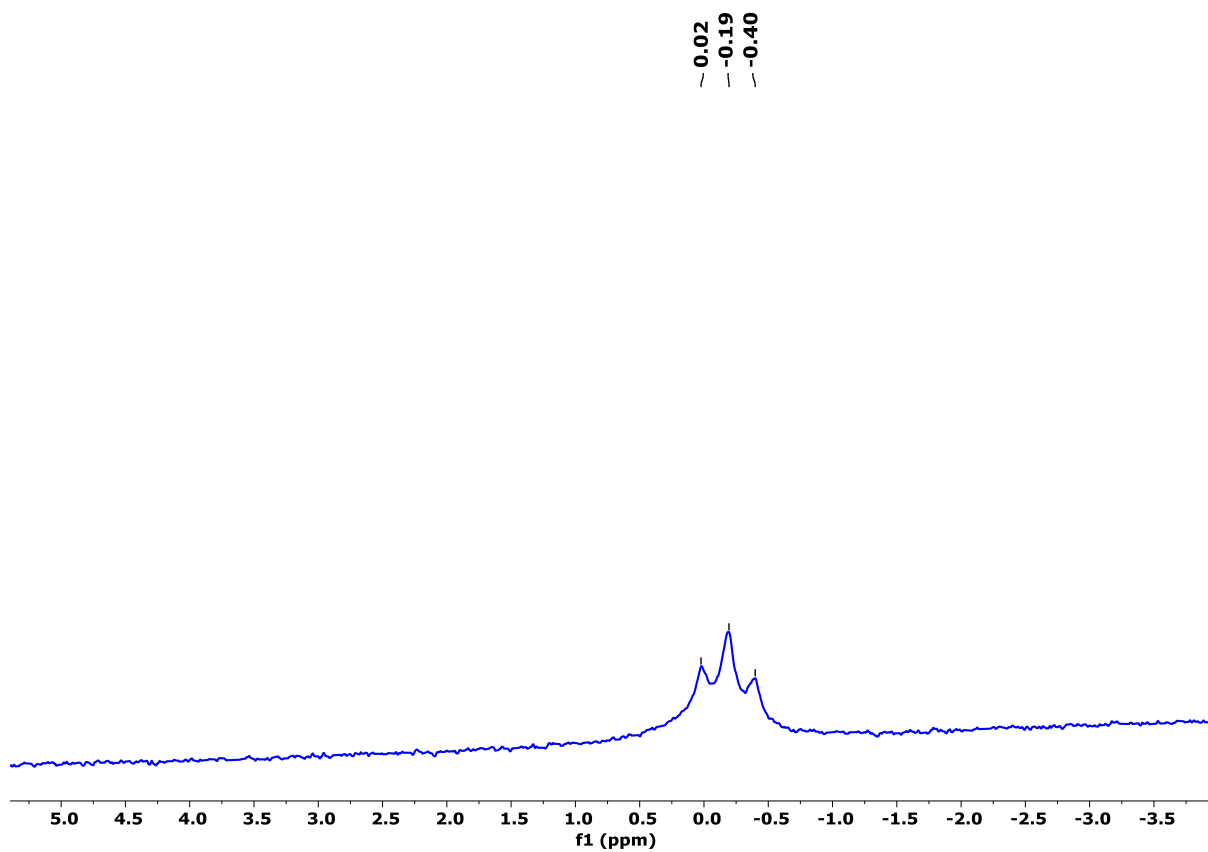
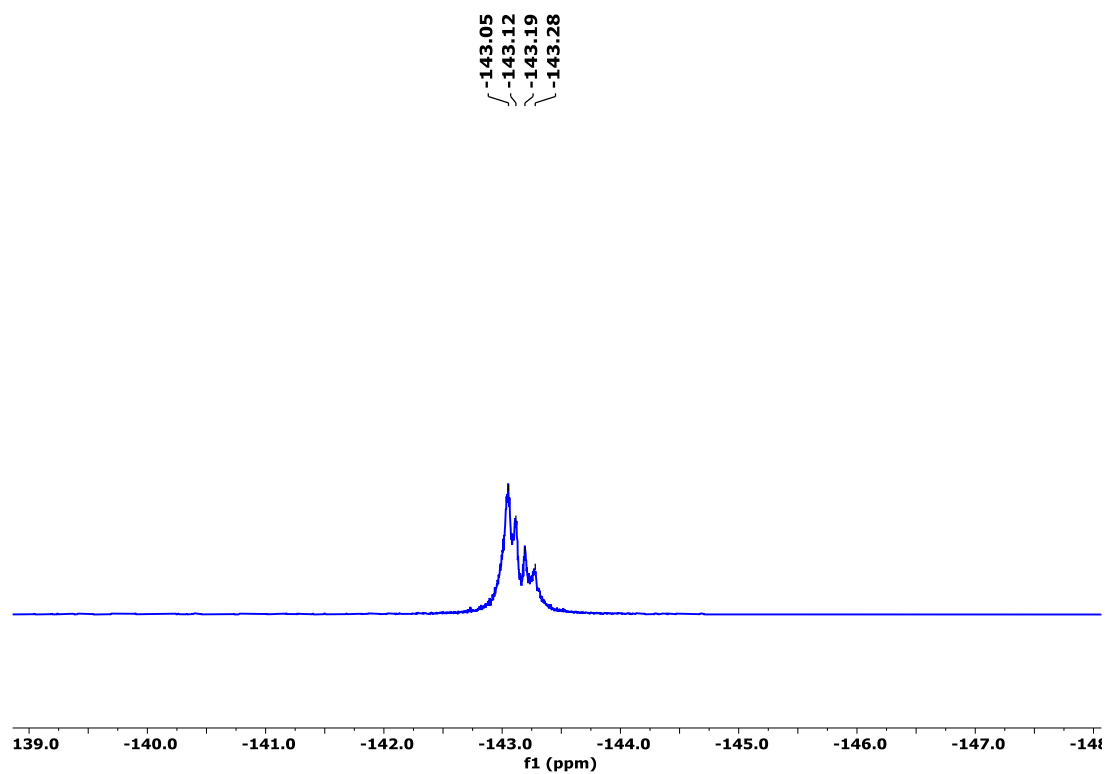


Figure S28. <sup>13</sup>C{<sup>1</sup>H} NMR spectrum (126 MHz, RT) of TPA-BDP-NMe<sub>3</sub> in DMSO-d<sub>6</sub>.



**Figure S29.**  $^{11}\text{B}\{^1\text{H}\}$  NMR spectrum (160.4 MHz, RT) of **TPA-BDP-NMe<sub>3</sub>** in DMSO-d<sub>6</sub>.



**Figure S30.**  $^{19}\text{F}\{^1\text{H}\}$  NMR spectrum (471 MHz, RT) of **TPA-BDP-NMe<sub>3</sub>** in DMSO-d<sub>6</sub>.

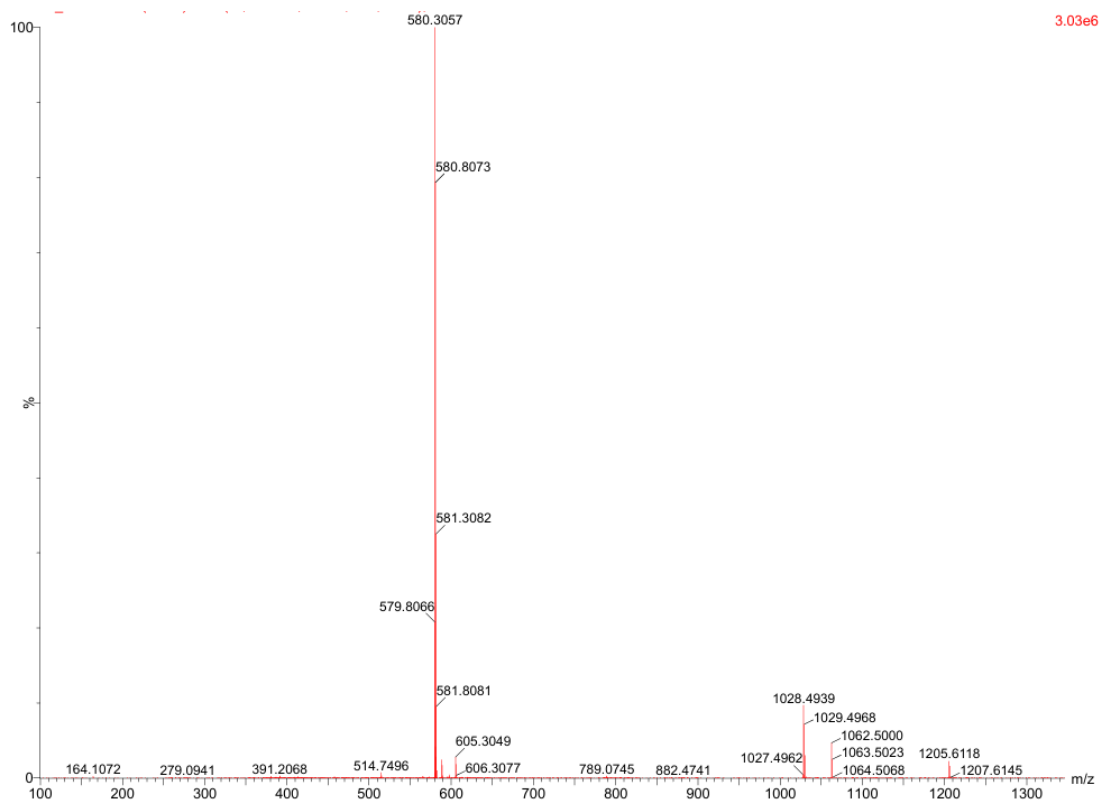


Figure S31. HRMS spectrum of TPA-BDP-NMe<sub>3</sub>.

#### 4. Photophysical studies of the target molecules

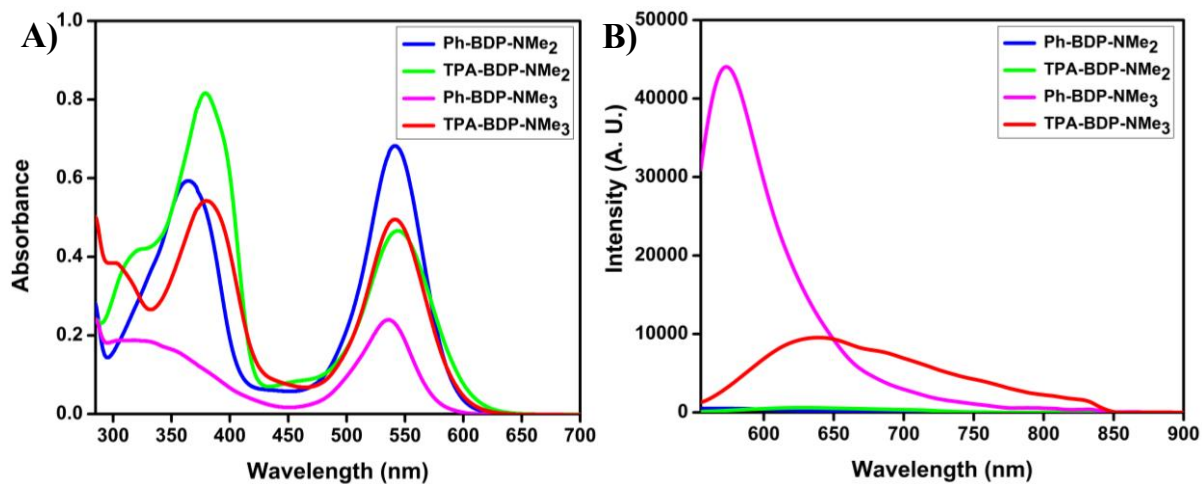
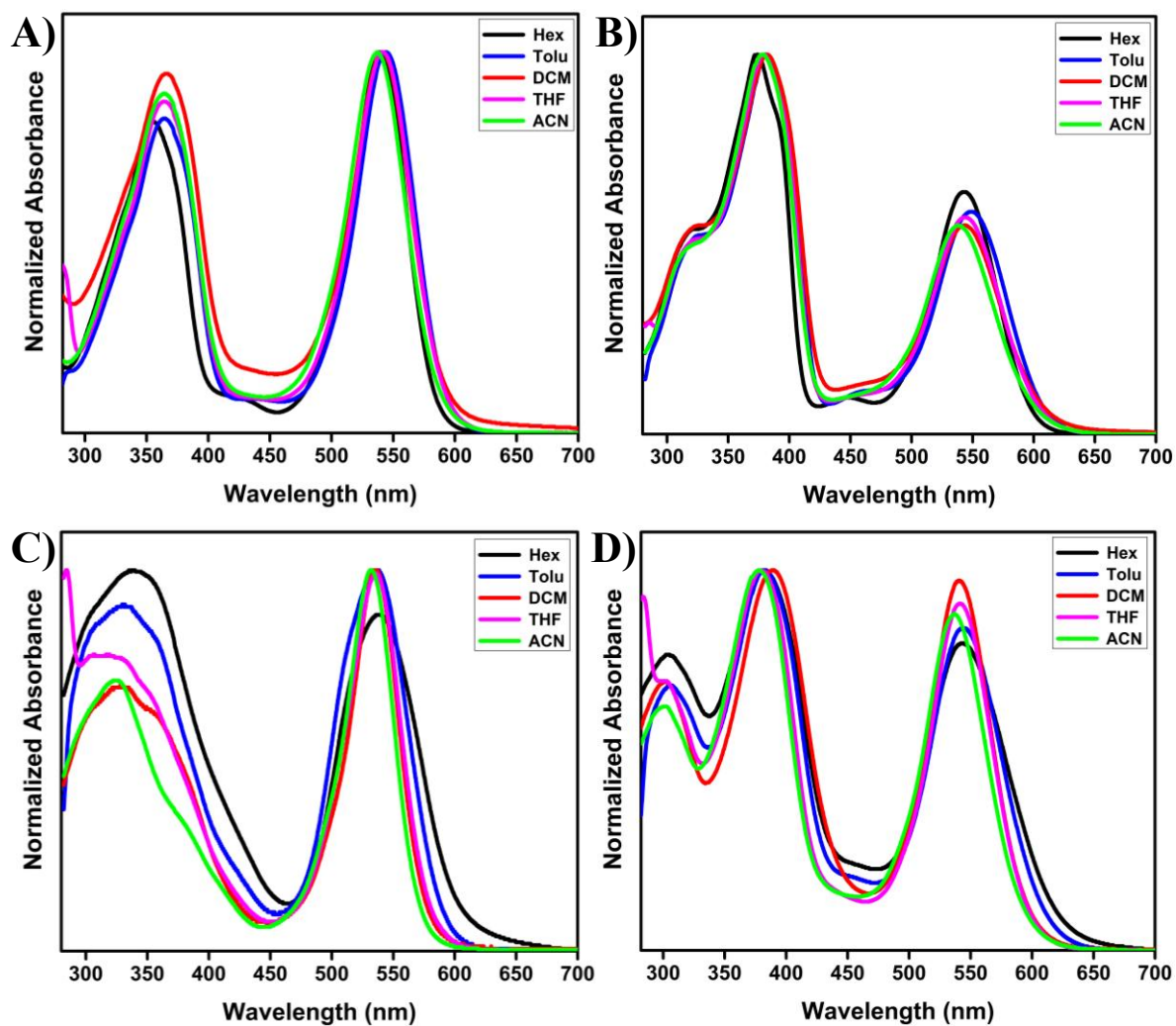


Figure S32. A) UV-Vis absorption (10  $\mu$ M) and B) emission spectra of target molecules (10  $\mu$ M,  $\lambda_{ex}$  = 540 nm) in THF.

**Table S1:** Photophysical characteristics of target molecules in solvents of different polarity.

<b>Compounds</b>	<b>Solvents</b>	$\lambda_{\text{max}}^{\text{[a]}}$ (nm)	$\lambda_{\text{max}}^{\text{[b]}}$ (nm)	$\Phi_{\text{F}}^{\text{[c]}}$	$\Delta\nu^{\text{[d]}}$ ( $\text{cm}^{-1}$ )
<b>Ph-BDP-NMe<sub>2</sub></b>	Hex	539	598	0.21	1830
	Toluene	544	616	0.17	2149
	DCM	541	559	0.05	595
	THF	541	570	0.03	940
	ACN	537	570	0.01	1078
<b>TPA-BDP-NMe<sub>2</sub></b>	Hex	544	619	0.27	2227
	Toluene	549	643	0.22	2663
	DCM	544	642	0.07	2806
	THF	544	637	0.02	2684
	ACN	538	581	0.01	1376
<b>Ph-BDP-NMe<sub>3</sub></b>	Hex	538	595	0.10	1781
	Toluene	537	605	0.11	2093
	DCM	536	577	0.22	1326
	THF	536	573	0.15	1205
	ACN	533	574	0.13	1340
<b>TPA-BDP-NMe<sub>3</sub></b>	Hex	543	597	0.35	1666
	Toluene	545	619	0.37	2194
	DCM	542	642	0.18	2874
	THF	542	640	0.21	2825
	ACN	538	-	0.02	-

[a] peak position of the absorption band maximum in nm. [b] peak position of the emission band maximum in nm. [c] Quantum yields were determined using Rhodamine B in ethanol as a standard ( $\Phi_{\text{F}} = 0.49$  in ethanol) and using the following formula  $\phi = \phi_{\text{F}} \times I/I_{\text{R}} \times A_{\text{R}}/A \times \eta^2 / \eta_{\text{R}}^2$  where  $\phi$  = quantum yield,  $I$  = integral area of emission peak,  $A$  = absorbance at  $\lambda_{\text{ex}}$ ,  $\eta$  = refractive index of solvent. [d] Stokes shift in  $\text{cm}^{-1}$ .



**Figure S33.** Normalized UV-Vis absorption spectra of compounds **Ph-BDP-NMe<sub>2</sub>** (A), **TPA-BDP-NMe<sub>2</sub>** (B), **Ph-BDP-NMe<sub>3</sub>** (C), and **TPA-BDP-NMe<sub>3</sub>** (D) in solvents of different polarity (10  $\mu$ M).

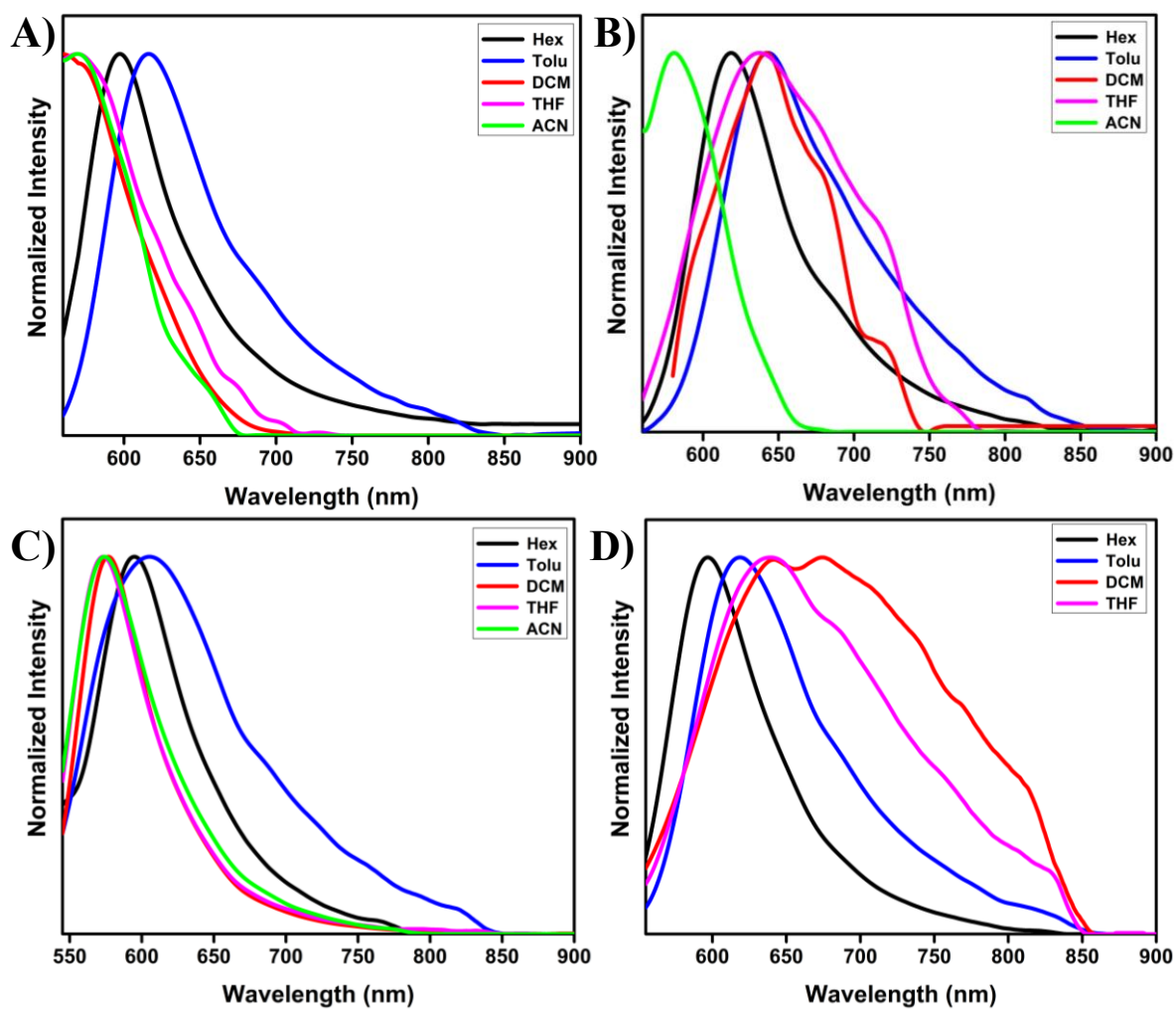


**Figure S34.** Normalized emission spectra of compounds **Ph-BDP-NMe<sub>2</sub>** (A), **TPA-BDP-NMe<sub>2</sub>** (B), **Ph-BDP-NMe<sub>3</sub>** (C), and **TPA-BDP-NMe<sub>3</sub>** (D) in solvents of different polarity (10  $\mu$ M).

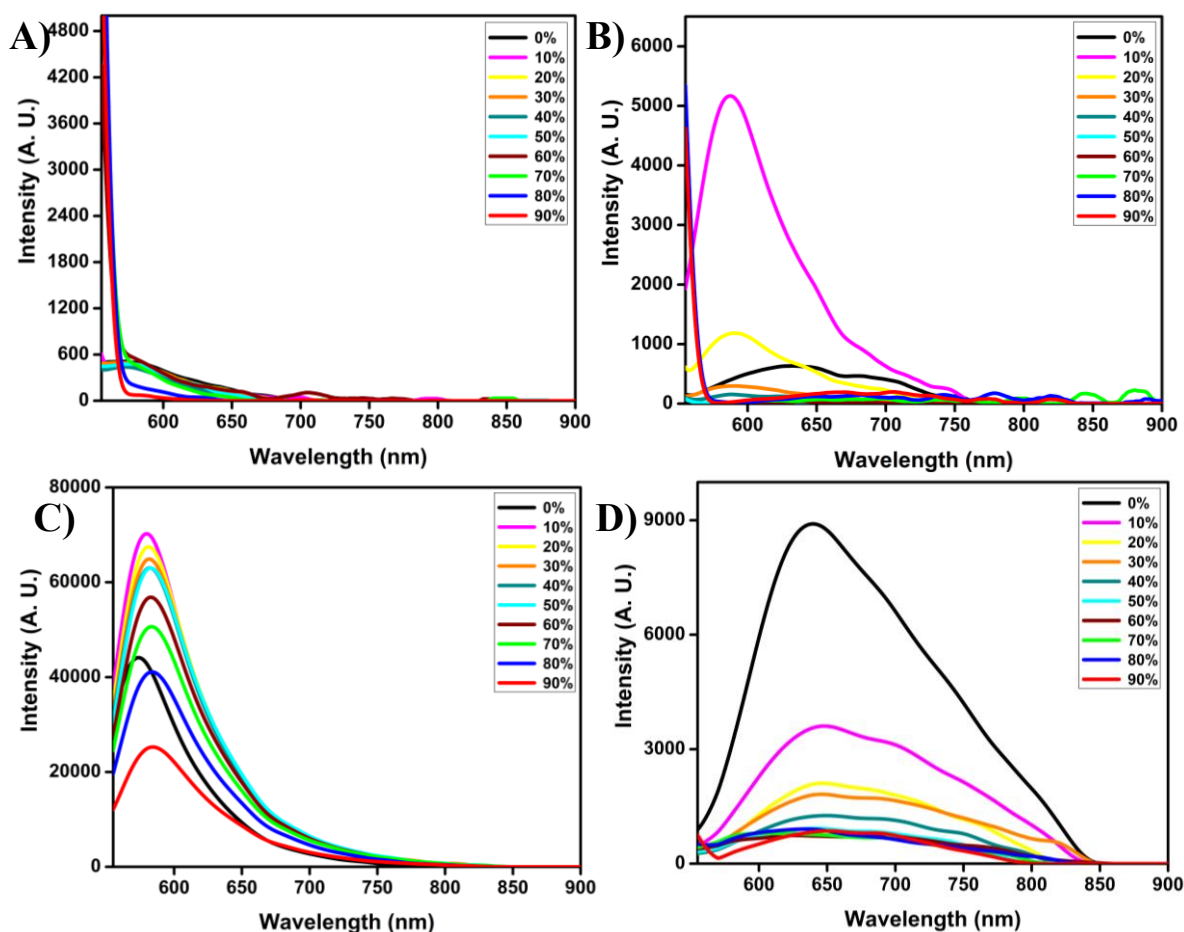


**Figure S35.** Emission spectra of compounds **Ph-BDP-NMe<sub>2</sub>** (A), **TPA-BDP-NMe<sub>2</sub>** (B), **Ph-BDP-NMe<sub>3</sub>** (C), and **TPA-BDP-NMe<sub>3</sub>** (D) in THF-water mixtures with increasing concentration of water from 0% to 90% (10  $\mu$ M,  $\lambda_{\text{ex}} = 540$  nm).

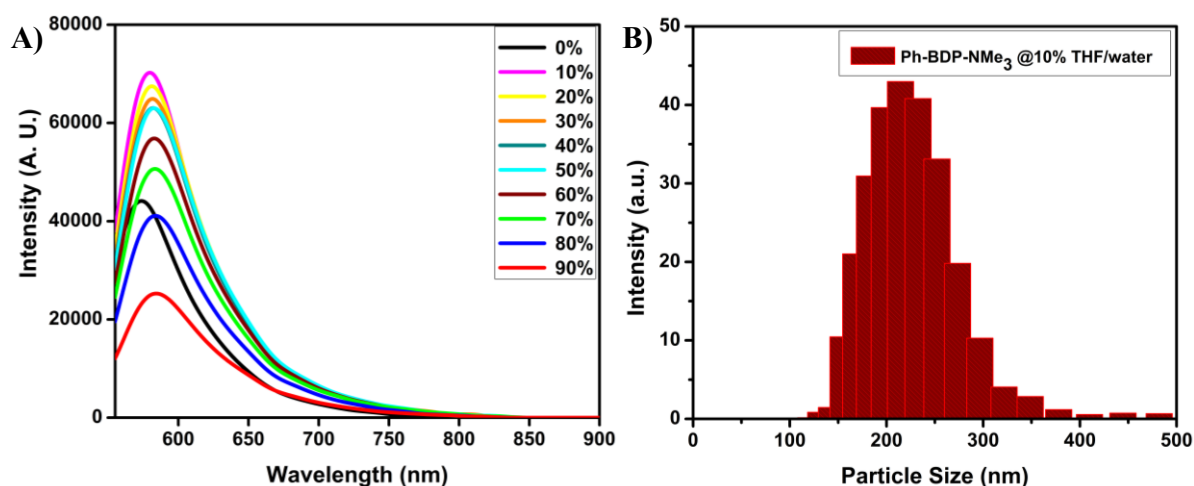


**Figure S36.** (A) Emission spectra of compound **Ph-BDP-NMe<sub>3</sub>** in THF-water mixtures with increasing concentration of water from 0% to 90%. (B) Size distributions of the aggregates of **Ph-BDP-NMe<sub>3</sub>** (10  $\mu$ M THF/H<sub>2</sub>O mixture with  $f_w = 10\%$ ).

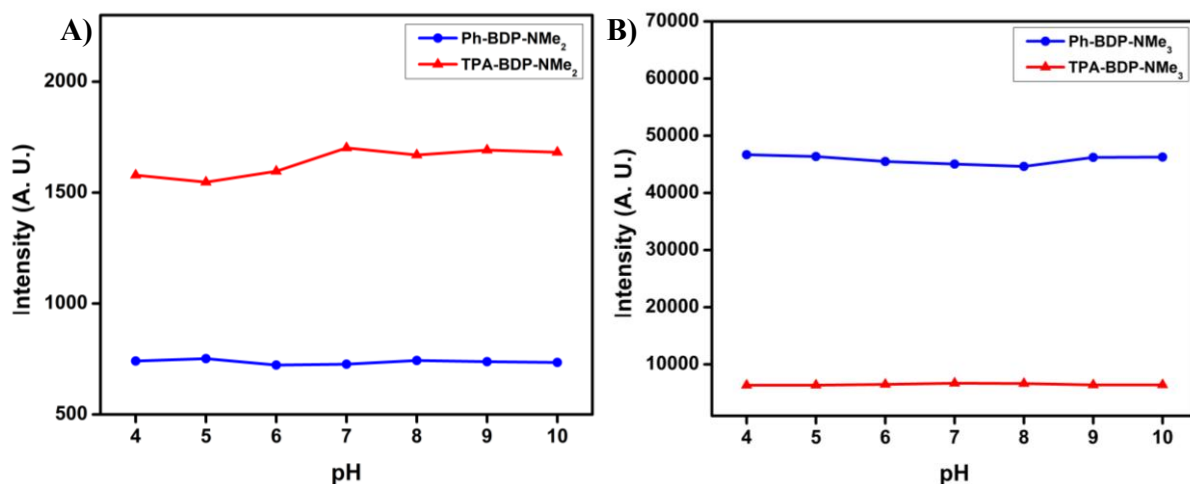


**Figure S37.** Fluorescence spectra of compounds (A) **Ph-BDP-NMe<sub>2</sub>** and **TPA-BDP-NMe<sub>2</sub>**, (B) **Ph-BDP-NMe<sub>3</sub>** and **TPA-BDP-NMe<sub>3</sub>** at different pH values (4-10) in THF solvent (10 μM, λ<sub>ex</sub> = 540 nm).

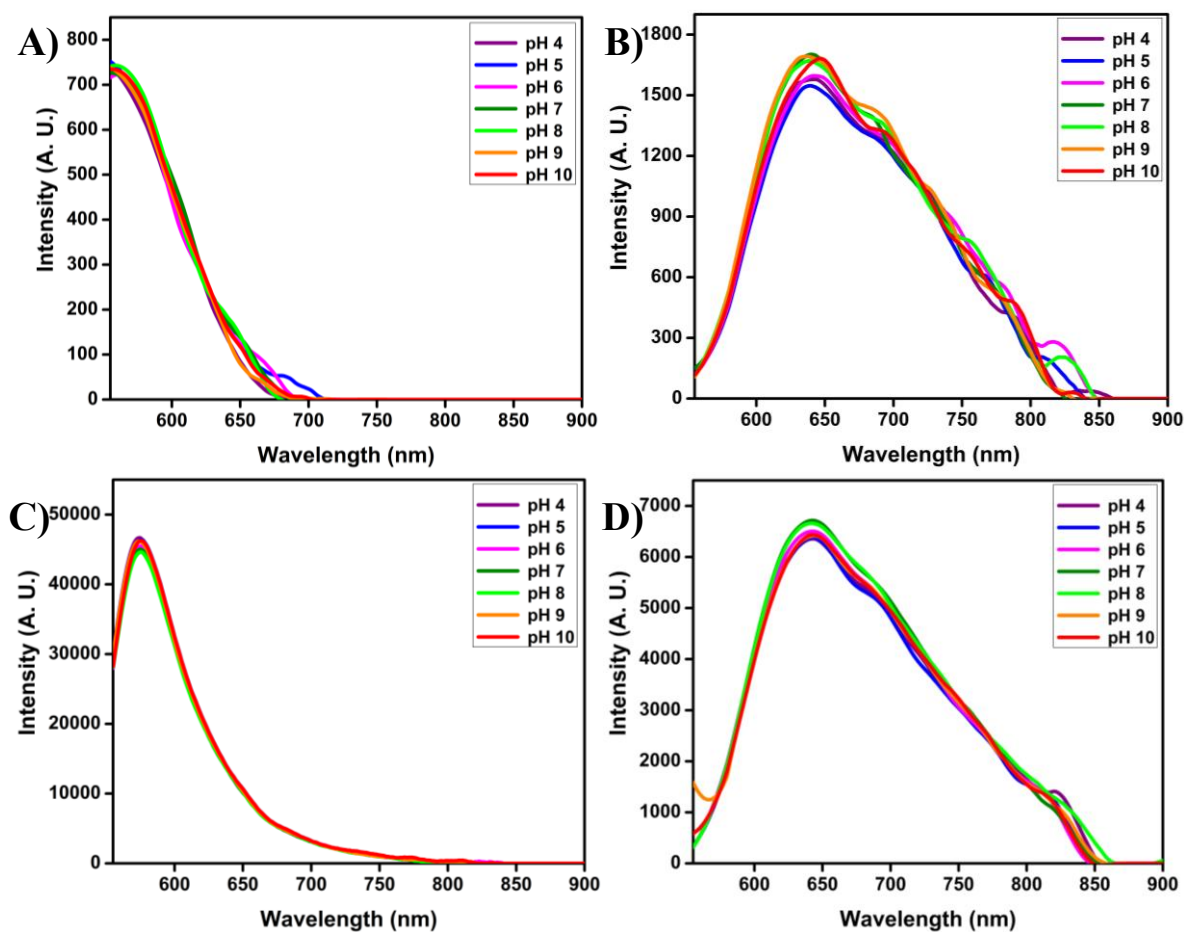


**Figure S38.** Fluorescence spectra of compounds **Ph-BDP-NMe<sub>2</sub>** (A), **TPA-BDP-NMe<sub>2</sub>** (B), **Ph-BDP-NMe<sub>3</sub>** (C), and **TPA-BDP-NMe<sub>3</sub>** (D) at different pH values (4-10) in THF solvent (10 μM, λ<sub>ex</sub> = 540 nm).

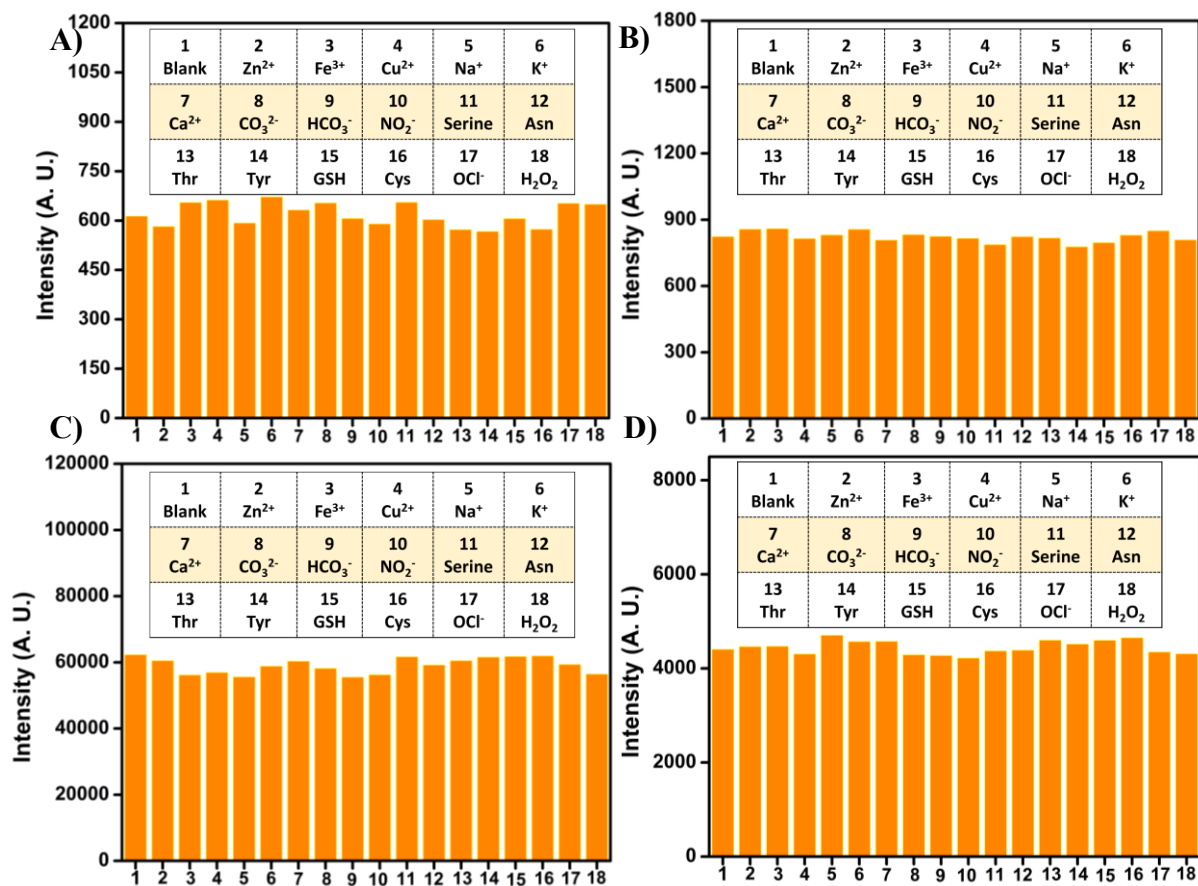


**Figure S39.** Emission spectra of compounds **Ph-BDP-NMe<sub>2</sub>** (A), **TPA-BDP-NMe<sub>2</sub>** (B), **Ph-BDP-NMe<sub>3</sub>** (C), and **TPA-BDP-NMe<sub>3</sub>** (D) in THF with various analytes (100 μM) (Blank, Zn(OAc)<sub>2</sub>, FeCl<sub>3</sub>, Cu(OAc)<sub>2</sub>, NaCl, KCl, CaCl<sub>2</sub>, K<sub>2</sub>CO<sub>3</sub>, NaHCO<sub>3</sub>, NaNO<sub>2</sub>, Ser, Asn, Thr, Tyr, GSH, Cys, OCl<sup>-</sup>, and H<sub>2</sub>O<sub>2</sub> (10 μM, λ<sub>ex</sub> = 540 nm).

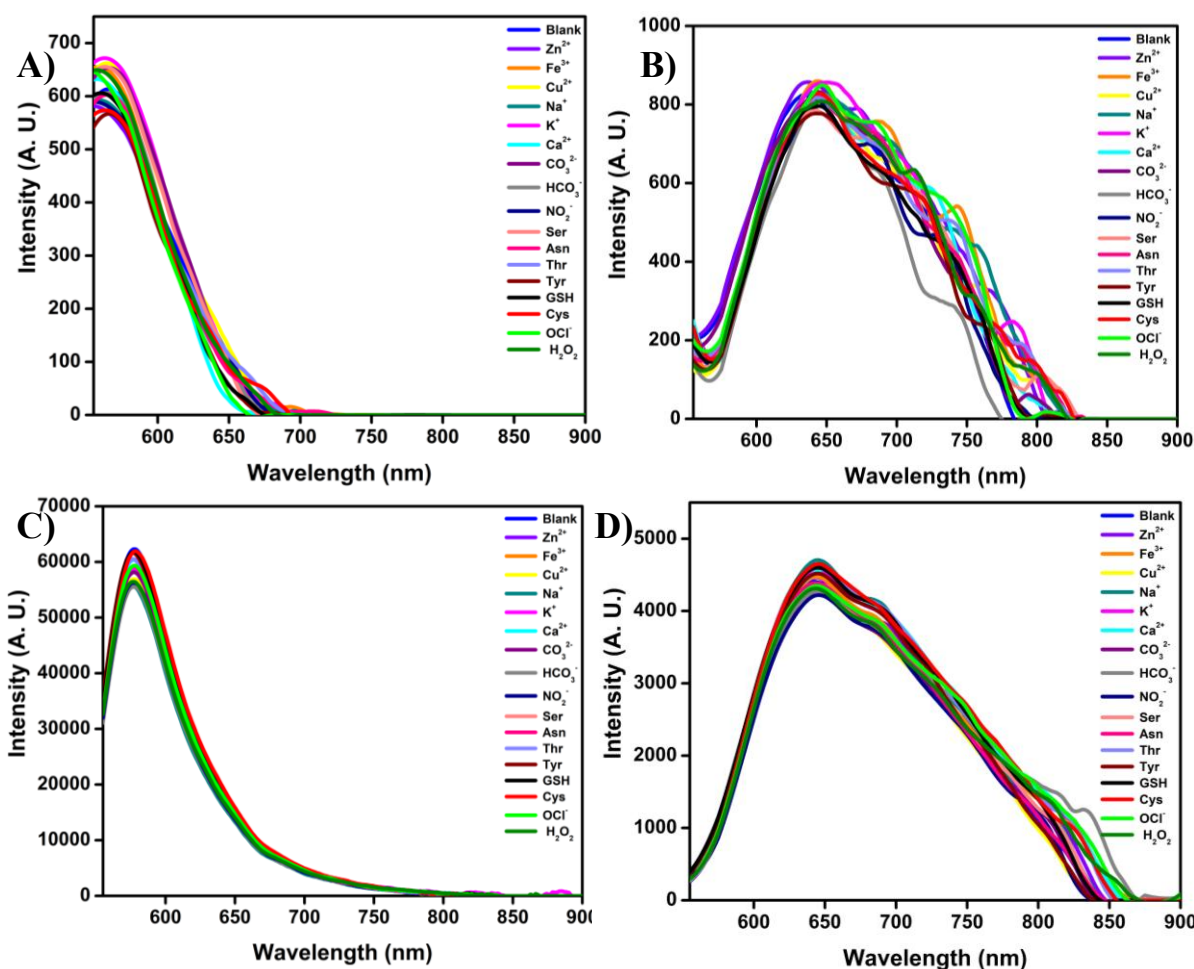


**Figure S40.** Emission spectra of compounds **Ph-BDP-NMe<sub>2</sub>** (A), **TPA-BDP-NMe<sub>2</sub>** (B), **Ph-BDP-NMe<sub>3</sub>** (C), and **TPA-BDP-NMe<sub>3</sub>** (D) in THF with various analytes (100  $\mu\text{M}$ ) (Blank,  $\text{Zn}(\text{OAc})_2$ ,  $\text{FeCl}_3$ ,  $\text{Cu}(\text{OAc})_2$ ,  $\text{NaCl}$ ,  $\text{KCl}$ ,  $\text{CaCl}_2$ ,  $\text{K}_2\text{CO}_3$ ,  $\text{NaHCO}_3$ ,  $\text{NaNO}_2$ , Ser, Asn, Thr, Tyr, GSH, Cys,  $\text{OCl}^-$ , and  $\text{H}_2\text{O}_2$ ) (10  $\mu\text{M}$ ,  $\lambda_{\text{ex}} = 540 \text{ nm}$ ).

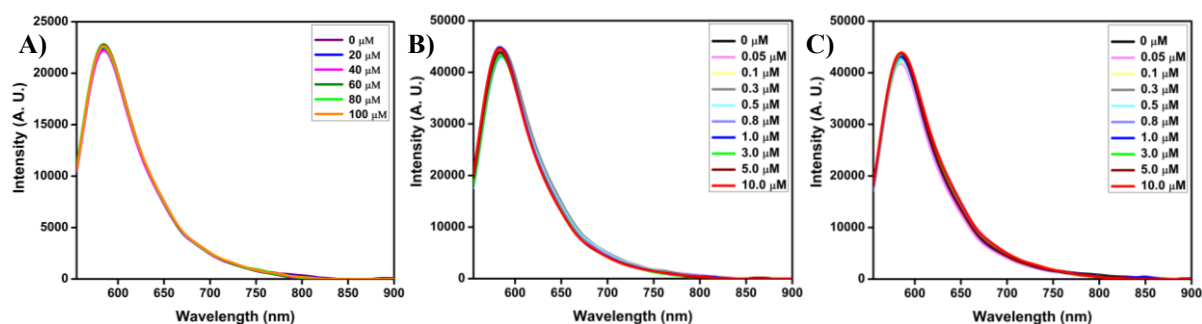


**Figure S41.** Emission spectra of probe **Ph-BDP-NMe<sub>3</sub>** (10  $\mu\text{M}$ ) upon addition of increasing concentrations of biomolecules such as reduced glutathione (0-100  $\mu\text{M}$ ) and serum albumins such as human serum albumin (HSA) and bovine serum albumin (BSA) (0-10  $\mu\text{M}$ ) in THF/PBS media (1:4, v/v; PBS 1 mM, pH 7.4) at 25  $^\circ\text{C}$  ( $\lambda_{\text{ex}} = 540 \text{ nm}$ ).

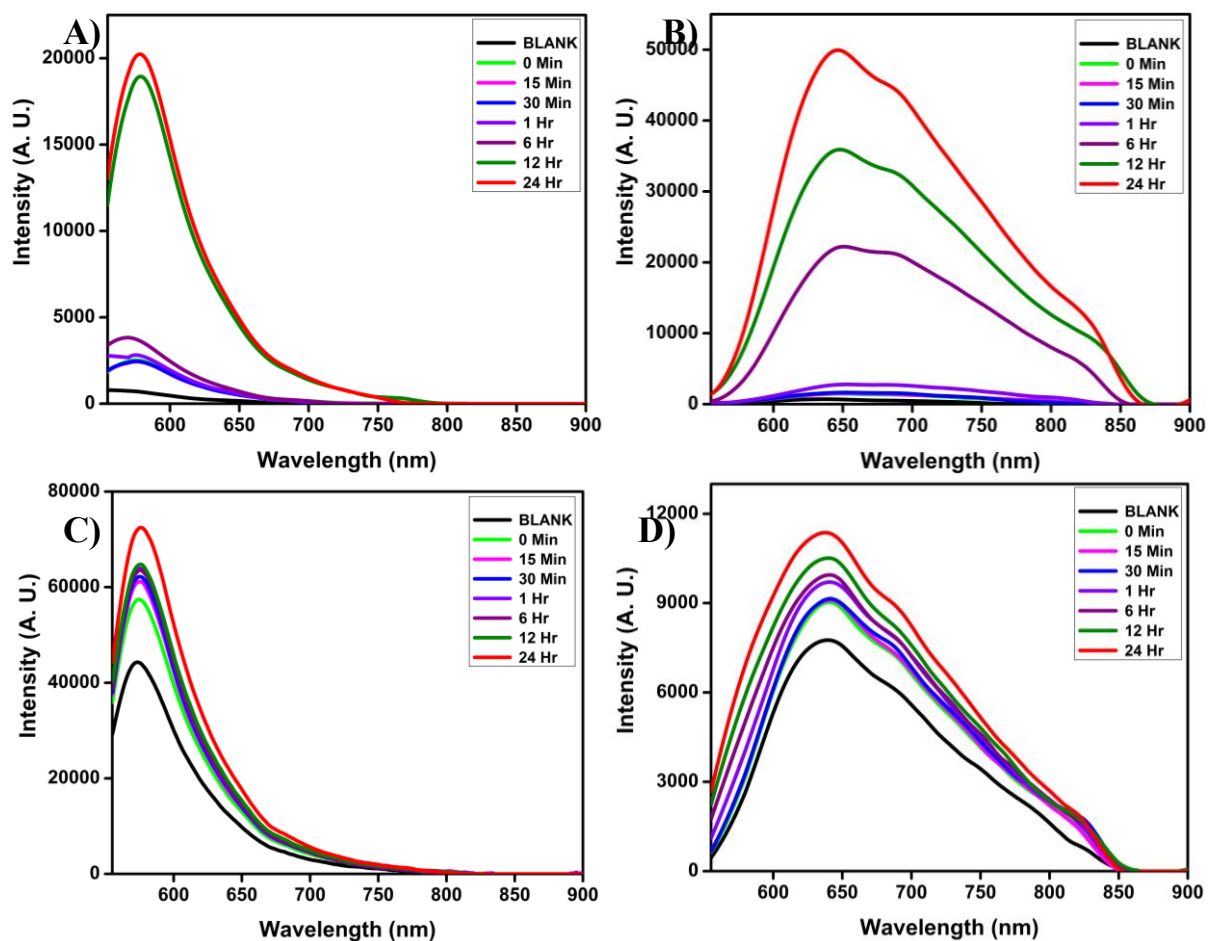


**Figure S42.** Emission spectra of compounds **Ph-BDP-NMe<sub>2</sub>** (A), **TPA-BDP-NMe<sub>2</sub>** (B), **Ph-BDP-NMe<sub>3</sub>** (C), and **TPA-BDP-NMe<sub>3s</sub>** (D) in THF (10 μM, λ<sub>ex</sub> = 540 nm) upon addition of 10 equivalents of TFA over a 24 h.

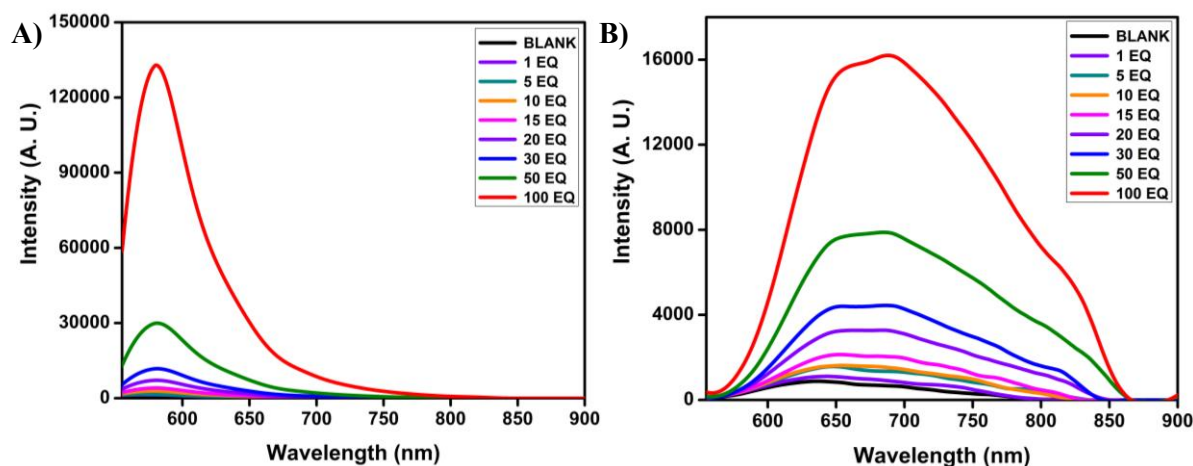


**Figure S43.** Emission spectra of compounds **Ph-BDP-NMe<sub>2</sub>** (A) and **TPA-BDP-NMe<sub>2</sub>** (B), in THF (10 μM, λ<sub>ex</sub> = 540 nm) upon addition with different equivalents of TFA.

## 5. DFT Calculations

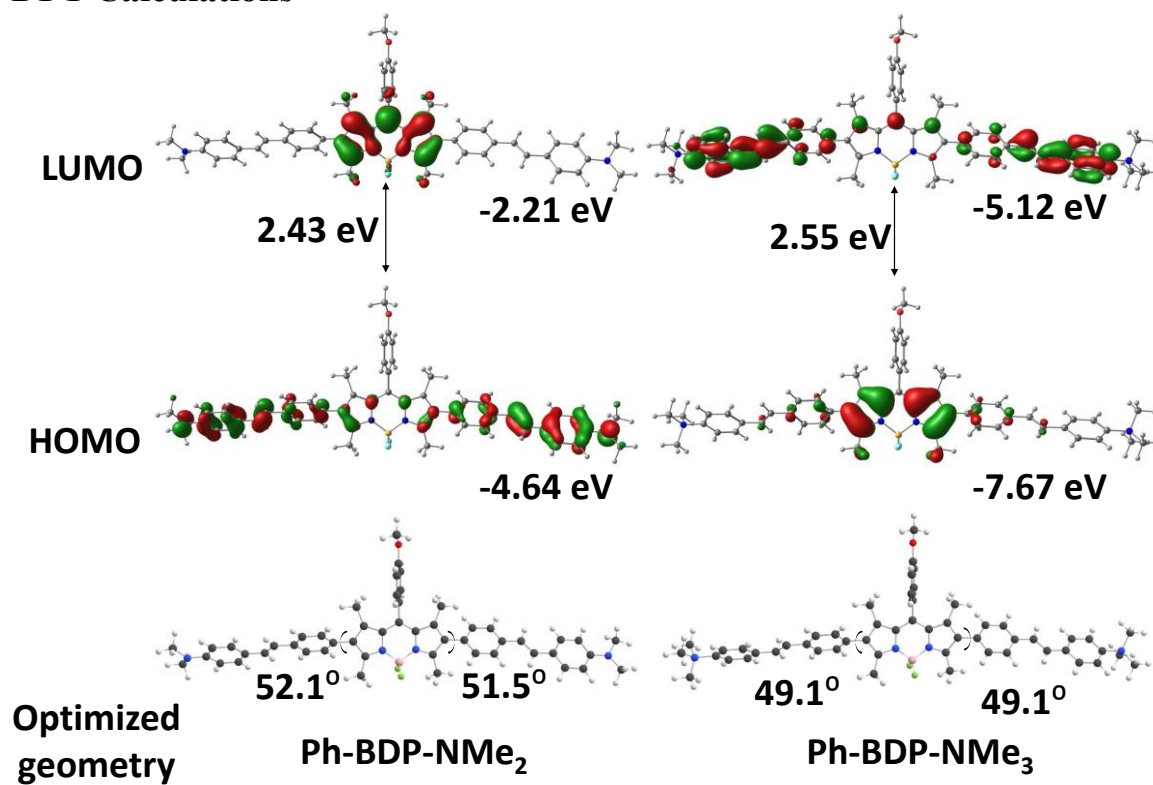


**Figure S44.** Optimized geometry and frontier molecular orbitals of compounds **Ph-BDP-NMe<sub>2</sub>** and **Ph-BDP-NMe<sub>3</sub>** in the ground state at the level of B3LYP/6-31G (d).

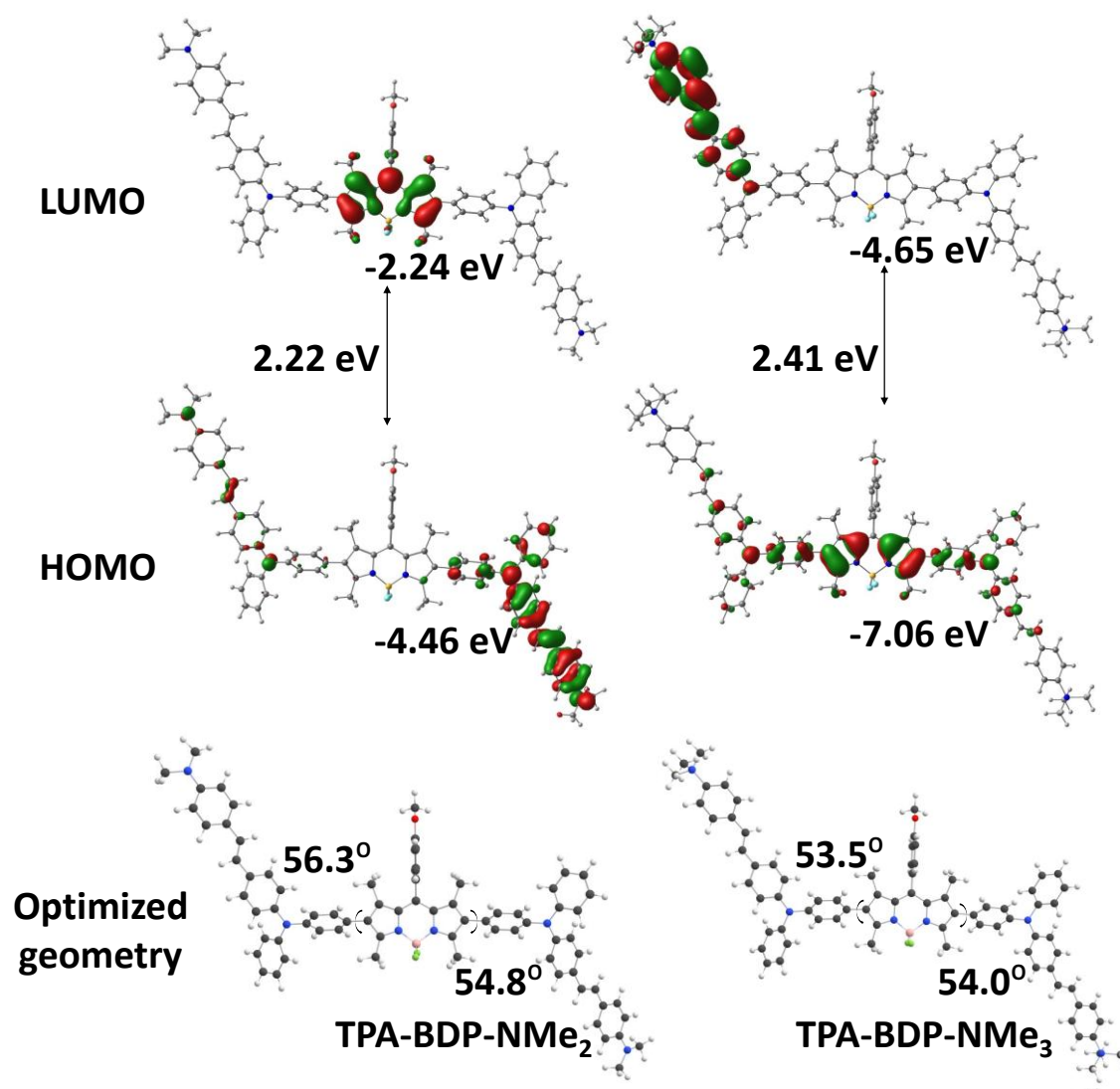


**Figure S45.** Optimized geometry and frontier molecular orbitals of compounds TPA-BDP-NMe<sub>2</sub> and TPA-BDP-NMe<sub>3</sub> in the ground state at the level of B3LYP/6-31G (d).

## 6. Cytotoxicity Assay

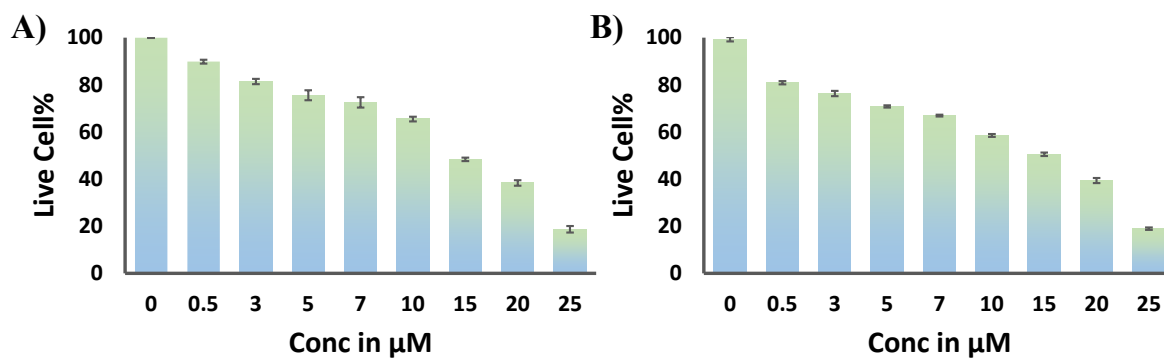


**Figure S46.** Cytotoxicity data of compounds Ph-BDP-NMe<sub>3</sub> (A) and TPA-BDP-NMe<sub>3</sub> (B) in HeLa cells.

## 7. Co-localization Studies

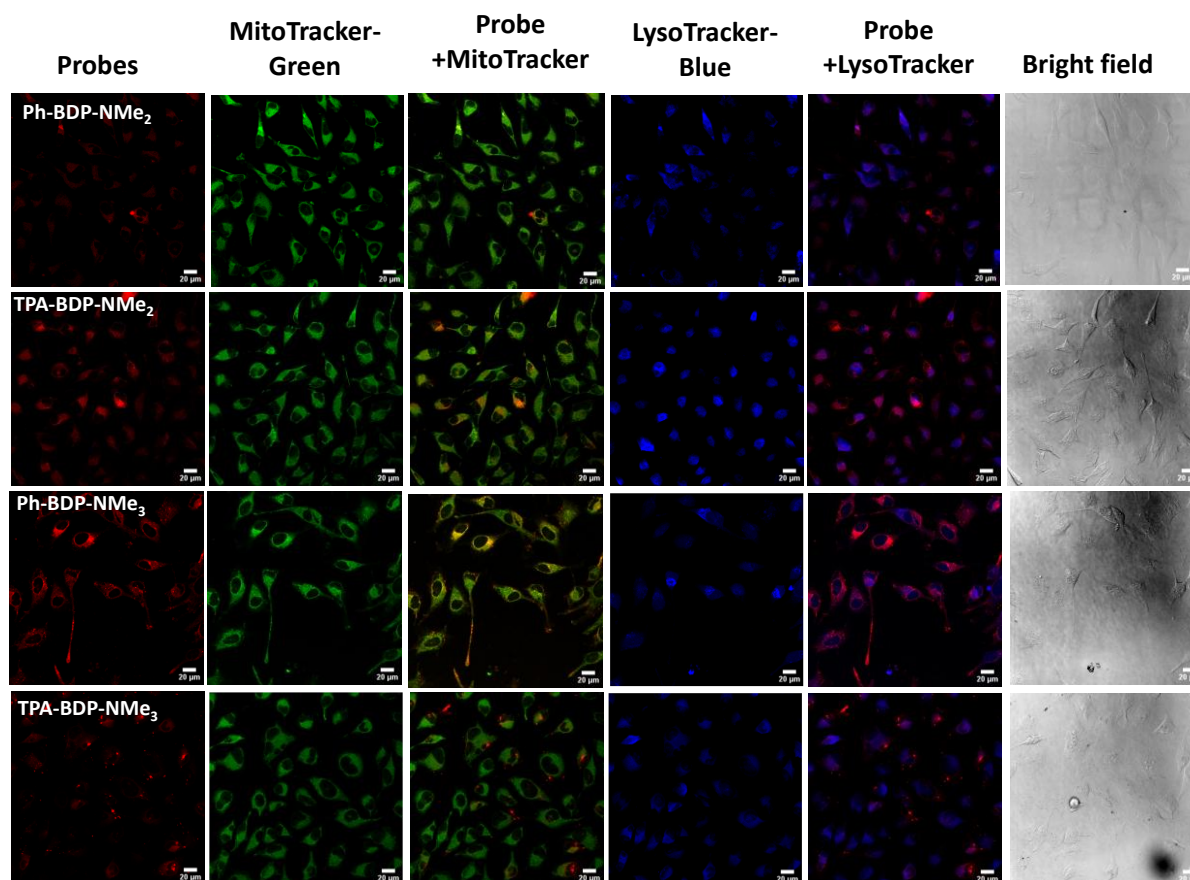


**Figure S47.** Fluorescence imaging of HeLa cells stained with probes (700 nM) for 30 mins and then incubated with lysotracker blue (100 nM) and mitotracker green (500 nM) for another 30 mins. Due to the low emission signals from the probes **Ph-BDP-NMe<sub>2</sub>** and **TPA-BDP-NMe<sub>2</sub>**, 30% laser power was used. For probes **Ph-BDP-NMe<sub>3</sub>** and **TPA-BDP-NMe<sub>3</sub>**, 3% laser power was utilized.

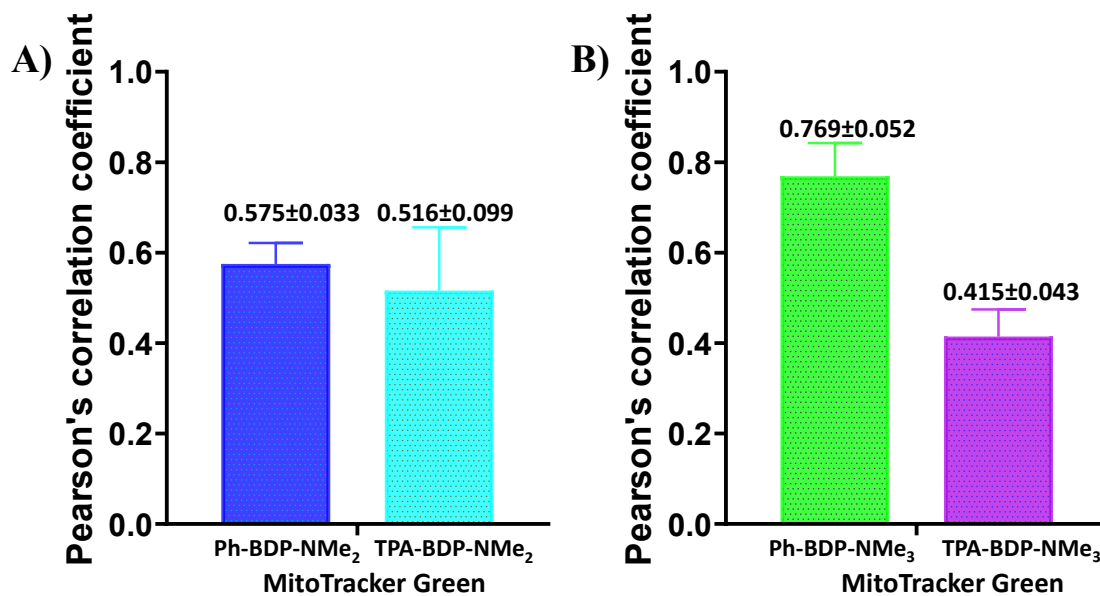


Figure S48. Pearson's correlation of compounds A) **Ph-BDP-NMe<sub>2</sub>** and **TPA-BDP-NMe<sub>2</sub>**, B) **Ph-BDP-NMe<sub>3</sub>** and **TPA-BDP-NMe<sub>3</sub>** with commercial MitoTracker-Green. Computation of Pearson correlation coefficient using JACoP with Fiji/ImageJ.

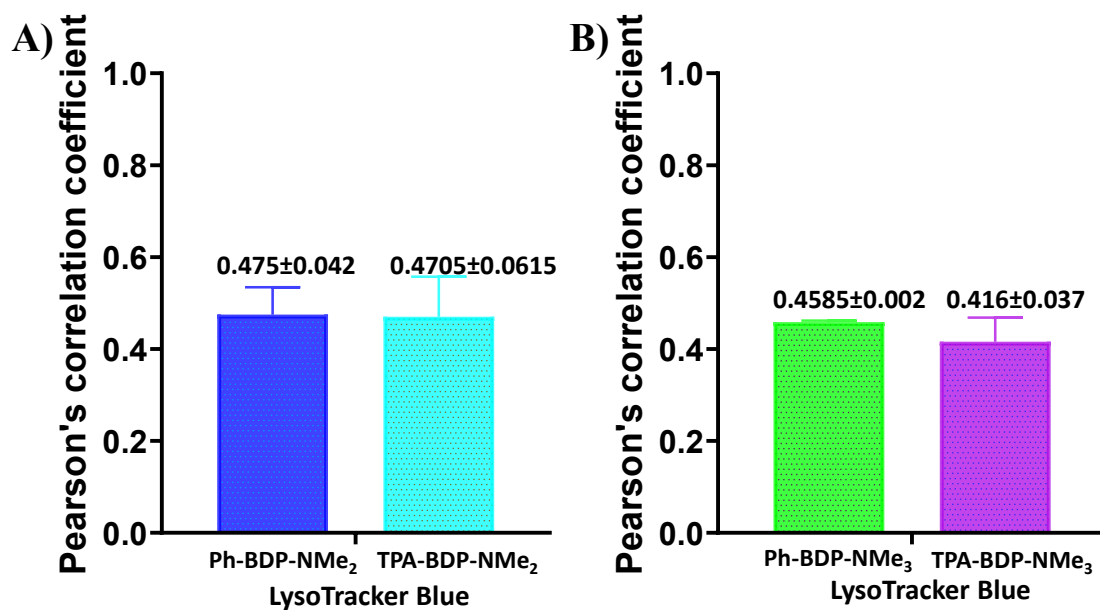
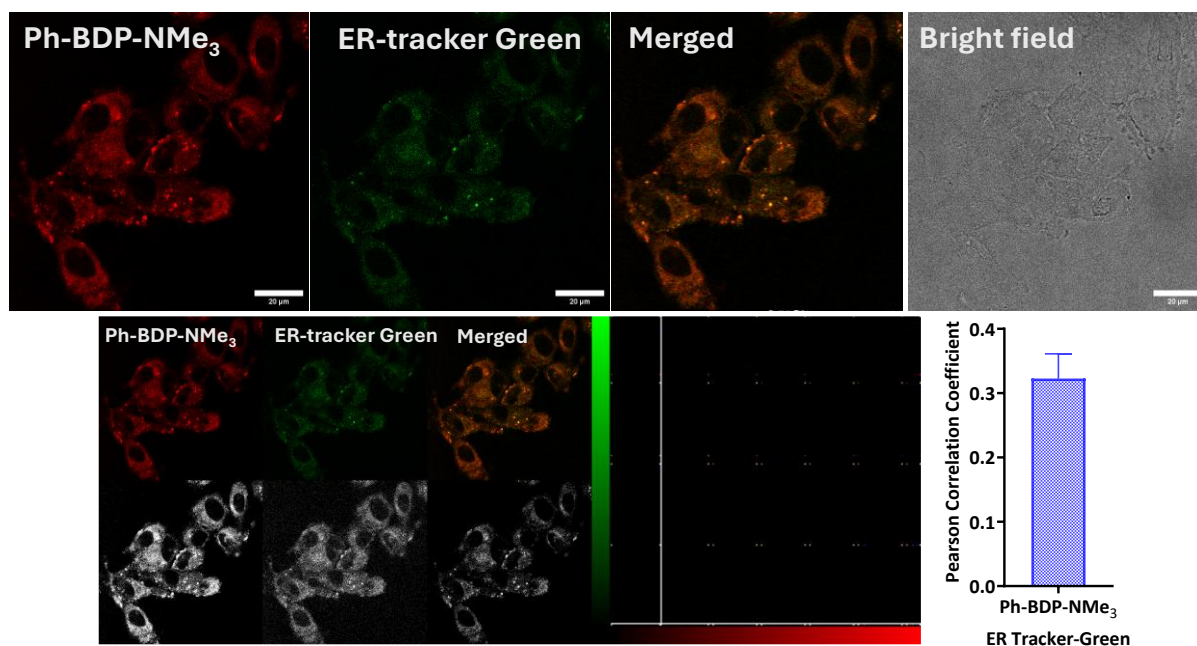


Figure S49. Pearson's correlation of compounds A) **Ph-BDP-NMe<sub>2</sub>** and **TPA-BDP-NMe<sub>2</sub>**, B) **Ph-BDP-NMe<sub>3</sub>** and **TPA-BDP-NMe<sub>3</sub>** with commercial LysoTracker-Blue. Computation of Pearson correlation coefficient using JACoP with Fiji/ImageJ.

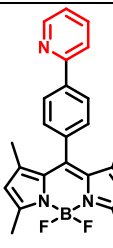
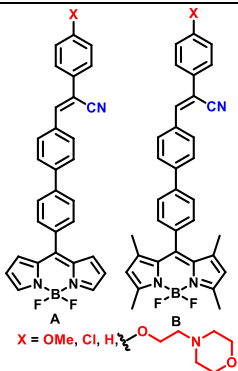
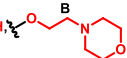
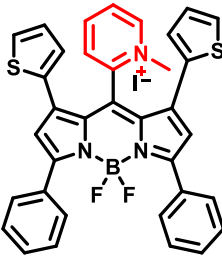
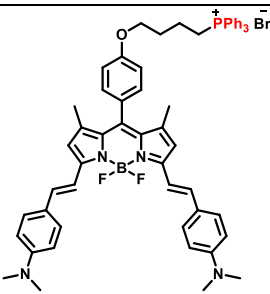
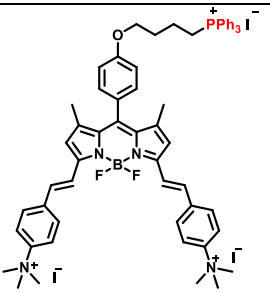


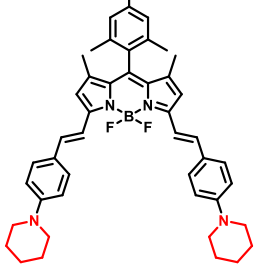
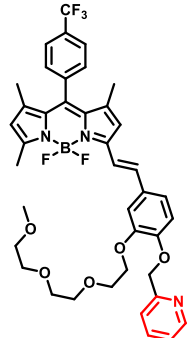
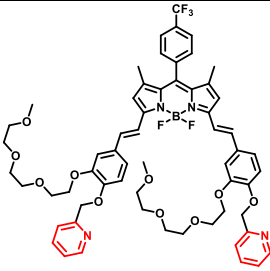
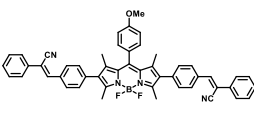
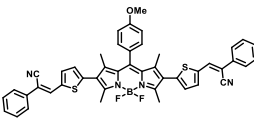
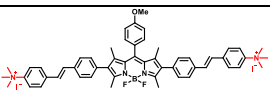
**Figure S50.** Fluorescence imaging of HeLa cells stained with **Ph-BDP-NMe<sub>3</sub>** (700 nM) for 30 mins and then incubated with ER-tracker green (1  $\mu$ M) and mitotracker green (500 nM) for another 30 mins. Ex/Em (ER-tracker green) = 488/516 nm, Ex/Em (**Ph-BDP-NMe<sub>3</sub>**) = 540/550-700 nm. Pearson's correlation of **Ph-BDP-NMe<sub>3</sub>** with commercial ER-tracker green. Computation of Pearson correlation coefficient using JACoP with Fiji/ImageJ.

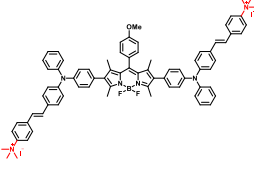
## 8. Comparative Table

**Table S2:** Comparative table summarizing key photophysical parameters of BODIPY derivatives with different substitution patterns

Probes (P)	Substitution position	Solvent	$\lambda_{ex}/\lambda_{em}$ (nm)	Stokes shift (nm)	QY ( $\phi_F$ )	Key characteristics	Ref
	<i>meso</i>	ACN	520/542	22	0.20	Membrane potential independent mitochondrial imaging, weak electronic coupling with the core, high rigidity, small Stokes shift, and limited ICT	<b>S7</b>
	<i>meso</i>	ACN	496/509	13	0.75	Mitochondrial labelling, weak electronic coupling with the core, high rigidity, small Stokes shift, and limited ICT	<b>S8</b>

	<i>meso</i>	DMSO	490/520	30	0.35	Super resolution imaging of mitochondrial membrane, weak electronic coupling with the core, high rigidity, small Stokes shift, and limited ICT	<b>S9</b>
 <p>X = OMe, Cl, H, </p>	<i>meso</i>	DCM	A. 500/524 B. 500/515	15-24	A. 0.07-0.10 B. 0.50	Lipid droplets imaging, weak electronic coupling with the core, small Stokes shift, and limited ICT	<b>S10</b>
	1,3,5,7	ACN	670/718	48	0.31	Pyridyl probe for membrane potential independent mitochondrial imaging, red-shifted emission via extended conjugation, largely locally excited (LE) character with a moderate Stokes shift	<b>S11</b>
	3,5	H <sub>2</sub> O DMSO	717/- 705/760	55	0.03	Not suitable for imaging due to aggregation caused quenching (ACQ) in water	<b>S12</b>
	3,5	H <sub>2</sub> O	617/630	13	0.43	High resolution mitochondrial imaging, red-shifted emission via extended conjugation, largely LE character with a small Stokes shift	<b>S12</b>

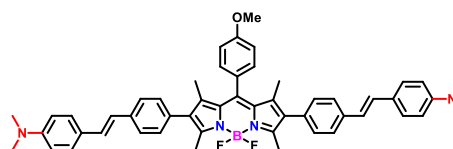
	3,5	ACN	681/751	70	0.04	Piperidinyl probe for mitochondrial imaging, red-shifted emission via extended conjugation, largely LE character with a moderate Stokes shift, and low quantum yield	<b>S13</b>
	3/5	ACN	570/589	19	0.42	Mitochondrial labelling, red-shifted emission via extended conjugation, largely LE character with a small Stokes shift	<b>S14</b>
	3,5	ACN	645/666	21	0.21	Mitochondrial labelling, red-shifted emission via extended conjugation, largely LE character with a small Stokes shift	<b>S14</b>
	2,6	DCM	535/570	35	0.19	Dual targeting of lipid droplets and lysosomes, red-shifted emission via extended conjugation, largely LE character with a small Stokes shift	<b>S15</b>
	2,6	DCM	543/655	112	0.04	Dual targeting of lipid droplets and lysosomes, red-shifted emission via increased geometry relaxation and enhanced ICT with a large Stokes shift, and low quantum yield	<b>S15</b>
 <p>Present work</p>	2,6	THF	536/573	37	0.15	Mitochondria labelling, red-shifted emission via extended conjugation, enhanced emission due to suppression of PET, and a small Stokes shift	

 <p>Present work</p>	2,6	THF	542/640 (600-850)	98	0.21	Not suitable for mitochondrial imaging due to bulky and hydrophobic TPA groups, red-shifted emission via extended conjugation and strong ICT, enhanced emission due to suppression of PET, and a large Stokes shift
---	-----	-----	----------------------	----	------	---

## 9. DFT Coordinates

**Table S3: The coordinates of compound Ph-BDP-NMe<sub>2</sub> (DFT/B3LYP/6-31G(d) level with Gaussian 09)**

5	-0.014303140	-1.821419196	-0.138522661
6	2.506200904	-1.311607992	-0.259639981
6	3.381229003	-0.190685131	-0.207679925
6	2.581097953	0.956263480	-0.095791687
6	1.220532222	0.506002534	-0.089643353
6	0.000123721	1.198833256	0.015836173
6	-1.226305641	0.510140033	0.059150068
6	-2.582252739	0.969566398	0.123363553
6	-3.392502352	-0.175551590	0.132385189
6	-2.528208031	-1.303865843	0.063921162
9	-0.128188715	-2.547020292	-1.323300561
9	0.091390743	-2.681294415	0.953428688
7	1.232238311	-0.889002834	-0.188418085
7	-1.250756826	-0.887770703	0.021248541
6	0.007692203	2.690566680	0.085348957
6	0.160407466	3.461228077	-1.070224415
6	-0.136439904	3.353986143	1.315037124
6	0.165153971	4.857778517	-1.017949254
1	0.271201590	2.966460113	-2.031387409
6	-0.121194247	4.740791212	1.384334219



1	-0.254128531	2.772213094	2.225179463
6	0.027375574	5.504578581	0.216117362
1	0.277460828	5.422456093	-1.936342582
1	-0.224657682	5.258674956	2.332705459
8	0.023985005	6.856453464	0.388768605
6	0.172481960	7.682197518	-0.756418051
1	0.144558605	8.709521750	-0.389245536
1	1.130999152	7.503225751	-1.261056219
1	-0.646270807	7.530502139	-1.472025281
6	-3.093353621	2.381248000	0.108931355
1	-2.941212543	2.891895927	1.067399677
1	-2.591647477	2.987462248	-0.650362093
1	-4.166164300	2.385515370	-0.101354714
6	-2.886388901	-2.755309353	0.062657279
1	-2.704677864	-3.197796795	-0.924025674
1	-2.254899364	-3.298353051	0.771240036
1	-3.936826140	-2.894455420	0.324975622
6	3.104839218	2.354537884	0.062288507
1	2.967605147	2.957228727	-0.843486309
1	2.600754464	2.889025675	0.872129367
1	4.175185063	2.327144822	0.282928241
6	2.851075004	-2.759589735	-0.399400288
1	2.667404455	-3.294544610	0.539979254
1	2.213906516	-3.225704958	-1.156098018
1	3.899961087	-2.882343627	-0.676254069
6	-4.866249004	-0.233398367	0.200614030
6	-5.612414320	-0.978439425	-0.733446520
6	-5.581722675	0.448619005	1.199276527
6	-6.998038118	-1.045347279	-0.669279333
1	-5.091919918	-1.495837178	-1.534911118

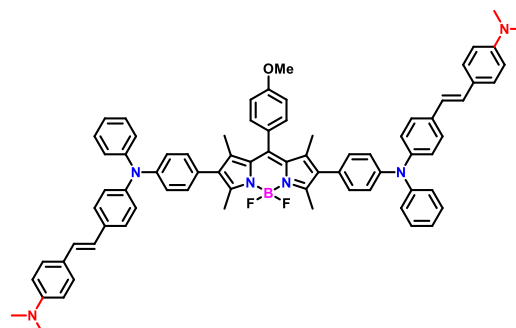
6	-6.969968757	0.385564051	1.260316900
1	-5.038313913	1.017423903	1.948763420
6	-7.718348686	-0.366816181	0.334873246
1	-7.528870051	-1.623253307	-1.420200763
1	-7.493148893	0.919228058	2.050910753
6	-9.175423530	-0.404690334	0.461753839
6	-10.037367171	-1.134777975	-0.279707596
1	-9.572120884	0.226189063	1.256312526
6	-11.491814068	-1.181888757	-0.162694439
6	-12.241614308	-0.387685403	0.726745612
6	-12.224121296	-2.061890017	-0.980005398
6	-13.622957590	-0.472744245	0.803870423
1	-11.736216962	0.325055391	1.372529248
6	-13.607580123	-2.161367232	-0.917706207
1	-11.688951379	-2.688461343	-1.690712013
6	-14.351895229	-1.374227801	-0.010180017
1	-14.140789861	0.172967945	1.503305996
1	-14.107815292	-2.856261406	-1.581701468
6	4.855285071	-0.256736887	-0.257134675
6	5.596011942	0.517314584	-1.166248421
6	5.577244565	-1.102200797	0.607848893
6	6.984936800	0.449952365	-1.204637928
1	5.072359251	1.164824685	-1.864207367
6	6.963386903	-1.173109162	0.565801273
1	5.037157952	-1.698463343	1.338381541
6	7.709645889	-0.396414984	-0.343788168
1	7.527851808	1.058753693	-1.924507173
1	7.473116306	-1.836265269	1.258656950
6	9.169442662	-0.424582339	-0.436773624
6	10.016762332	-1.180577144	0.295635541

1	9.582855033	0.246418833	-1.188797267
6	11.473828180	-1.217437054	0.213150225
6	12.239308736	-0.417466176	-0.657654092
6	12.192440089	-2.092775346	1.047465612
6	13.622852073	-0.490400121	-0.699125227
1	11.744392962	0.288168428	-1.319142757
6	13.577857136	-2.179914424	1.021048010
1	11.644633314	-2.724313838	1.744003591
6	14.338464658	-1.385419048	0.133698553
1	14.152848382	0.158613821	-1.386287026
1	14.066842580	-2.871070522	1.697168489
1	9.597660460	-1.854998963	1.041877157
1	-9.633353306	-1.782234769	-1.057575824
7	15.721790609	-1.482028181	0.073679937
7	-15.732330391	-1.482474283	0.085077518
6	16.426004451	-2.255026547	1.082287888
1	16.102392931	-3.302659120	1.070907620
1	17.495314770	-2.239075970	0.862513163
1	16.277155993	-1.864615903	2.102006986
6	16.474582976	-0.504146678	-0.693216756
1	16.345352441	0.524705163	-0.320214853
1	17.536355853	-0.753978269	-0.645734772
1	16.179280956	-0.520843591	-1.749043957
6	-16.455208368	-2.263283580	-0.904050243
1	-16.122878282	-3.308265176	-0.898722995
1	-17.518814950	-2.255520803	-0.657756594
1	-16.334949822	-1.873896608	-1.927917075
6	-16.473733434	-0.510797969	0.870689248
1	-16.361865893	0.519068508	0.494936203
1	-17.534326776	-0.769049274	0.849172896

1 -16.152532105 -0.525232905 1.918976165

**Table S4: The coordinates of compound TPA-BDP-NMe<sub>2</sub> (DFT/B3LYP/6-31G(d) level with Gaussian 09)**

5	0.644598358	-1.802856261	0.522978398
6	-1.871161889	-2.307077516	0.291590130
6	-3.088430484	-1.614479426	0.042262430
6	-2.765810933	-0.264669955	-0.157488055
6	-1.342188278	-0.161784201	-0.025641008
6	-0.466289253	0.934584945	-0.123875367
6	0.919288082	0.776916775	0.059950102
6	2.005051935	1.711083617	0.008581316
6	3.173110100	0.980706743	0.270221768
6	2.786845427	-0.373361651	0.474510408
9	0.787546422	-2.281547138	1.826306449
9	1.079777244	-2.752470454	-0.396971843
7	-0.845387633	-1.439138704	0.252469256
7	1.452908647	-0.482716250	0.349746615
6	-1.018529079	2.290889947	-0.423181848
6	-1.380224163	3.165380699	0.613946179
6	-1.187371139	2.719749731	-1.742183041
6	-1.896176277	4.425376219	0.338145864
1	-1.255676661	2.850970788	1.646620875
6	-1.703408526	3.985002617	-2.035546102
1	-0.912694782	2.057199712	-2.558736271
6	-2.062062835	4.845201461	-0.990536412
1	-2.179320200	5.104902588	1.135895068
1	-1.819858588	4.283294085	-3.071080344
8	-2.575830194	6.096823280	-1.155719630
6	-2.773969370	6.574816071	-2.477652320
1	-3.191847102	7.577524089	-2.372897762



1	-1.828080743	6.632457603	-3.032135640
1	-3.480186350	5.943719760	-3.033004517
6	1.960018914	3.177645096	-0.309475360
1	1.426699297	3.376422354	-1.243732718
1	1.448942141	3.755524263	0.469414361
1	2.975440590	3.570089034	-0.406360394
6	3.647353236	-1.548224715	0.811585785
1	3.236214010	-2.078600143	1.675613417
1	3.664983295	-2.265123905	-0.017338474
1	4.668374660	-1.229574284	1.029361284
6	-3.753618743	0.816722498	-0.487696023
1	-3.782493797	1.599276344	0.278768642
1	-3.511979832	1.315535578	-1.431477546
1	-4.756892674	0.392850007	-0.575843994
6	-1.670847043	-3.757268362	0.593988704
1	-1.126494022	-4.251387571	-0.219039028
1	-1.061032463	-3.872380638	1.495066140
1	-2.630751569	-4.257514740	0.735122255
6	4.558504557	1.491532078	0.332389851
6	4.910874172	2.553790856	1.183144913
6	5.580158850	0.931496678	-0.454789971
6	6.215172555	3.033662983	1.249631473
1	4.153420584	2.990571286	1.828253287
6	6.885190752	1.410913151	-0.405141530
1	5.340327466	0.124695389	-1.142190483
6	7.224878571	2.471269236	0.451316832
1	6.460027313	3.842807981	1.930204925
1	7.648549942	0.970208010	-1.038189823
6	-4.431251044	-2.232349994	0.017906246
6	-5.463932847	-1.770797216	0.852811947

6	-4.725924655	-3.309421947	-0.836250467
6	-6.727447300	-2.353070967	0.839508659
1	-5.262132754	-0.960267732	1.547787577
6	-5.989128460	-3.892452368	-0.865587381
1	-3.958391706	-3.677071010	-1.512102192
6	-7.011680730	-3.423040954	-0.024731576
1	-7.500318504	-1.986989068	1.507704094
1	-6.192247591	-4.711078836	-1.548604516
7	-8.303108120	-4.010997492	-0.048783343
6	-9.456646206	-3.186990736	0.047513291
6	-10.542173744	-3.554515089	0.856757159
6	-9.539490015	-1.981615918	-0.672542039
6	-11.667642364	-2.742319226	0.935063184
1	-10.498345697	-4.479534965	1.423093452
6	-10.660948054	-1.170704839	-0.574978826
1	-8.714084105	-1.688703277	-1.313948252
6	-11.761721823	-1.524969592	0.232718008
1	-12.494630726	-3.048062568	1.572212828
1	-10.688022667	-0.252681577	-1.154673298
6	-8.446402440	-5.420640274	-0.165163292
6	-9.444569481	-5.969294738	-0.986967566
6	-7.595542839	-6.286825535	0.540941907
6	-9.589469590	-7.351283723	-1.090351544
1	-10.102285419	-5.307086033	-1.540808825
6	-7.736648799	-7.667552062	0.416211202
1	-6.827052270	-5.871540883	1.185003357
6	-8.735533458	-8.210117919	-0.395005572
1	-10.367553295	-7.757439644	-1.731560999
1	-7.068831662	-8.322144213	0.970310908
1	-8.846989723	-9.286998012	-0.483813413

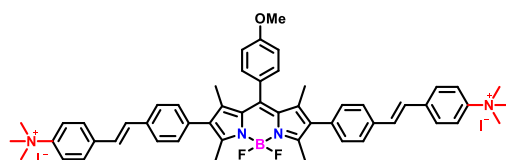
7	8.555836453	2.958908362	0.509396322
6	8.803464524	4.353001980	0.636512482
6	9.810666050	4.821160764	1.496102227
6	8.050677343	5.283801932	-0.098443865
6	10.060461154	6.187442820	1.608856691
1	10.392600524	4.108796348	2.072070239
6	8.295979679	6.648959889	0.035114924
1	7.276098166	4.930242875	-0.771499000
6	9.303700593	7.110954171	0.884623321
1	10.843942203	6.530797785	2.279493141
1	7.703434407	7.354423331	-0.541798910
1	9.496707781	8.175655515	0.980408838
6	9.649114692	2.052377357	0.449691963
6	10.776917248	2.340201340	-0.339594917
6	9.631540768	0.850683263	1.173317038
6	11.848805031	1.460781672	-0.394870915
1	10.802945148	3.261923161	-0.912623931
6	10.703604238	-0.030862267	1.098120126
1	8.773611518	0.612153861	1.794136357
6	11.845583982	0.245492565	0.321107110
1	10.666826684	-0.955390597	1.670067898
6	-12.968351892	-0.711261595	0.371935861
6	-13.201655452	0.500674276	-0.178810982
1	-13.739115913	-1.158173753	0.998954553
1	-12.421777518	0.950323190	-0.793046208
6	-14.401897240	1.321776562	-0.049261552
6	-14.448694925	2.581420740	-0.673743044
6	-15.552418699	0.939032167	0.667868515
6	-15.556251424	3.414809924	-0.591923658
1	-13.586637722	2.916695163	-1.247038091

6	-16.667453583	1.757432967	0.761973370
1	-15.584036986	-0.027853630	1.162466788
6	-16.701084015	3.030550622	0.141930195
1	-15.526366191	4.368900761	-1.104511915
1	-17.523388946	1.400776777	1.322706093
7	-17.805384221	3.864143449	0.257539889
6	-19.034729647	3.347151750	0.834023064
1	-18.875856349	3.014920695	1.866904303
1	-19.780832050	4.143972283	0.856682318
1	-19.451705338	2.500663090	0.264957234
6	-17.877748311	5.065774571	-0.555211140
1	-17.035622939	5.734986377	-0.341954099
1	-17.876626402	4.852483575	-1.636429799
1	-18.795537297	5.605844532	-0.314207373
1	12.697235337	1.717502791	-1.022427697
6	12.942007068	-0.721202999	0.297037417
6	14.119523868	-0.604057137	-0.355930811
1	12.756687766	-1.620560827	0.883266384
1	14.305755207	0.301284211	-0.933321455
6	15.218117216	-1.565222772	-0.386968744
6	15.198603064	-2.813037426	0.266553719
6	16.384660521	-1.260800441	-1.111840755
6	16.269025026	-3.691811571	0.207599366
1	14.321759432	-3.112586055	0.833813219
6	17.466742268	-2.128004766	-1.183790371
1	16.442560291	-0.311674648	-1.640988502
6	17.445815425	-3.371663976	-0.513055875
1	18.330833681	-1.832202463	-1.766718456
1	16.187381443	-4.639486985	0.726723730
7	18.530508080	-4.236794376	-0.549861354

6	19.631913528	-3.960941854	-1.455572600
1	20.094847840	-2.993036379	-1.228073538
1	20.397822083	-4.729064946	-1.331709552
1	19.323231792	-3.949106328	-2.513350612
6	18.392250522	-5.581660338	-0.018284965
1	18.134938826	-5.559071507	1.047515805
1	17.622598250	-6.171849713	-0.541225324
1	19.346462779	-6.103339410	-0.114685985

**Table S5: The coordinates of compound Ph-BDP-NMe<sub>3</sub> (DFT/B3LYP/6-31G(d) level with Gaussian 09)**

5	0.007450345	-1.787914200	0.124685378
6	-2.509540658	-1.274120081	0.236478602
6	-3.381786226	-0.149196052	0.189117189
6	-2.580181666	0.999932113	0.090061169
6	-1.222030841	0.545577203	0.085624696
6	-0.000244973	1.238453138	-0.017303781
6	1.224568426	0.544778865	-0.062737060
6	2.579986331	1.003019714	-0.123035119
6	3.386905096	-0.146615189	-0.129925954
6	2.520507226	-1.275210123	-0.064624104
9	0.119339611	-2.514987871	1.305411385
9	-0.100192304	-2.636937800	-0.972355839
7	-1.237559976	-0.850398148	0.176851264
7	1.246813186	-0.853754867	-0.028505234
6	-0.004182962	2.729278129	-0.085418941
6	-0.168318865	3.500232277	1.069075576
6	0.156196370	3.391054517	-1.314726714
6	-0.166982238	4.896418378	1.015987112
1	-0.290110125	3.007166898	2.029933336
6	0.144451521	4.777311967	-1.384375505
1	0.281394262	2.809390257	-2.224072482



6	-0.013990728	5.543486232	-0.217425147
1	-0.285894850	5.462241226	1.932708171
1	0.258273649	5.294718578	-2.331691280
8	-0.004131316	6.890489404	-0.391323438
6	-0.160581564	7.725614078	0.749460651
1	-0.124473486	8.749441348	0.374953469
1	-1.125104218	7.552827069	1.243629094
1	0.651240972	7.573795083	1.472130641
6	3.090020371	2.414781242	-0.097826360
1	2.956032437	2.924365285	-1.059310261
1	2.569899911	3.019119404	0.649687091
1	4.157550628	2.425119582	0.137548670
6	2.870149415	-2.729127207	-0.065758027
1	2.726625697	-3.163184359	0.931051386
1	2.207709904	-3.272595052	-0.744310338
1	3.907345745	-2.881495695	-0.370485349
6	-3.097127502	2.400833897	-0.065517657
1	-2.973827181	2.993838035	0.848317915
1	-2.574306751	2.939762571	-0.859697808
1	-4.162607768	2.383435274	-0.309414204
6	-2.852397852	-2.723783771	0.367104638
1	-2.692176342	-3.247849697	-0.582684382
1	-2.197512769	-3.198141618	1.102676268
1	-3.893202726	-2.853628644	0.670164748
6	4.857465736	-0.209066923	-0.192740886
6	5.592190224	-1.007270176	0.709474134
6	5.581161377	0.514538465	-1.157973671
6	6.975539618	-1.083856603	0.647930630
1	5.063234457	-1.559548420	1.480180871
6	6.967463156	0.441028172	-1.218387700

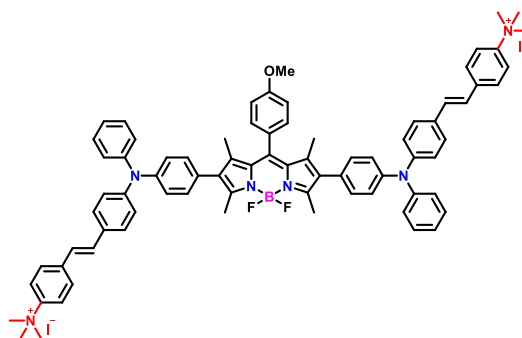
1	5.045317484	1.118835976	-1.883300940
6	7.700284691	-0.358506357	-0.319944669
1	7.496797570	-1.713220768	1.363150417
1	7.498315621	1.004719378	-1.982207808
6	9.152340712	-0.398270668	-0.440957371
6	10.026850461	-1.047350183	0.362607074
1	9.542536118	0.177034860	-1.279923870
6	11.476938895	-1.078446321	0.213614644
6	12.175989556	-0.514030691	-0.872680558
6	12.253335796	-1.715942385	1.205391784
6	13.562854485	-0.571960626	-0.965874228
1	11.633679927	-0.022930081	-1.673209026
6	13.637607228	-1.782709398	1.127000223
1	11.756522022	-2.167041187	2.059303340
6	14.298304761	-1.208146209	0.036888004
1	14.033898703	-0.118715701	-1.828585504
1	14.177295895	-2.284051818	1.924161329
6	-4.853078306	-0.215256727	0.229350513
6	-5.600908420	0.585473734	1.111675525
6	-5.564540025	-1.093582933	-0.615066897
6	-6.988147054	0.510820803	1.146637742
1	-5.083814600	1.253986384	1.793003065
6	-6.948720068	-1.170333971	-0.579442891
1	-5.016242576	-1.709861895	-1.321042725
6	-7.697928688	-0.365814135	0.303409165
1	-7.538067363	1.136426674	1.846090037
1	-7.451036174	-1.862905459	-1.248323606
6	-9.152720556	-0.399065010	0.389876587
6	-10.005250134	-1.109673928	-0.384838283
1	-9.564907669	0.239138027	1.170859423

6	-11.458666299	-1.132260689	-0.273036194
6	-12.184311820	-0.488397089	0.754057969
6	-12.210161124	-1.839875617	-1.231377165
6	-13.568786933	-0.543921858	0.811243074
1	-11.661145655	0.059466412	1.530071035
6	-13.600491159	-1.905512001	-1.187817712
1	-11.693025356	-2.352555390	-2.037101063
6	-14.283769797	-1.253083799	-0.162266332
1	-14.070817177	-0.032096042	1.626061534
1	-14.110207597	-2.466648053	-1.960260097
1	-9.603863369	-1.725916799	-1.186030490
1	9.648362996	-1.601433228	1.218565392
7	-15.791757525	-1.295110770	-0.059176556
7	15.806768273	-1.300307370	-0.019912167
6	-16.429838658	-2.079754781	-1.178857069
1	-16.179387427	-1.615579014	-2.132191558
1	-16.073122021	-3.108623761	-1.147200008
1	-17.509618061	-2.058543505	-1.029187518
6	-16.197119839	-1.949872083	1.246879820
1	-15.798362662	-1.371380822	2.078008480
1	-17.286948847	-1.980229469	1.300954670
1	-15.783261267	-2.958207986	1.266159954
6	-16.350218332	0.113352150	-0.114117191
1	-15.957073027	0.690102352	0.720835951
1	-16.040319487	0.566874344	-1.055701738
1	-17.438669203	0.060725179	-0.051779240
6	16.231886308	-2.755529374	-0.031241360
1	17.321207677	-2.802070333	-0.083770989
1	15.881675164	-3.240221015	0.878004854
1	15.784285754	-3.235611463	-0.901647567

6	16.384034927	-0.648464919	-1.251921879
1	17.467905876	-0.760177925	-1.213124989
1	15.992982148	-1.145062408	-2.139309236
1	16.121560313	0.408861956	-1.255720345
6	16.407539922	-0.606761010	1.186942590
1	16.092067836	0.436672461	1.173124275
1	16.048608625	-1.088904133	2.094063411
1	17.495108550	-0.680945072	1.128709037

**Table S6: The coordinates of compound TPA-BDP-NMe<sub>3</sub> (DFT/B3LYP/6-31G(d) level with Gaussian 09)**

5	0.687620855	-1.633279163	0.053158744
6	-1.841916723	-2.093846454	-0.065957468
6	-3.065000161	-1.369982133	-0.147107883
6	-2.741428202	-0.006393538	-0.195294667
6	-1.311317035	0.074048182	-0.141610957
6	-0.430241984	1.171075221	-0.155277942
6	0.963103038	0.984162011	-0.090691838
6	2.054206194	1.913605926	-0.081103160
6	3.227105558	1.147846430	-0.003673201
6	2.838847554	-0.220425538	0.034271135
9	0.917274928	-2.267566296	1.274054463
9	1.040942968	-2.462437501	-1.005399254
7	-0.813274511	-1.230301459	-0.060982070
7	1.499277761	-0.305042887	-0.014272290
6	-0.983750439	2.557698481	-0.224608143
6	-1.314375653	3.254788195	0.948644936
6	-1.183653621	3.192023900	-1.453711727
6	-1.826533567	4.544550370	0.891530513
1	-1.165618478	2.779076052	1.914282849
6	-1.698923108	4.489148766	-1.526901592
1	-0.932728920	2.669373502	-2.373095463



6	-2.023270470	5.173027555	-0.348282735
1	-2.081525625	5.089575927	1.794970880
1	-1.839452662	4.950062478	-2.497792314
8	-2.529476786	6.435134762	-0.296586841
6	-2.734956465	7.133224384	-1.517141103
1	-3.131311262	8.110631220	-1.237918954
1	-1.794764395	7.266565673	-2.067559304
1	-3.460600018	6.616808932	-2.158911405
6	2.004870925	3.410489600	-0.183400059
1	1.444585689	3.740059158	-1.063152495
1	1.517378396	3.868245018	0.684890808
1	3.016548592	3.817083727	-0.255260368
6	3.703325039	-1.434989732	0.147185139
1	3.329539848	-2.088673545	0.940484049
1	3.676071897	-2.018321240	-0.780546110
1	4.736998403	-1.156614633	0.361103475
6	-3.734309134	1.111578548	-0.330093716
1	-3.764810255	1.748335140	0.561722459
1	-3.495837645	1.767889684	-1.171808698
1	-4.736855642	0.705877100	-0.488470252
6	-1.633735292	-3.570693699	0.038953553
1	-1.176524429	-3.963752520	-0.876528179
1	-0.942335323	-3.794299297	0.856416909
1	-2.580526674	-4.085697433	0.211300685
6	4.621622253	1.634594353	0.040349501
6	5.040003772	2.573842319	0.999621544
6	5.583525106	1.166501092	-0.873139349
6	6.356477750	3.023428134	1.050200559
1	4.328181895	2.934767084	1.736207360
6	6.901078346	1.614129937	-0.833844726

1	5.285463253	0.463597171	-1.645832967
6	7.302572798	2.544770945	0.134469728
1	6.658976156	3.740523792	1.807009853
1	7.621137184	1.253041861	-1.562042776
6	-4.409363284	-1.982878831	-0.158945192
6	-5.394535960	-1.606447098	0.771417925
6	-4.741323512	-2.988452614	-1.084488451
6	-6.647154601	-2.214420956	0.790049906
1	-5.158943058	-0.855169813	1.519598364
6	-5.992464393	-3.597288650	-1.078644387
1	-4.011677103	-3.284450480	-1.832607881
6	-6.958805710	-3.219922865	-0.136187039
1	-7.378911326	-1.928581806	1.539547150
1	-6.226032013	-4.370354512	-1.803866714
7	-8.219508275	-3.891387854	-0.099224523
6	-9.422336417	-3.191867772	0.014054698
6	-10.560076657	-3.793576531	0.594897528
6	-9.545116757	-1.862892409	-0.459622281
6	-11.753434749	-3.099095126	0.685620105
1	-10.494172711	-4.804565707	0.979663846
6	-10.743730373	-1.181470099	-0.360595143
1	-8.690475391	-1.381711712	-0.921585421
6	-11.890413550	-1.776295151	0.213040830
1	-12.609699525	-3.587251724	1.145814845
1	-10.795303511	-0.169921814	-0.753090855
6	-8.212652413	-5.324448286	-0.150337020
6	-8.991992491	-6.002020012	-1.097812319
6	-7.405852057	-6.052944696	0.733075868
6	-8.971619908	-7.395216917	-1.148753472
1	-9.605916895	-5.434081482	-1.790370324

6	-7.380056942	-7.445362494	0.665934261
1	-6.802326410	-5.524695624	1.464709914
6	-8.164499030	-8.121914972	-0.270579804
1	-9.577262052	-7.912462437	-1.887685988
1	-6.751283296	-8.002335837	1.354856876
1	-8.144878989	-9.206731508	-0.317902676
7	8.649452830	3.023365601	0.175224033
6	8.854144676	4.439336835	0.243699626
6	9.670187430	4.992369839	1.240482400
6	8.214204754	5.282505882	-0.674194522
6	9.853232592	6.373076664	1.305057180
1	10.153058018	4.338846388	1.960741559
6	8.391405471	6.662976154	-0.593807138
1	7.581130961	4.851213422	-1.443492272
6	9.213680134	7.213786381	0.391526891
1	10.485990043	6.792751424	2.082184387
1	7.891789281	7.308702258	-1.310551289
1	9.352542489	8.289369567	0.449041876
6	9.731569133	2.140702173	0.177077219
6	11.000533848	2.547565096	-0.302205997
6	9.598913393	0.818291376	0.653472687
6	12.074988087	1.678854341	-0.294841915
1	11.125470056	3.551846496	-0.690456388
6	10.684038809	-0.041480654	0.651334181
1	8.643355015	0.478935397	1.036134488
6	11.955733337	0.354954758	0.185199010
1	10.553527348	-1.050044611	1.037462474
6	-13.175574263	-1.120245270	0.331181810
6	-13.517734187	0.131760488	-0.069922893
1	-13.942083963	-1.739045518	0.797086424

1	-12.766614496	0.761411860	-0.541655698
6	-14.830479111	0.739863577	0.056088063
6	-15.042492071	2.042119367	-0.444589592
6	-15.945602951	0.107199943	0.656220514
6	-16.275960740	2.681165545	-0.366559889
1	-14.215816559	2.568862194	-0.912312589
6	-17.180156169	0.730256957	0.741323323
1	-15.849276075	-0.892243812	1.065749480
6	-17.353321063	2.022843774	0.228124652
1	-16.360596556	3.679884080	-0.775834814
1	-17.996049801	0.190225938	1.211684902
7	-18.718499726	2.662703196	0.334808380
6	-19.737952182	1.823522823	-0.409391534
1	-19.769983863	0.827083254	0.026909396
1	-20.716023506	2.301117250	-0.324748542
1	-19.429840687	1.759316700	-1.453073952
6	-19.123101454	2.773949182	1.791319223
1	-18.375495447	3.376300622	2.307629506
1	-20.105491817	3.246854553	1.848378475
1	-19.162227709	1.779017567	2.230386450
6	-18.755912875	4.050263777	-0.253872191
1	-18.052337538	4.686994444	0.281344764
1	-18.498318651	3.998878856	-1.311097331
1	-19.768654570	4.436978208	-0.137569149
1	13.024970736	2.032282518	-0.685126213
6	13.048877641	-0.593922985	0.225180012
6	14.339839513	-0.392902827	-0.146859045
1	12.768062484	-1.574966407	0.607834076
1	14.634164671	0.582542081	-0.527416637
6	15.412696219	-1.369714909	-0.086037122

6	15.262560114	-2.692054965	0.386723831
6	16.707299572	-0.999634038	-0.518721506
6	16.325984395	-3.585867946	0.429998150
1	14.295202089	-3.039028343	0.732892916
6	17.778371522	-1.880142297	-0.482161634
1	16.872065894	0.006974911	-0.891806696
6	17.591618415	-3.181990160	-0.004494156
1	16.135697336	-4.582994271	0.806225712
1	18.746201520	-1.530915608	-0.828613063
7	18.779717914	-4.116292810	0.028366399
6	19.861859088	-3.539155185	0.918842430
1	19.447919393	-3.411720873	1.919213099
1	20.707773527	-4.229110320	0.936700152
1	20.175283682	-2.574528392	0.524422084
6	18.430303552	-5.481199106	0.564933147
1	17.673715344	-5.935650919	-0.073718172
1	19.336230713	-6.087910189	0.555465674
1	18.061526542	-5.382945761	1.585334047
6	19.325610390	-4.302979384	-1.373170738
1	18.531725875	-4.715741279	-1.995807410
1	19.639513254	-3.338599314	-1.767878121
1	20.176797764	-4.985317409	-1.331451155

## 10. References

1. A. N. S. Chauhan and R. D. Erande, *Tetrahedron Lett.*, **2024**, 151, 155317–155320.
2. T. Akasaka, H. Watanabe and M. Ono, *J. Med. Chem.*, **2023**, 66, 14029–14046.
3. M. Gigante, M. A. Esteves, N. Pires, M. L. Davies, P. Douglas, S. M. Fonseca, H. D. Burrows, R. A. E. Castro, J. Pinac and J. S. de Melo, *New J. Chem.*, **2009**, 33, 877–885.
4. J. Kulhánek, F. Bureš and M. Ludwig, *Beilstein J. Org. Chem.*, **2009**, 5, 11.
5. M. Wang, Y. Zhang, T. Wang, C. Wang, D. Xue and J. Xiao, *Org. Lett.*, **2016**, 18, 1976–1979.

6. X. Li, X. Sun, H. Chen, X. Chen, Y. Li, D. Li, Z. Zhang, H. Chen and Y. Gao, *Eur. J. Med. Chem.*, **2024**, 264, 116035–116047.
7. S. Zhang, T. Wu, J. Fan, Z. Li, N. Jiang, J. Wang, B. Dou, S. Sun, F. Song and X. Peng, *Org. Biomol. Chem.*, **2013**, 11, 555–558.
8. T. Gao, H. He, R. Huang, M. Zheng, F.-F. Wang, Y.-J. Hu, F.-L. Jiang and Y. Liu, *Dyes Pigm.*, **2017**, 141, 530–535.
9. T. Zhu, G. Yang, X. Liu, P. Xiang, Z. Yang, S. Zhang, J. Chen, H. Wang, S. C. De Souza, Z. Zhang, R. Zhang, Y. Tian, J. Wu and X. Tian, *Biosens. Bioelectron.*, **2021**, 178, 113036.
10. (a) C. Kalarikkal, Anjali, S. Bhattacharjee, K. Mapa and P. C. A. Swamy, *J. Mater. Chem. B*, **2025**, 13, 1474–1486; (b) C. Kalarikkal, Anjali, K. Mapa and P. C. A. Swamy, *New J. Chem.*, **2025**, 49, 16914–16924.
11. N. Jiang, J. Fan, T. Liu, J. Cao, B. Qiao, J. Wang, P. Gao and X. Peng, *Chem. Commun.*, **2013**, 49, 10620–10622.
12. J.-L. Wang, L. Zhang, L.-X. Gao, J.-L. Chen, T. Zhou, Y. Liu and F.-L. Jiang, *J. Mater. Chem B*, **2021**, 9, 8639–8645.
13. J. Yang, R. Zhang, Y. Zhao, J. Tian, S. Wang, C. P. Gros and H. Xu, *Spectrochim. Acta, Part A*, **2021**, 248, 119199.
14. T. Gayathri, S. Karnewar, S. Kotamraju and S. P. Singh, *ACS Med. Chem. Lett.*, **2018**, 9, 618–622.
15. C. Kalarikkal, S. Bhattacharjee, K. Mapa and P. C. A. Swamy, *Sens. Diagn.*, **2026**, 5, 337–347.